S-N/99205--029

STOLLER-NAVARRO

Integrated Analysis Report for Single- and Multiple-Well Aquifer Testing at Frenchman Flat Well Cluster RNM-2s, Nevada Test Site, Nevada

Revision No.: 0

September 2004

Prepared for U.S. Department of Energy under Contract No. DE-AC52-03NA99205

Available for public sale, in paper, from:

U.S. Department of Commerce
National Technical Information Service
5285 Port Royal Road
Springfield, VA 22161
Phone: 800.553.6847
Fax: 703.605.6900
Email: *orders@ntis.gov*
Online ordering: *http://www.ntis.gov/ordering.htm*

Available electronically at *http://www.osti.gov/bridge*

Available for a processing fee to U.S. Department of Energy and its contractors, in paper, from:

U.S. Department of Energy
Office of Scientific and Technical Information
P.O. Box 62
Oak Ridge, TN 37831-0062
Phone: 865.576.8401
Fax: 865.576.5728
Email: *reports@adonis.osti.gov*

S-N/99205--029

STOLLER-NAVARRO

INTEGRATED ANALYSIS REPORT FOR SINGLE- AND MULTIPLE-WELL AQUIFER TESTING AT FRENCHMAN FLAT WELL CLUSTER RNM-2s, NEVADA TEST SITE, NEVADA

Revision No.: 0

September 2004

E. Bhark, G. Ruskauff, J. Pickens, L. Scheinost, B. Fryer
Stoller-Navarro Joint Venture
7710 W. Cheyenne, Building 3
Las Vegas, NV 89129

Prepared for U.S. Department of Energy under Contract No. DE-AC52-03NA99205

INTEGRATED ANALYSIS REPORT FOR SINGLE- AND MULTIPLE-WELL AQUIFER TESTING AT FRENCHMAN FLAT WELL CLUSTER RNM-2s, NEVADA TEST SITE, NEVADA

Approved by: Approved Signature Date: 9/21/2004

John McCord, UGTA Project Manager
Stoller-Navarro Joint Venture

Table of Contents

Table of Contents *(Continued)*

List of Figures

List of Figures *(Continued)*

List of Figures *(Continued)*

List of Tables

List of Acronyms and Abbreviations

AA	Alluvial aquifer
amsl	Above mean sea level
BE	Barometric efficiency
bgs	Below ground surface
BN	Bechtel Nevada
cm	Centimeter
CZ	Completion zone
DOE	U.S. Department of Energy
DRI	Desert Research Institute
FCVF	Finite conductivity vertical fracture
FF	Frenchman Flat
fpm	Feet per minute
ft	Foot
FY	Fiscal Year
gal	Gallons
gpm	Gallons per minute
HSU	Hydrostratigraphic unit
ICVF	Infinite conductivity vertical fractures
in.	Inch
ITLV	IT Corporation, Las Vegas
JD	Julian day
LANL	Los Alamos National Laboratory
LCA	Lower carbonate aquifer
LLNL	Lawrence Livermore National Laboratory
LTCU	Lower Tuff Confining Unit
m	Meter
m^3	Cubic meter
mbar	Millibar
MWAT	Multiple-well aquifer test
NNSA/NSO	U.S. Department of Energy, National Nuclear Security Administration Nevada Site Office
NTS	Nevada Test Site
psi	Pounds per square inch

psig	Pounds per square inch gauge
PXD	Pressure transducer
PZ	Piezometer
QTa	Quarternary-Tertiary Alluvium
RNM	Radionuclide Migration Study
RWMS	Radioactive Waste Management Site
Shaw	Shaw Environmental, Inc.
sec	Second
SNJV	Stoller-Navarro Joint Venture
SS	Stainless-steel
SSE	Sum of squared errors
SWL	Static water level
Tcb	Bullfrog Tuff
TCU	Tuff confining unit
TD	Total depth
TFM	Thermal flow meter
Tma	Ammonia Tanks Tuff
Tmr	Rainier Mesa Tuff
TVD	Time vertical depth
UGTA	Underground Test Area
UNLV-HRC	University of Nevada, Las Vegas - Harry Reid Center
UTM	Universal Transverse Mercator

1.0 Introduction

This report documents the analysis and interpretation of the hydraulic data collected for the Well ER-5-4 single-well test, the Well ER-5-4#2 single-well test, and the well cluster RNM-2s multiple-well aquifer test (MWAT). All wells are located in south-central Frenchman Flat (FF) within Area 5 of the Nevada Test Site (NTS), Nevada. Figure 1-1 shows the well cluster location within Frenchman Flat, and Figure 1-2 shows the well cluster in greater spatial detail. Wells ER-5-4 and ER-5-4#2 are components of the RNM-2s well cluster and functioned as observation wells during the MWAT; however, prior to the MWAT each well was tested individually and independent of the other wells within the cluster.

The RNM-2s MWAT was developed in response to the U.S. Department of Energy, National Nuclear Security Administration Nevada Site Office (NNSA/NSO) review of the *Phase I Frenchman Flat Corrective Action Unit Model* and proposed in the *Addendum to the Corrective Action Plan for Corrective Action Unit 98 Frenchman Flat, Nevada Test Site, Nevada* (DOE/NV, 2000). Shaw Environmental, Inc. (Shaw) and Stoller-Navarro Joint Venture (SNJV) documents occasionally refer to the MWAT as the ER-5-4 MWAT because the aquifer test followed drilling of ER-5-4 and ER-5-4#2 at the cluster. This report refers to the test as the RNM-2s MWAT to reflect the name of the production well during the test.

During design of the MWAT, consideration was given to three underground nuclear tests conducted near RNM-2s. The CAMBRIC (drillhole U-5e) test, located 301 feet (ft) north of RNM-2s, had a working point in alluvium below the static water level (SWL) at 968 ft below ground surface (bgs). The DILUTED WATERS (drillhole U-5b) test, located 3,577 ft southeast of RNM-2s, had a working point in alluvium above the SWL at 633 ft bgs. The WISHBONE (U-5a) test, located 5,436 ft southeast of RNM-2s, had a working point in alluvium above the SWL at 574 ft bgs. A summary of the location and depth of each test is presented in Table 1-1.

The site of this MWAT was previously used by the Los Alamos National Laboratory (LANL) to conduct a long-term Radionuculide Migration Study (RNM) which involved nearly 16 years of continuous pumping from well RNM-2s in an effort to understand migration of radionuculides from the CAMBRIC (U-5e) underground test. Spatial- (scale-) dependent hydraulic properties of the local alluvium were not studied, rather activity levels of radionuclides at RNM-2s as a function of time and groundwater volume produced were investigated (Bryant, 1992). Hence, the RNM-2s MWAT was designed to investigate hydraulic properties of the alluvium at known support scales.

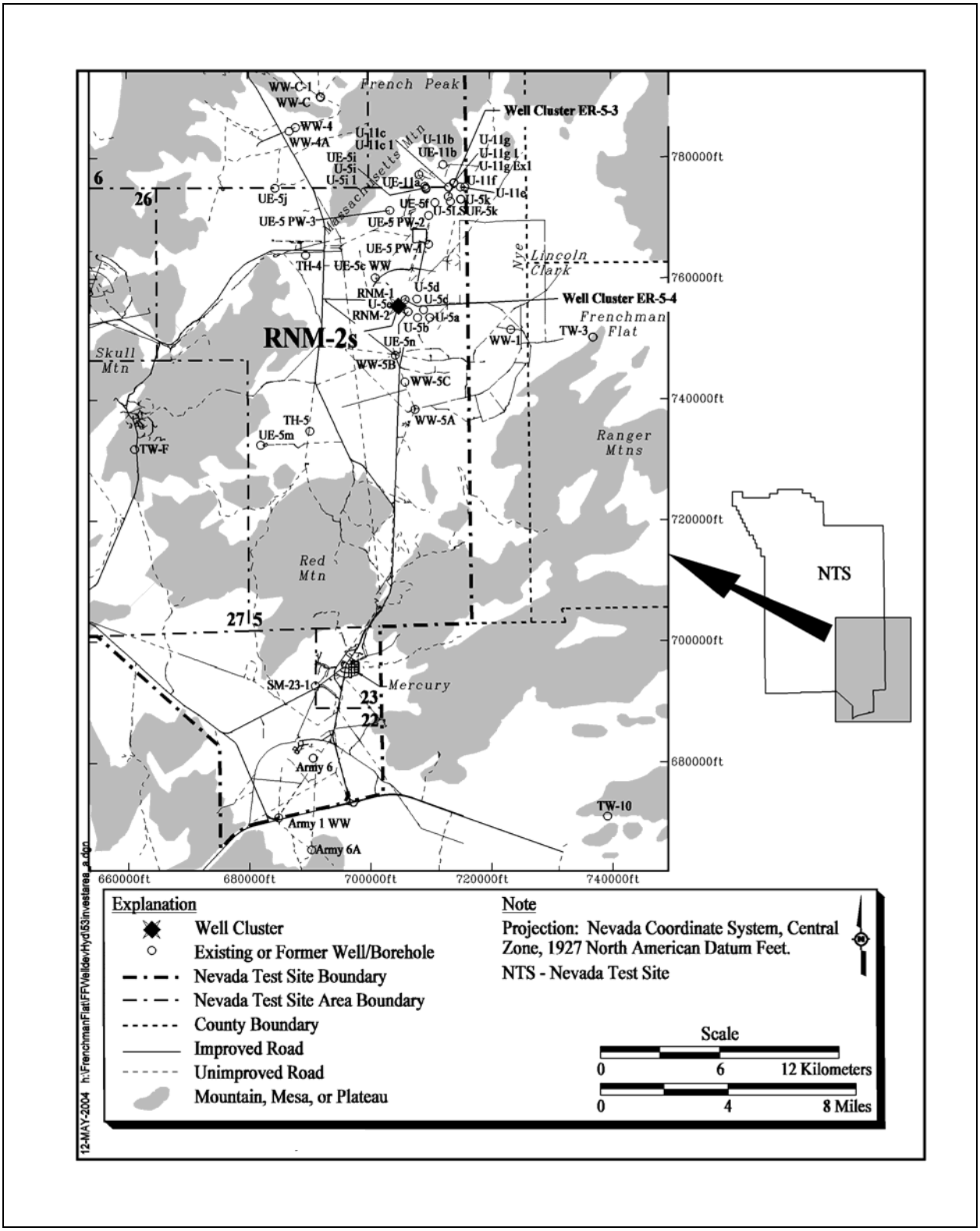

Figure 1-1
Well Cluster RNM-2s within the Frenchman Flat CAU

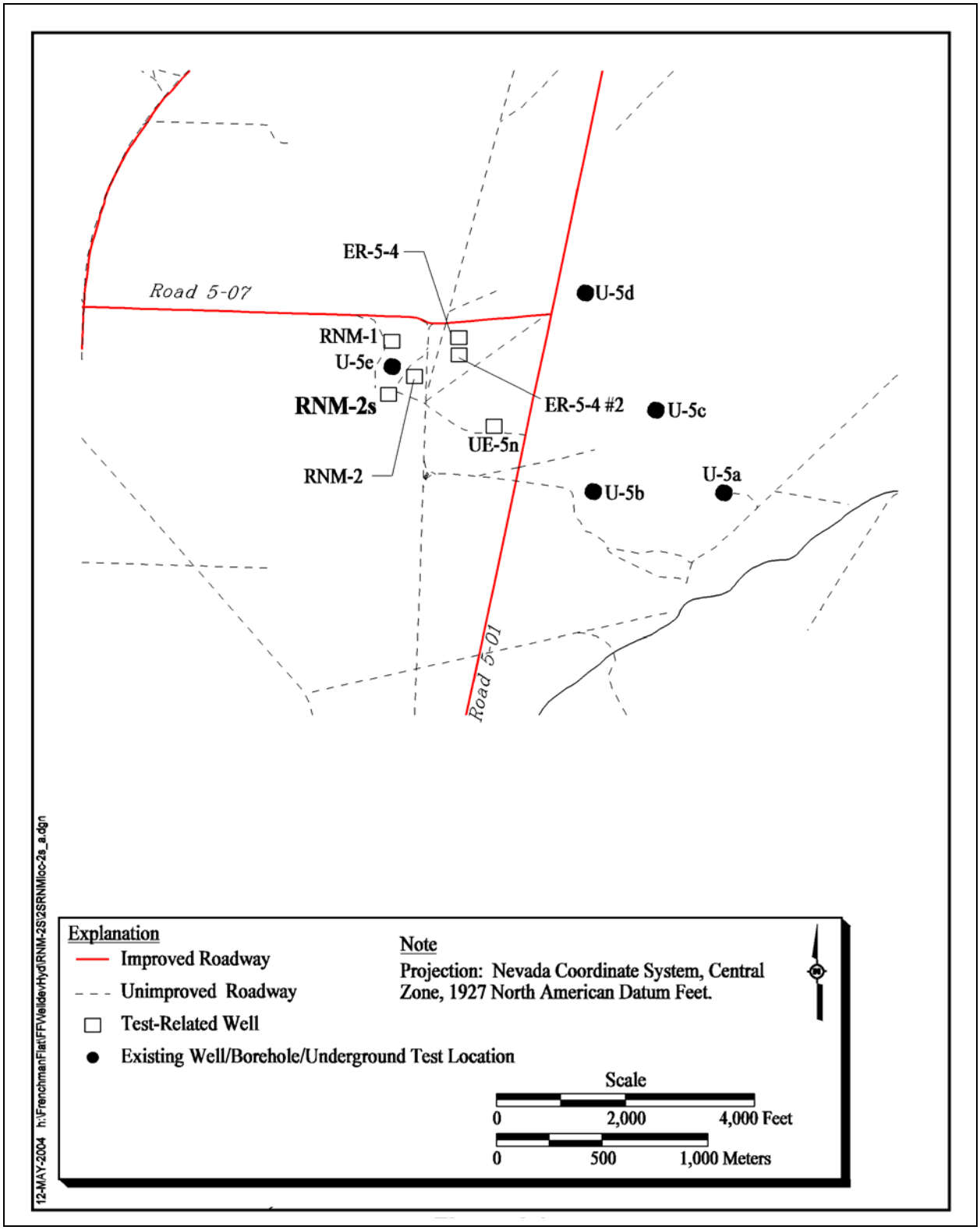

Figure 1-2
Well Cluster RNM-2s in Spatial Detail

Table 1-1
Well and Nearby Nuclear Test Locations, Elevations, Distances from RNM-2s, and Completion HSUs
(Page 1 of 2)

Well	Nevada State Plane NAD 27 (ft)		Source	UTM Zone 11 NAD 27 (m)		Ground Surface Elevation (ft amsl)	Distance from RNM-2s (ft)	Completion HSU[a]
	Northing	Easting		Northing	Easting			
Multi-Well Aquifer Test Production Well								
RNM-2s	755,119.13	704,809.78	BN Survey 4/30/2001	4,075,483.95	592,136.58	3,130.45	0	AA
RNM-2s access line	755,119.13	704,809.78	BN Survey 4/30/2001	4,075,483.95	592,136.58	3,130.45	0	AA
Multi-Well Aquifer Test Observation Wells								
RNM-2s Outer West Piezometer	755,119.13	704,809.78	BN Survey 4/30/2001	4,075,483.95	592,136.58	3,130.45	0	AA
RNM-2	755,264.43	705,088.20	BN Survey 4/30/2001	4,075,528.53	592,221.27	3,128.80	314.05	AA
RNM-1 (Slant-Angle Well)	755,825.38	704,831.25	BN Survey 4/30/2001	4,075,699.19	592,142.37	3,135.17	706.58	AA
ER-5-4 #2	755,651.18	705,819.62	BN Survey 8/2003	4,075,647.16	592,443.74	3,131.70	1,141.43	LTCU
ER-5-4 Upper Completion Zone	755,751.32	705,819.92	BN Survey 8/2003	4,075,677.67	592,443.72	3,131.70	1,191.66	AA
ER-5-4 Lower Completion Zone	755,751.32	705,819.92	BN Survey 8/2003	4,075,677.67	592,443.72	3,131.70	1,191.66	AA1
ER-5-4 Piezometer	755,751.32	705,819.92	BN Survey 8/2003	4,075,677.67	592,443.72	3,131.70	1,191.66	AA
UE-5n	754,460.79	706,415.49	BN Survey 4/30/2001	4,075,285.05	592,626.58	3,113.36	1,735.43	AA
ER-5-3 #3	773,574.10	713,100.80	BN Survey	4,081,116.46	594,643.44	3,337.40	20,231.83	OAA
TW-3	750,189.00	736,937.00	Borehole Index	4,074,015.75	601,931.81	3,484.12	48,886.23	LCA
Radioactive Waste Management Site Pilot Wells								
UE-5 PW-1	765,702.14	709,831.52	RWMS Records	4,078,714.20	593,655.58	3,177.98	11,714.01	AA
UE-5 PW-2	770,395.87	709,893.59	RWMS Records	4,080,144.56	593,669.50	3,246.19	16,100.43	AA
UE-5 PW-3	771,290.88	703,460.01	RWMS Records	4,080,410.45	591,708.08	3,295.47	16,277.98	TM-WTA
Nearby Water Supply Wells								
UE-5c WW	760,133.73	700,997.24	BN Survey 4/30/2001	4,077,007.97	590,969.48	3,216.27	6,299.34	AA/LTCU
WW-5B	747,360.25	704,262.81	BN Survey 4/30/2001	4,073,119.05	591,978.15	3,093.27	7,778.14	AA
WW-5C	741,654.28	706,305.21	BN Survey 4/30/2001	4,071,382.47	592,606.58	3,083.09	13,547.64	AA
WW-5A	738,359.48	707,518.36	BN Survey 4/30/2001	4,070,379.75	592,979.75	3,093.73	16,977.11	AA

Table 1-1
Well and Nearby Nuclear Test Locations, Elevations, Distances from RNM-2s, and Completion HSUs
(Page 2 of 2)

Well	Nevada State Plane NAD 27 (ft)		Source	UTM Zone 11 NAD 27 (m)		Ground Surface Elevation (ft amsl)	Distance from RNM-2s (ft)	Completion HSU[a]
	Northing	Easting		Northing	Easting			
U-5e CAMBRIC	755,419.00	704,831.00	Borehole Index	4,075,575.35	592,142.73	3,136.78	300.62	AA
U-5b DILUTED WATERS	753,500.00	707,999.00	Borehole Index	4,074,993.95	593,110.14	3,095.18	3,576.69	AA
U-5a WISHBONE	753,500.00	709,999.00	Borehole Index	4,074,996.08	593,719.59	3,085.70	5,435.95	AA

[a]Refer to Table 1-4 and Table 1-5 for HSU descriptions.

BN - Bechtel Nevada
ft - Feet
amsl - Above mean sea level
HSU - Hydrostratigraphic unit
m - Meters
NAD 27 - North American Datum 1927
RWMS - Radioactive Waste Management Site
UTM - Universal Transverse Mercator

Well RNM-2s was last pumped in 1999 for a period of approximately 7 days by the U.S. Air Force as part of a short-term test unrelated to hydraulic testing.

Participants in the field development and hydraulic testing activities of wells within the RNM-2s well cluster included IT Corporation, Las Vegas (ITLV), Shaw, Bechtel Nevada (BN), Weatherford, Desert Research Institute (DRI), LANL, Lawrence Livermore National Laboratory (LLNL), U.S. Geological Survey (USGS), and the University of Nevada, Las Vegas - Harry Reid Center (UNLV-HRC). The analyses of the data collected from the development and testing activities were performed by the SNJV team which includes Stoller, Navarro, Battelle, INTERA, Inc., and Weston Solutions, Inc.

1.1 Well ER-5-4

Well ER-5-4 is the first of two wells within Well Cluster RNM-2s that was drilled and completed during the fiscal years (FYs) 2001 and 2002 for the Underground Test Area Project (UGTA) of the NNSA/NSO. Figure 1-2 shows the location of Well ER-5-4 within the RNM-2s well cluster. During FY 2001, the activities conducted at the well included well development, hydraulic testing, and groundwater sampling. These activities provide information on the hydraulic characteristics of hydrostratigraphic units (HSUs) underlying the Frenchman Flat area. Section 2.1 of the document presents the data collected during well development and hydraulic testing for Well ER-5-4. Section 3.1 includes the testing data analysis and interpretation.

development and hydraulic testing for Well ER-5-4. Section 3.1 includes the testing data analysis and interpretation.

Well ER-5-4 was constructed with one main production string and one nested piezometer. The main production string includes two completion intervals that are defined as zones of slotted casing surrounded by gravel/sand pack in the annular space and separated by cement grout. Both zones were completed in the Quarternary-Tertiary alluvium (QTa), which is assigned to the Alluvial Aquifer (AA) HSU. The well completion and lithologic log are shown in Figure 1-3 and Figure 1-4, respectively. The upper zone was completed from 1,715 to 2,192 ft bgs with the slotted interval spanning from 1,770 to 2,113 ft bgs. The lower zone was completed from 3,014 to 3,732 ft bgs with the slotted interval spanning from 3,136 to 3,350 ft bgs. The piezometer was completed between 723 and 813 ft bgs in the upper portion of the AA to monitor the water table elevation.

Well development activities began on May 5, 2001, with the measurement of water levels in the production string and piezometer, although general mobilization did not begin until May 21, 2001. Work continued until July 18, 2001 when partial demobilization activities were completed. A total of 59 operational days were spent conducting development and testing field activities at Well ER-5-4. Complete demobilization did not occur because site support facilities were used to support the subsequent drilling and completion of nearby Well ER-5-4#2 in FY 2002. A summary of activities performed at Well ER-5-4, from predevelopment through the partial demobilization, is presented in Table 1-2.

1.2 Well ER-5-4#2

Well ER-5-4#2 is the second of two wells within the Well Cluster RNM-2s that was drilled and completed during the FYs 2001 and 2002 for the NNSA/NSO UGTA Project. The well cluster location within the larger Frenchman Flat investigation area is presented in Figure 1-2. A detailed map of the Well ER-5-4#2 location, particularly in relation to the location of Well ER-5-4, is shown in Figure 1-5.

The purpose of drilling ER-5-4#2 was to attempt to penetrate the lower carbonate aquifer (LCA). The depth of the LCA prior to drilling was uncertain. Carbonate rocks were predicted below a minimum depth of 4,300 ft based on structural inferences. It was expected that the LCA would be located below a fault, inferred at a depth of approximately 6,000 ft bgs. The USGS predicted depth was below 8,000 ft bgs. In actuality, the LCA was not encountered during drilling through 7,000 ft, the well total depth (TD).

The well is completed with one main production string, constructed with 5.5-inch (in.) stainless-steel (SS) casing, to a maximum depth of 6,658 ft bgs. Below the casing (i.e., below 4,848 ft bgs), the borehole is open to a depth of 7,000 ft. There is no piezometer string. The main production casing is blank from the ground surface to 6,486 ft bgs, and slotted from 6,486 to 6,658 ft bgs. The slotted casing interval extends through the Crater Flat Group Bullfrog Tuff (Tcb), a section of

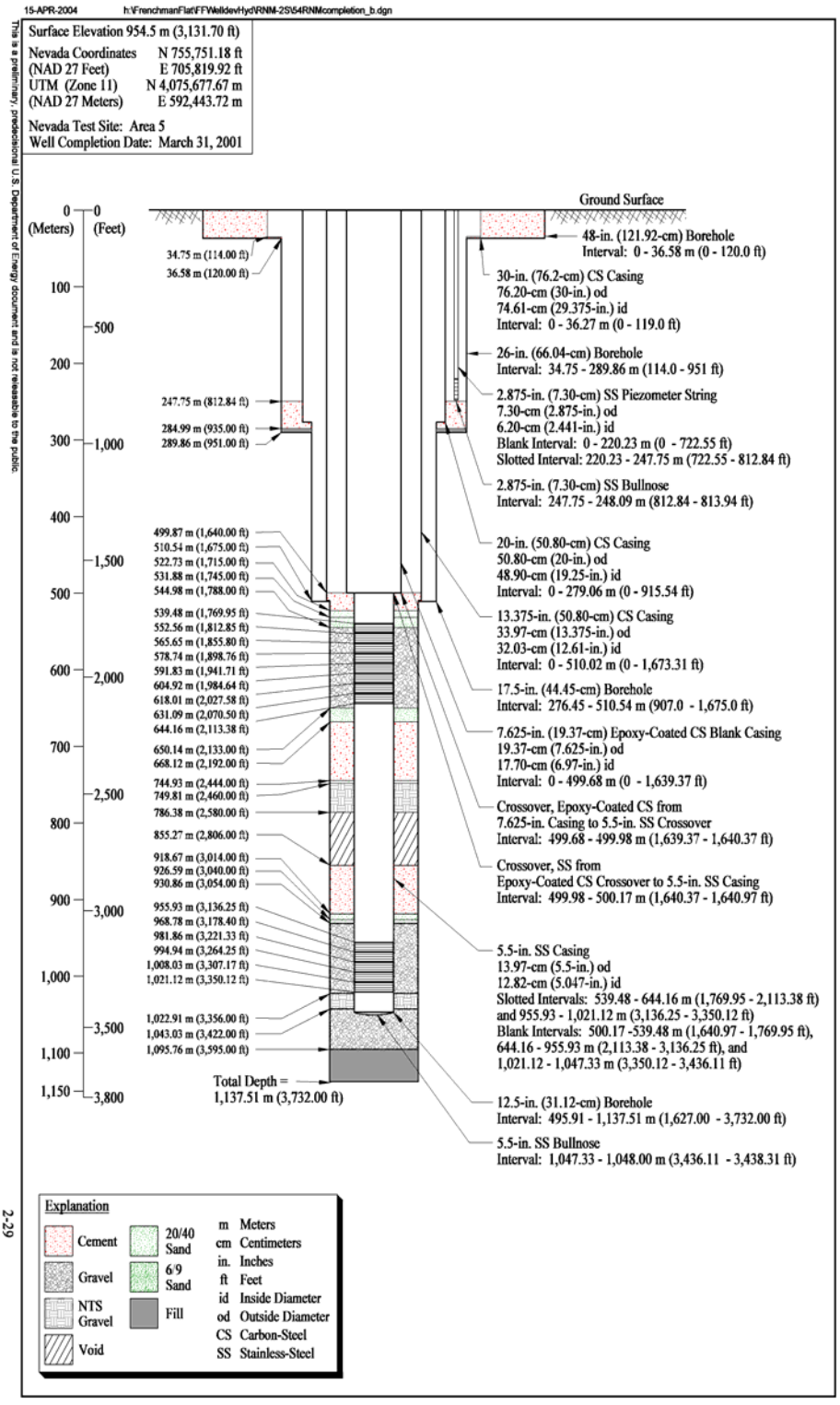

Figure 1-3
Well Completion Diagram for Well ER-5-4

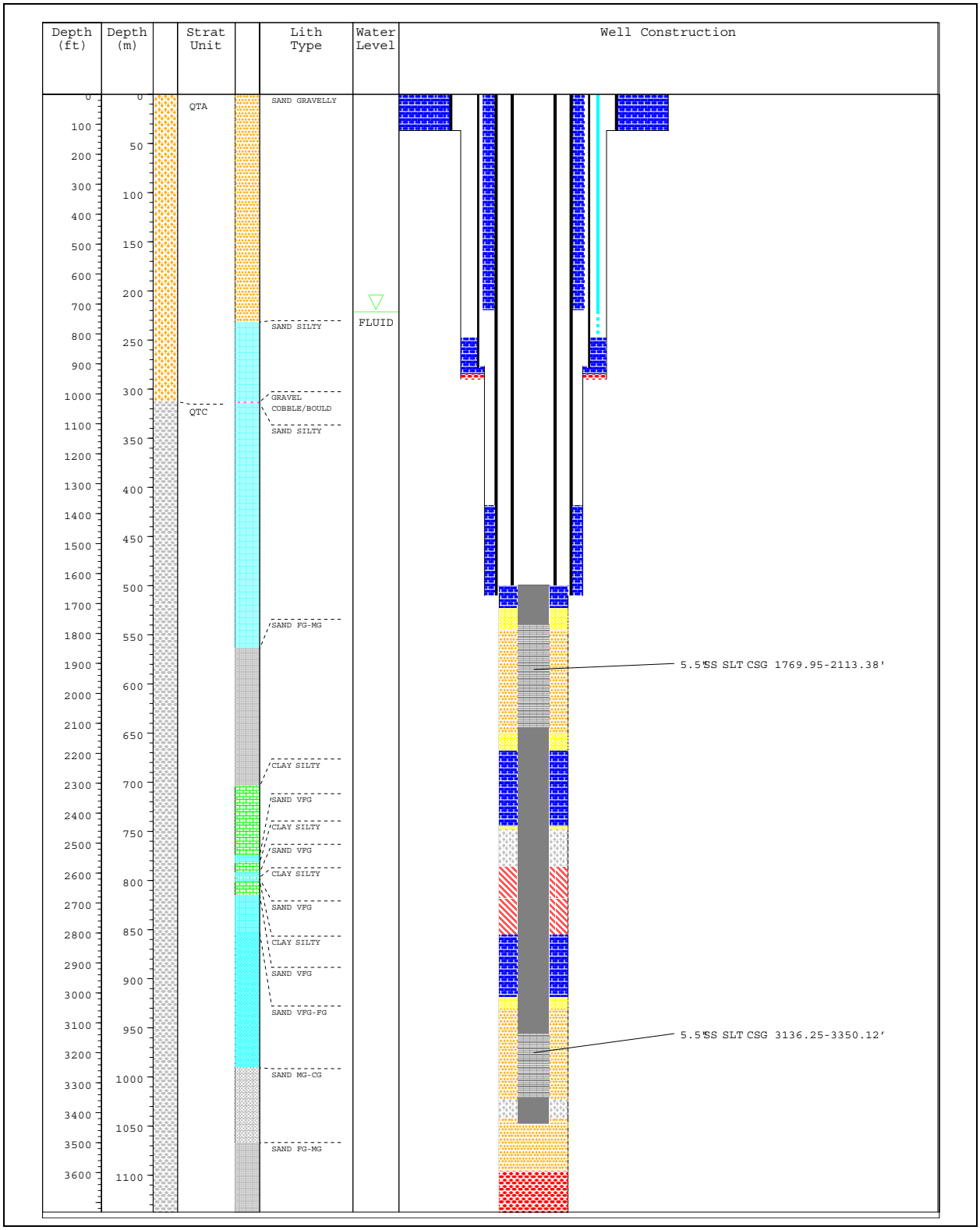

Figure 1-4
Well ER-5-4 Lithologic Log

Table 1-2
Summary of work performed at Well ER-5-4

Activity	Start Date	Finish Date	Duration in Days[a]
Pre-air-lift development water-level monitoring	5/4/2001	5/15/01	12 (5)
Site mobilization	5/21/2001	5/24/01	3.5
Air-lift development	5/24/2001	5/31/01	8 (3.5)
Install access line, testing pump, and check pump functionality	5/31/2001	6/05/01	6 (2.5)
Predevelopment water-level monitoring	6/7/2001	6/10/01	5
Develop well and conduct step drawdown testing	6/11/2001	6/18/01	8
Conduct stressed flow logging, collect discrete depth samples, install check valve, and shutdown pump	6/18/2001	6/20/01	3
Monitor water-level recovery (pretest conditions)	6/21/2001	6/26/01	6
Constant-rate test	6/26/2001	7/5/01	10
Composite well head sampling	7/5/2001	7/5/01	1
Monitor water-level recovery, remove PXDs	7/6/2001	7/10/01	5
Remove access line and testing pump	7/11/2001	7/12/01	2
Thermal flow and chemistry tool logging under ambient conditions	7/13/2001	7/13/01	1
Slug test piezometer	7/16/2001	7/16/01	1
Demobilize (partial)	7/17/2001	7/18/01	2

[a]Days in parenthesis are operational days within the duration.

the Lower Tuff Confining Unit (LTCU) HSU. The well completion diagram and well lithologic log are shown in Figure 1-6 and Figure 1-7, respectively.

A total of 47 operational days were spent conducting field development and testing activities at Well ER-5-4#2. Well development and hydraulic testing activities began on September 25, 2002, with the measurement of water levels in the production string. Mobilization began on October 14, 2002. Work continued until December 14, 2002, when partial demobilization activities were completed. A chronological summary of activities performed at Well ER-5-4#2 from predevelopment through site demobilization is presented in Table 1-3.

1.3 Well Cluster RNM-2s

The aquifer test was configured using RNM-2s as the high-volume production well and nine observation wells as hydraulic response monitoring points. The observation wells were selected from available monitoring points in FF based on proximity to RNM-2s, accessibility, and ability to instrument the well. The nine observation wells, in increasing order with respect to the distance from RNM-2s,

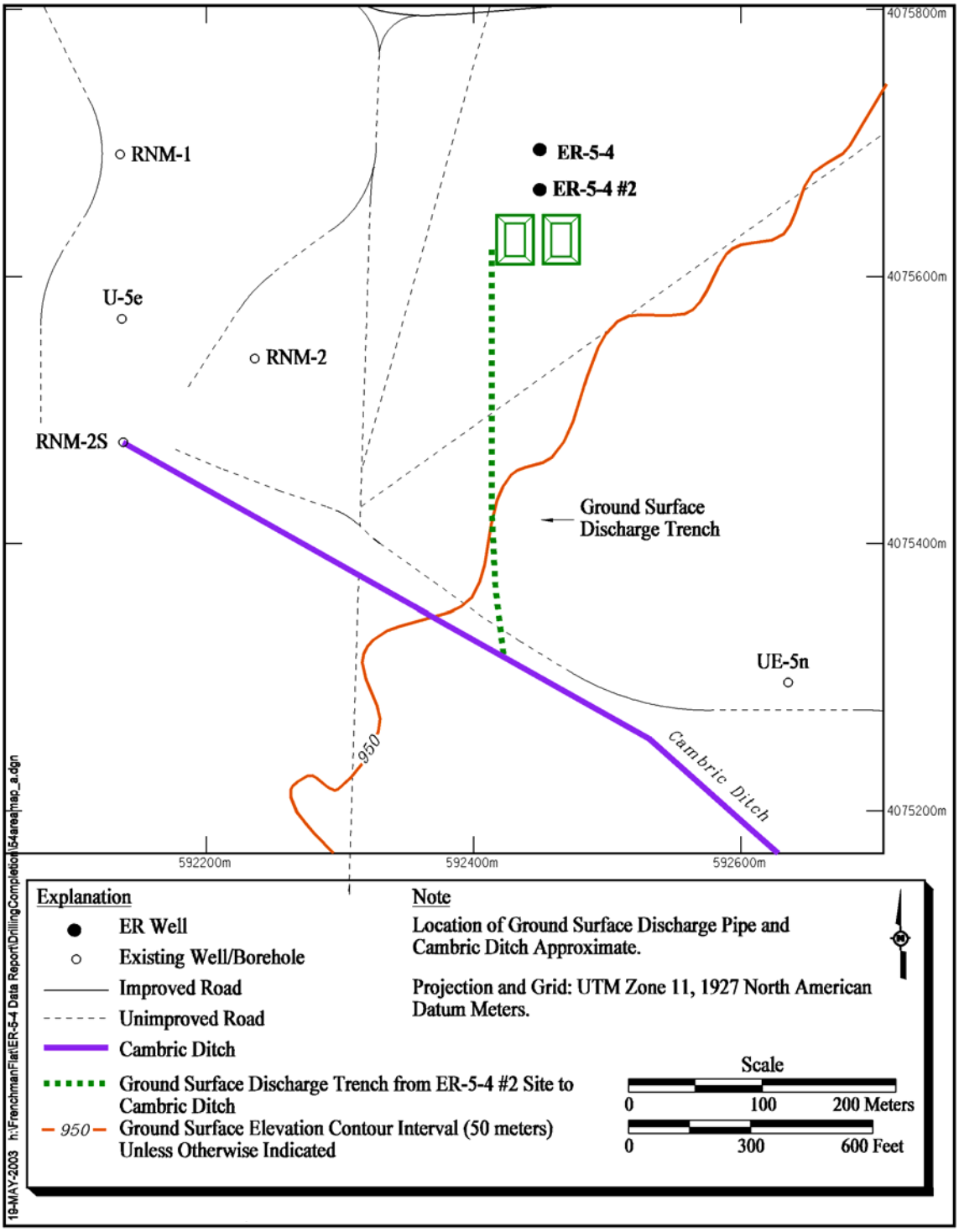

Figure 1-5
Detailed Map of Well Cluster ER-5-4

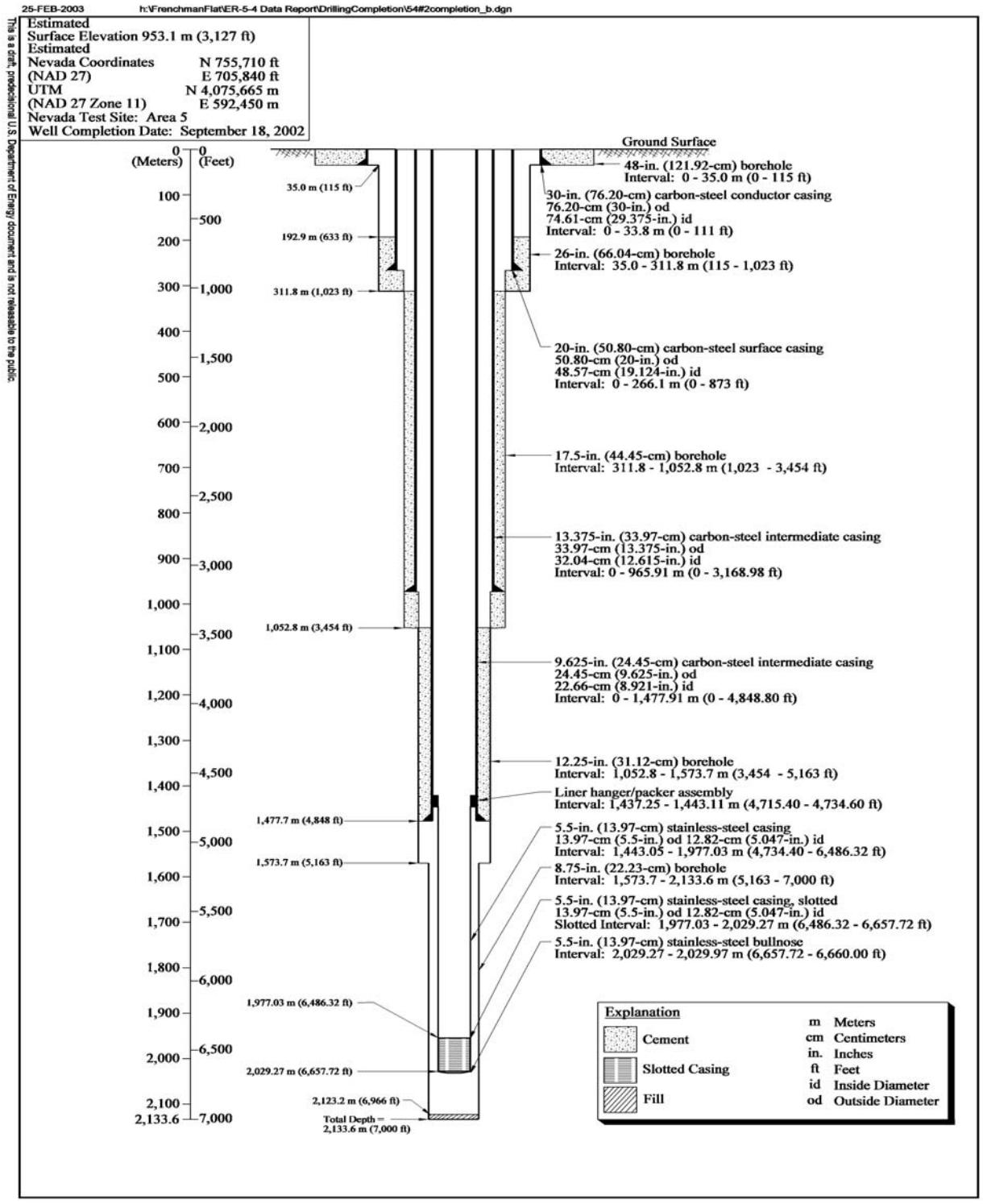

Figure 1-6
Well ER-5-4#2 Completion Diagram

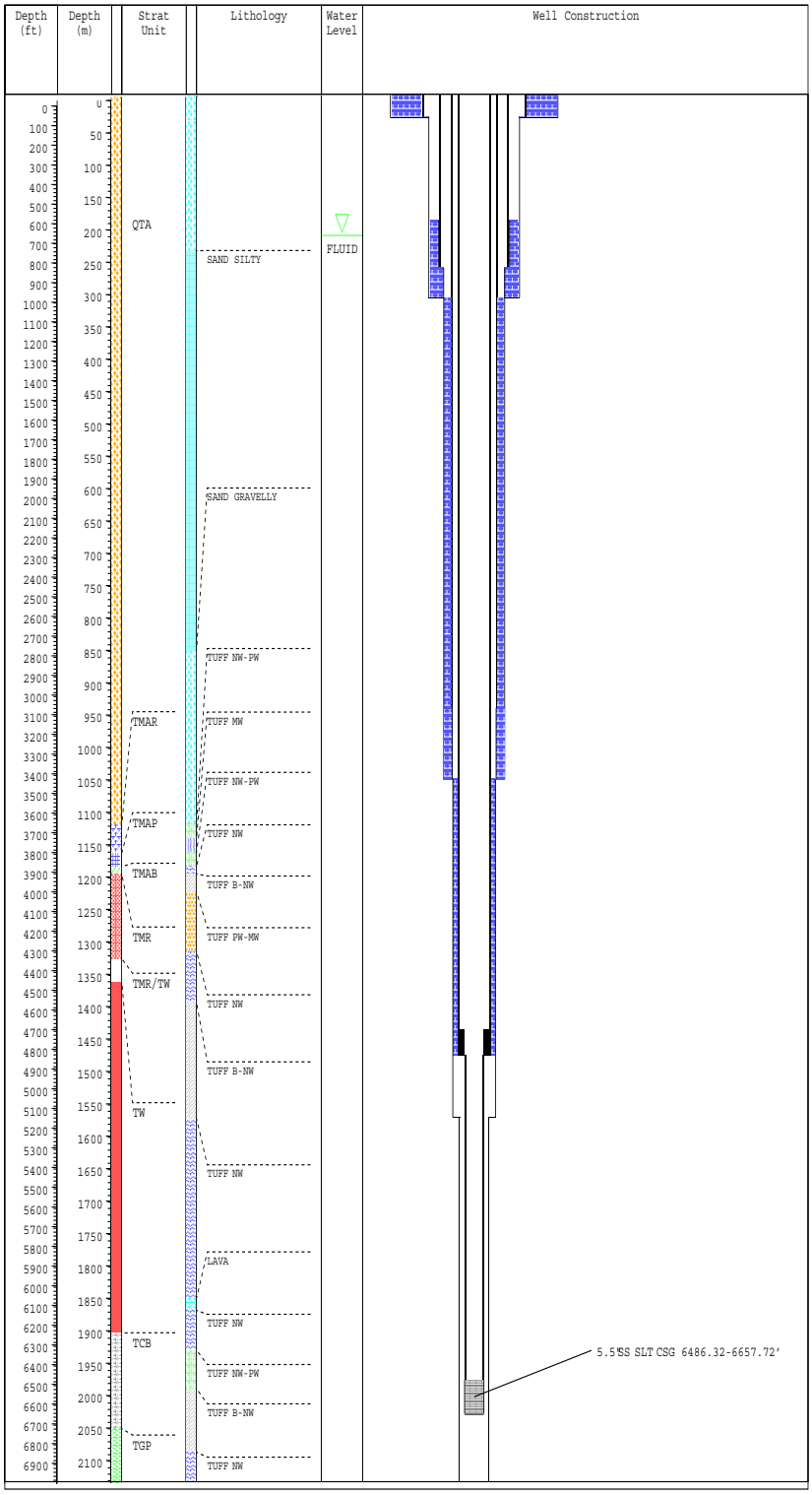

Figure 1-7
Well ER-5-4#2 Lithologic Log

Table 1-3
Summary of work performed at Well ER-5-4#2

Activity	Start Date	Finish Date	Duration in Days
Site mobilization activities	9/29/2002	10/15/2002	17
Predevelopment water-level monitoring	9/29/2002	10/14/2002	15
Install access line, and check pump functionality	10/15/2002	10/18/2002	3.5
Develop well and conduct step-drawdown testing	10/19/2002	10/25/2002	7
Conduct stressed flow logging and collect discrete depth samples. Attempt to troubleshoot pump problems	10/26/2002	10/30/2002	5
Remove and replace pump, and check new pump functionality, install check valve, and shutdown pump	10/31/2002	11/07/2002	8
Monitor water-level recovery (pretest conditions)	11/07/2002	11/12/2002	5
10-day constant-rate test	11/12/2002	11/23/2002	12
Monitor water-level recovery, remove PXDs	11/24/2002	12/02/2002	9
Trip out pump assembly and access line. Perform thermal flow and chemistry tool logging under ambient conditions.	12/02/2002	12/05/2002	4
Wellbore survey	12/06/2002	12/06/2002	1
Install low-volume sampling pump, functionality test	12/09/2002	12/12/2002	4
Demobilize	12/13/2002	12/14/2002	2

PXD = Pressure transducer

are: the RNM-2s nested outer west piezometer; RNM-2 (314 ft east); RNM-1 (707 ft north); ER-5-4#2 (1,141 ft east); ER-5-4 upper and lower completion zones (1,192 ft east); the ER-5-4 nested piezometer; UE-5n (1,735 ft southwest); ER-5-3#3 (3.8 miles north); and TW-3 (9.2 miles east). Well ER-5-4 was equipped with a bridge plug during the MWAT permitting separate hydraulic monitoring of the upper and lower completion zones. A summary of the well coordinate locations and distances from RNM-2s is presented in Table 1-1.

Well surface elevations and the HSUs accessed are also provided in Table 1-1. All wells with the exception of ER-5-4#2 and TW-3 are completed in the AA. The AA extends from ground surface to about 3,676 ft bgs. ER-5-4#2 is completed in the LTCU, and TW-3 is completed in the LCA. Table 1-4 provides further details on the hydrostratigraphy tested in each well. Table 1-5 explains the nomenclature referenced in Table 1-4. Well construction diagrams for RNM-2s, RNM-2, RNM-1, and ER-5-3#3 are shown in Figure 1-8 through Figure 1-11, respectively. Construction diagrams for UE-5n and TW-3 were not available during preparation of the report and are not provided. However, principal construction elements for each well, including UE-5n and TW-3, are summarized in Table 1-6.

Table 1-4
Hydrostratigraphy for Wells and Underground Tests Near RNM-2s
(Page 1 of 2)

Well	Top Depth[1] (Feet)	Elevation[2] (Feet)	Total Depth[3] (Feet)	Lithology[4]	Major Alteration[4]	Stratigraphy[4]	HGU[5]	HSU[6]
RNM-2s	0.0	3,133.0	1,156.0	AL	CC	QTa	AA	AA
RNM-2	0.0	3,132.0	935.0	AL	CC	QTa	AA	AA
RNM-1[7]	0.0	3,136.0	1,302.0	AL	CC	QTa	AA	AA
ER-5-4 #2	0.0	3,131.7	7,000.0	AL	CC/ZE	QTa	AA	AA
ER-5-4 #2	2,312.0	819.7		P	CC	QTp	PCU	PCU1U
ER-5-4 #2	2,940.0	191.7		AL	CC	QTa	AA	AA1
ER-5-4 #2	3,676.0	-544.3		PWT	DV/GL/ZE	Tma	VTA	TM-WTA
ER-5-4 #2	4,306.0	-1,174.3		PWT	GL	Tmr	WTA	TM-LVTA
ER-5-4 #2	4,472.0	-1,340.3		NWT/BED	ZE	Tw	TCU	LTCU
ER-5-4	0.0	3,131.7	3,732.0	AL	CC	QTa	AA	AA
ER-5-4	2,312.0	819.7		P	CC	QTp	PCU	PCU1U
ER-5-4	2,940.0	191.7		AL	CC	QTa	AA	AA1
ER-5-4	3,670.0	-538.3		PWT	DV	Tma	WTA	TM-WTA
UE-5n	0.0	3,112.0	1,687.0	AL	CC	QTa	AA	AA
ER-5-3 #3	0.00	3,334.3	1,800.0	AL	CC/ZE	QTa	AA	AA
ER-5-3 #3	610.0	2,724.3		AL	CC	QTa	AAA	OAA1
ER-5-3 #3	910.0	2,424.3		BS	DV	Tybf	LFA	BLFA
ER-5-3 #3	950.0	2,384.3		AL	CC/ZE	QTa	AAA	OAA
TW-3	0.00	3,477.0	1,860.0	AL	CC	QTa	AA	AA
TW-3	157	3,320.0		LS		Op	CA	LCA
UE-5 PW-1	0.0	3,180.0	839.0	AL	CC	QTa	AA	AA
UE-5 PW-2	0.0	3,248.0	919.5	AL	CC	QTa	AA	AA
UE-5 PW-3	0.0	3,298.0	955.0	AL	CC	QTa	AA	AA
UE-5 PW-3	617.0	2,681.0			CC	Tma	WTA	TM-WTA
UE-5c WW	0.0	3,216.0	2,682.0	AL		QTa	AA	AA
UE-5c WW	1,350.0	1,866.0		NWT		Tw	TCU	LTCU
WW-5B	0.0	3,092.0	900.0	AL		QTa	AA	AA
WW-5B	57.0	3,035.0		P	CC	QTp	PCU	PCU2T
WW-5B	432.0	2,660.0		AL		QTa	AA	AA
WW-5C	0.0	3,081.0	1,200.0	AL		QTa	AA	AA
WW-5C	10.0	3,071.0		P	CC	QTp	PCU	PCU2T
WW-5C	732.0	2,349.0		AL	CC/QZ	QTa	AA	AA
WW-5A	0.0	3,093.0	910.0	AL	CC	QTa	AA	AA3
WW-5A	80.0	3,013.0		P	CC	QTp	PCU	PCU2T
WW-5A	550.0	2,543.0		AL	CC	QTa	AA	AA

Table 1-4
Hydrostratigraphy for Wells and Underground Tests Near RNM-2s
(Page 2 of 2)

Well	Top Depth[1] (Feet)	Elevation[2] (Feet)	Total Depth[3] (Feet)	Lithology[4]	Major Alteration[4]	Stratigraphy[4]	HGU[5]	HSU[6]
U-5e	0.0	3,137.0	1,000.0	AL		QTa	AA	AA
U-5b	0.0	3,095.0	675.0	AL		QTa	AA	AA
U-5a	0.0	3,086.0	628.0	AL	CC	QTa	AA	AA

Lithology:
AL - Alluvium
BS - Basalt
BED - Bedded tuff
LS - Limestone
NWT - Nonwelded tuff
P - Playa
PWT - Partially welded tuff

Major Alteration:
CC - Calcite
DV - Devitrified
GL - Vitric
QZ - Silicic
ZE - Zeolitic

Notes:
1-Top Depth - Distance from ground surface to top of unit
2-Top Elevation - Elevation above mean sea level
3-Total depth of borehole below ground level
4-Lithology, major alterations, and stratigraphy compiled from Drellack (2004) and well-specific completion reports
5-HGU - Hydrogeologic unit (reference Table 1-5)
6-HSU - Hydrostratigraphic unit (reference Table 1-5)
7-RNM-1 is a slant-angle well deviated 21 degrees from vertical. Total depth is measured depth rather than true vertical depths.

1.3.1 Summary of Field Operations and Measured Well-Test Data

Objectives of the RNM-2s MWAT (Section 1.0) were achieved by constant-rate pumping of RNM-2s for a period of 75 days and monitoring formation responses in RNM-2s and the nine observation wells before, during, and after pumping. Table 1-7 summarizes the RNM-2s field activities. Operations generally proceeded as scheduled with minor interruptions during production. The pump shut down twice during production due to power problems and was restarted after approximately one hour each time. The pump was stopped a third time when maintenance was performed on the RNM-2s piezometer. The pump was restarted after approximately 2.5 hours.

Clear responses to the test are observed in the pumping well (RNM-2s), RNM-2, RNM-1, and the ER-5-4 upper completion zone. Although the RNM-2s outer piezometer shows a response, it is inconsistent with expectations and differs from what has been recorded during previous studies. Monitoring records for ER-5-4#2, the ER-5-4 lower completion zone, ER-5-3#3, TW-3, and UE-5n appear good, but do not indicate a response to pumping.

In general, recovery records show that well formation pressures approach the static formation pressure after turning off the pump at RNM-2s; however, none of the records show complete recovery. Many of the wells appear to be equilibrating to a post-production water level lower than the preproduction water level. In the case where well completion zones intersect or are near to the water table, recovery to an equilibrium water level would take months. Insufficient pre- and post-test

Table 1-5
Hydrostratigraphic Units of the Frenchman Flat Hydrostratigraphic Framework

Hydrostratigraphic Unit	Dominant Hydrogeologic Unit(s)	Stratigraphic Unit Map Symbols	General Description
alluvial aquifer (AA, AA1, AA2, AA3) (this term is also used to designate a hydrogeologic unit)	AA	Qay, QTc, Qai, QTa, Tt	Consists mainly of alluvium that fills extensional basins. Also includes generally older Tertiary gravels and very thin air-fall tuffs.
playa confining unit (PCU2T)	PCU	Qp	Clayey silt and sandy silt. Forms Frenchman Flat playa (dry lake).
basalt lava flow aquifer (BLFA)	LFA	Tybf	Several (possibly dissected) basalt flows recognized in the middle of the alluvial section of northeastern Frenchman Flat. Related to other basalt flows in Nye Canyon.
older altered alluvial aquifer (OAA, OAA1)	AAA	QTa	Older, denser, zeolitized alluvium recognized only in northern Frenchman Flat.
older playa confining unit (PCU1U)	PCU	QTp	Deep, subsurface playa deposits in the deepest portion of Frenchman Flat. Recognized in ER-5-4 #2 and with 3-D seismic data.
Timber Mountain - welded tuff aquifer (TM-WTA)	Mostly WTA, minor VTA	Tma, Tmab, Tmr	Consists mainly of extra-caldera welded ash-flow tuffs of Ammonia Tanks Tuff and Rainier Mesa Tuff. Unit occurs mostly in north and central Frenchman Flat. Prolific aquifer when saturated.
Timber Mountain - lower vitric tuff aquifer (TM-LVTA)	VTA	Tma, Tmab, Tmr, Tmrh, Tp, Th	Defined to include all unaltered (nonzeolitic), nonwelded, and bedded tuffs below the welded Tmr and above the level of pervasive zeolitization. The presence of the welded Tpt (see Tsa) complicates this general description.
upper tuff confining unit (UTCU)	TCU	Tmr (lower most), Tmrh, Tp	Relatively thin TCU above the TSA. Grouped with the LTCU where the TSA is not present.
Topopah Spring aquifer (TSA)	WTA	Tpt	The welded ash-flow lithofacies of the Topopah Spring Tuff in Massachusetts Mountain/French Peak area and north-central Frenchman Flat.
lower vitric tuff aquifer (LVTA)	VTA	Th	Relatively thin VTA unit below the TSA. Grouped with the TM-LVTA where TSA is not present.
lower tuff confining unit (LTCU, LTCU1)	TCU, minor WTA	Th, Tw, Tc, Tn, To	Generally includes all the zeolitic nonwelded and bedded tuffs in southeastern NTS. May include all units from base of Tmr to top of Paleozoic-age rocks.
Wahmonie confining unit (WCU)	TCU, minor LFA	Tw (Twu, Twm, Twl, Twls)	Mixture of lava flows, debris flows, lahars, ash-flows, and air-falls. Typically zeolitic, argillic, or hydrothermally altered. Grades/interfingers laterally with the LTCU.
volcaniclastic confining unit (VCU)	TCU, minor AA and CA	Tgp, Tgw	Older Tertiary sedimentary rocks of variable lithologies including silts, clays, limestones, gravels, and tuffaceous units. Present in southeastern half of Frenchman Flat.
lower carbonate aquifer (LCA)	CA	Dg through Cc	Cambrian through Devonian mostly limestone and dolomite. Regional carbonate aquifer present throughout the model area.

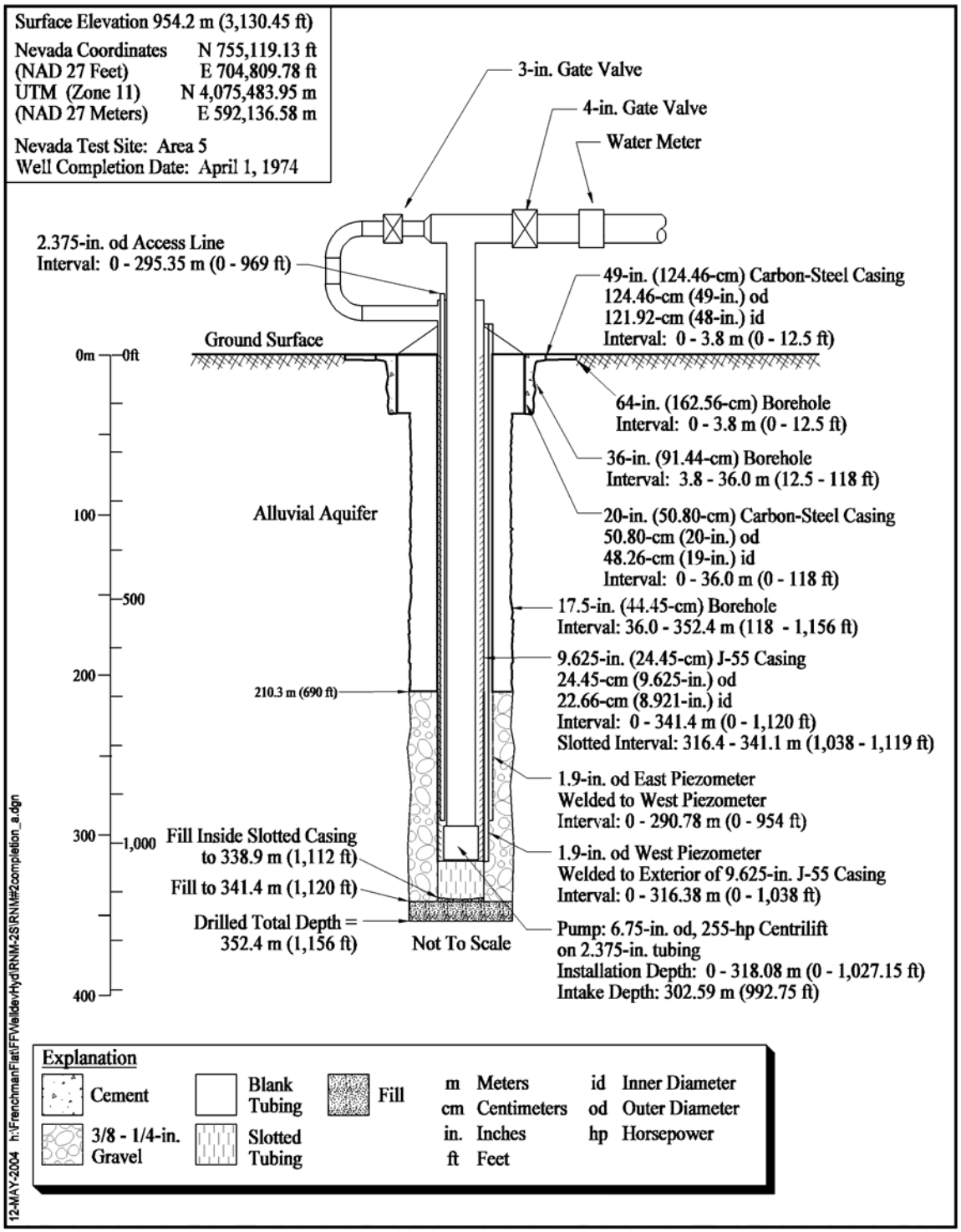

Figure 1-8
Well RNM-2s Completion Diagram

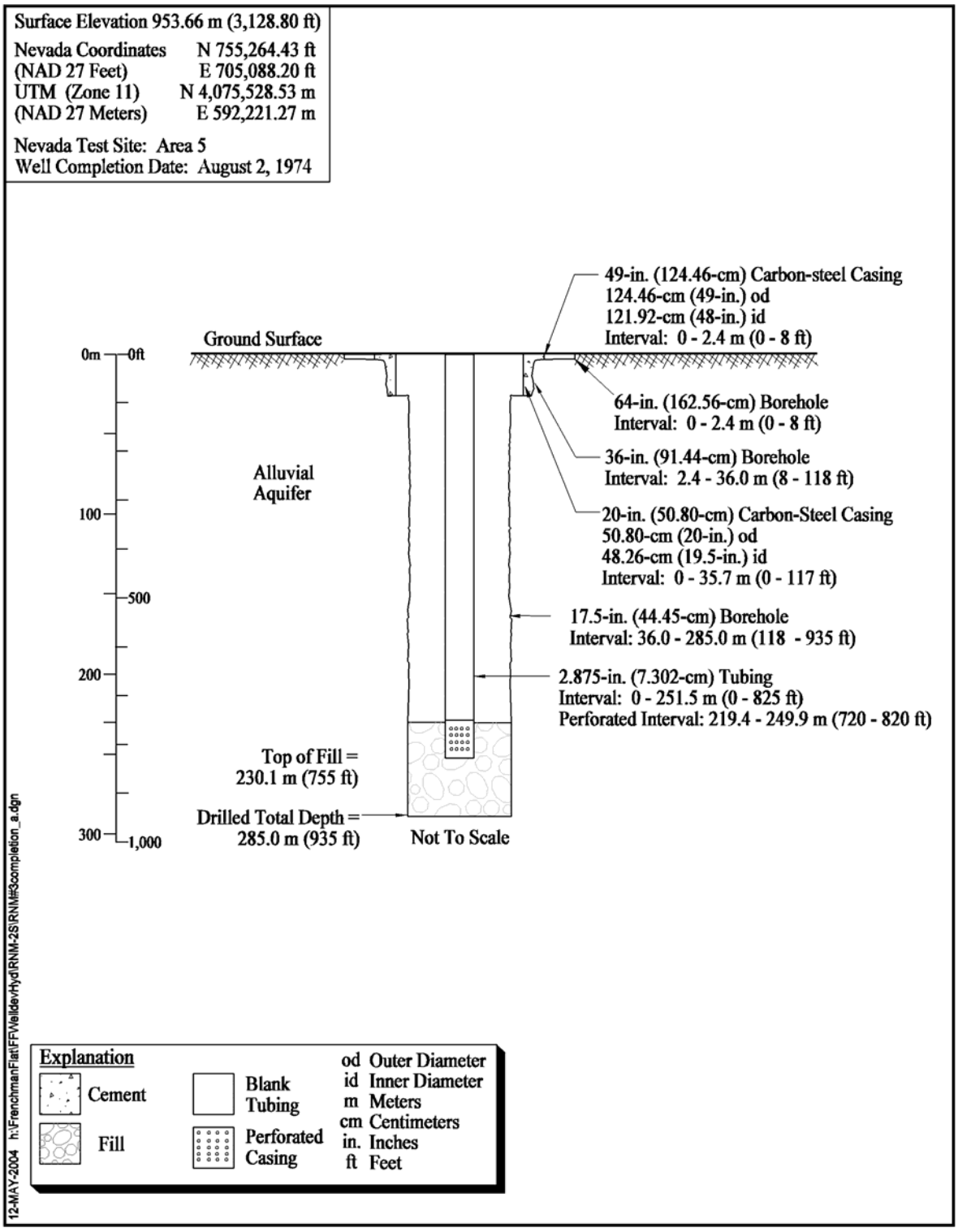

Figure 1-9
Well RNM-2 Completion Diagram

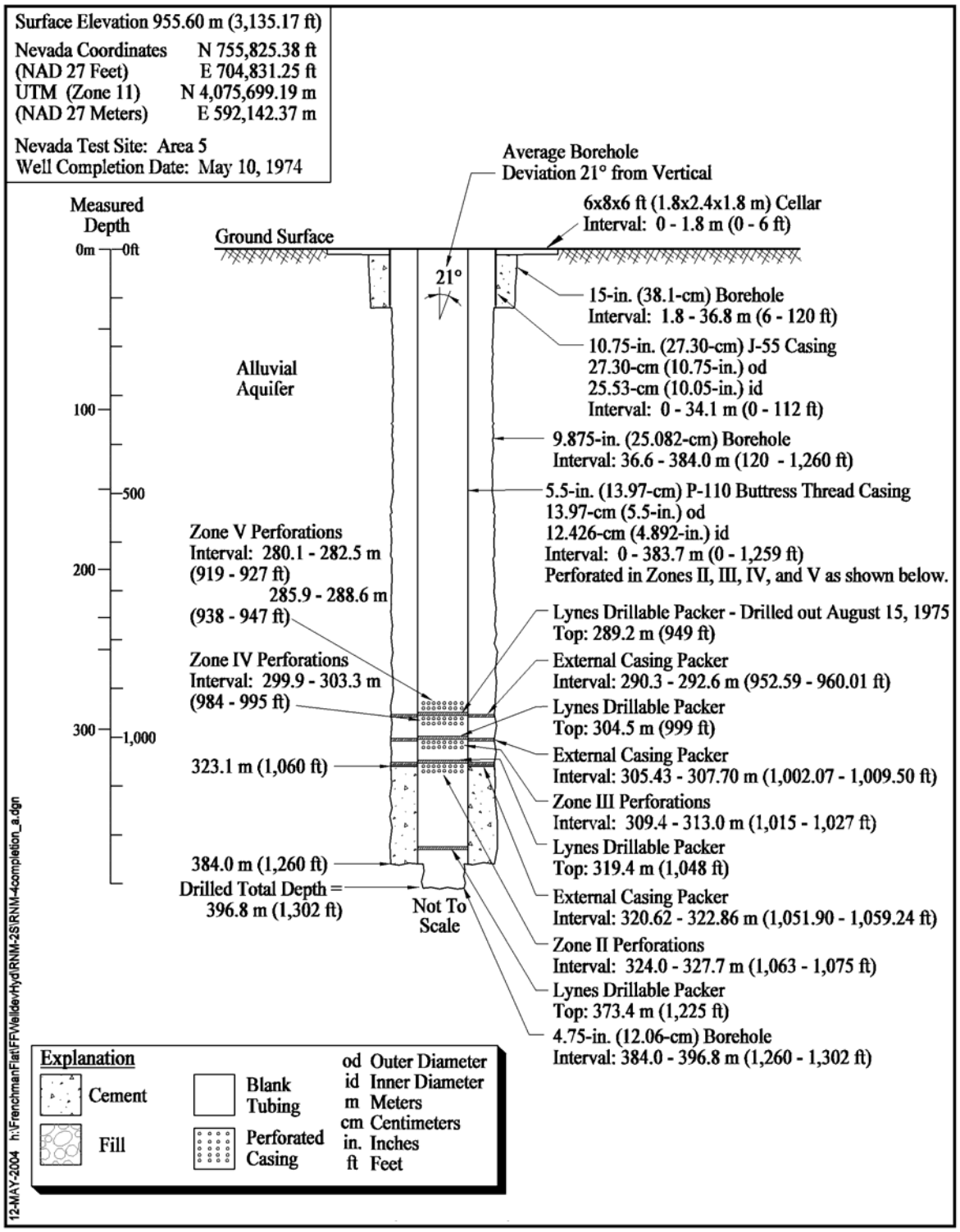

Figure 1-10
Well RNM-1 Completion Diagram

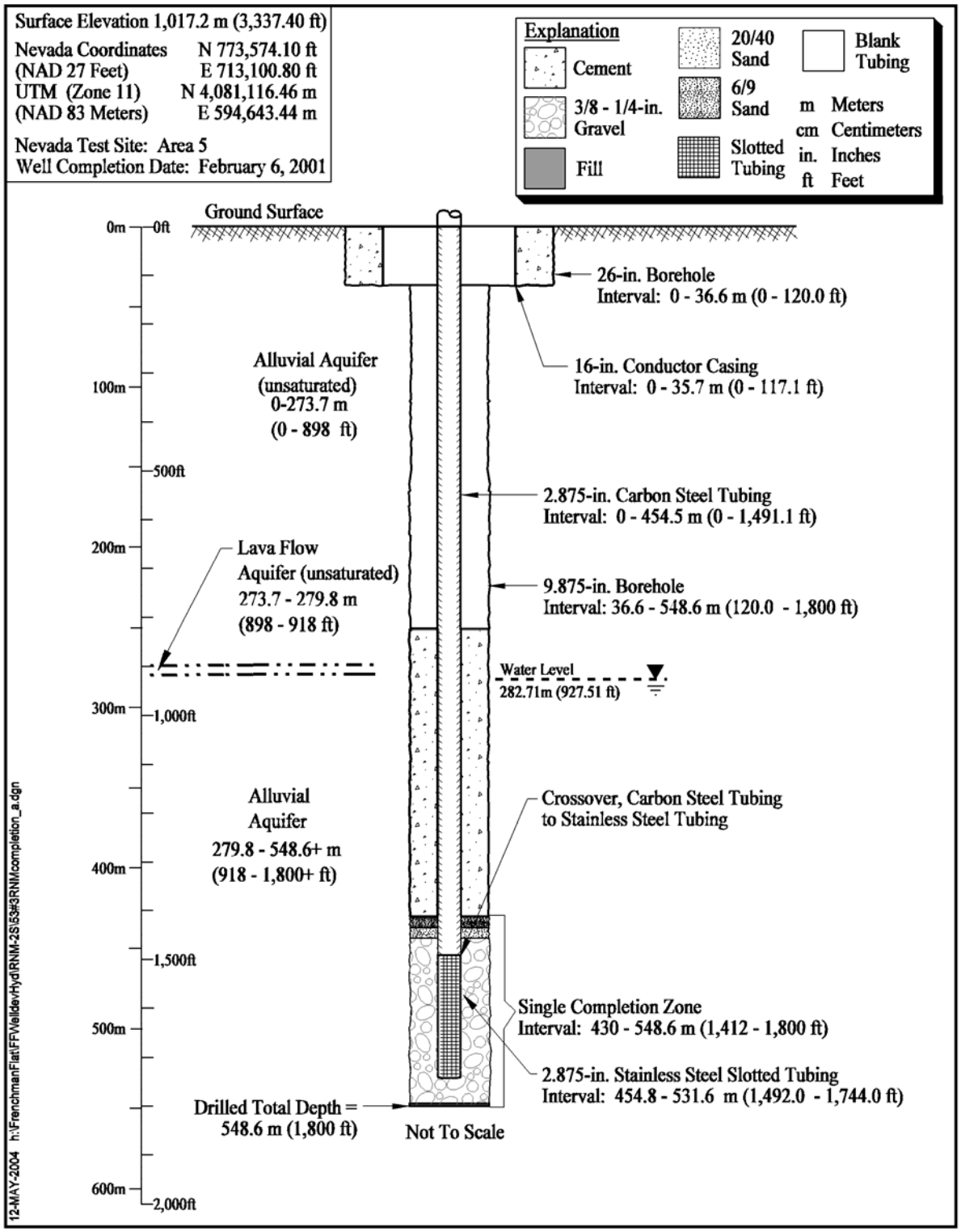

Figure 1-11
Well ER-5-3#3 Completion Diagram

Table 1-6
Well Construction Data for RNM-2s MWAT Wells

Well	Ground Surface Elevation (ft amsl)	Drilled Depth (ft bgs)	Cased Depth (ft bgs)	Gravel Pack (ft bgs)	Perforations (ft bgs)	Notes
RNM-2s	3,130.45	1,156	1,120	690 - 1,120	1,038 - 1,119	Fill below casing, open borehole above gravel pack
RNM-2s Access Line	3,130.45	1,156	969	690 - 1,120	NA	Open-ended tubing
RNM-2s Outer West Piezometer	3,130.45	1,156	1,038	690 - 1,120	NA	Open-ended tubing, obstruction at 994 ft bgs
RNM-2	3,128.80	935	825	NA	720 - 820	Fill to 755 ft bgs
RNM-1 (Slant-Angle Well)	3,135.17	935.51	935.51	NA	857.96 - 865.43 875.70 - 884.10 918.64 - 928.91	True vertical depths to top of second external packer
ER-5-4 #2	3,131.70	7,000	6,660.00	NA	6,486.32 - 6,657.72	Open annulus below 4,848 ft bgs to 6,966 ft bgs
ER-5-4 Upper Zone	3,131.70	3,732	3,438.31	1,745 - 2,192	1,769.95 - 2,113.38	Bridge plug in main casing at 2,290 ft bgs during test
ER-5-4 Lower Zone	3,131.70	3,732	3,438.31	3,014 - 3,595	3,136.25 - 3,350.12	Bridge plug in main casing at 2,290 ft bgs during test
ER-5-4 Piezometer	3,131.70	813.94	813.94	NA	722.55 - 812.84	Located in main well annulus above cement seal
UE-5n	3,113.36	1,687	1,523	NA	720 - 730	Cemented at bottom, obstruction at 1,184 ft bgs
ER-5-3 #3	3,337.40	1,800	1,744	1,412 - 1,800	1,492 - 1,744	Gravel-packed completion
TW-3	3,484.12	1,860	1,356	NA	NA	Open hole
UE-5c WW	3,216.27	2,682	1,682	NA	1,100 - 1,682	Open annulus
WW-5B	3,093.27	900	900	NA	687 - 900	Open interval 687 - 900 ft bgs
WW-5C	3,083.09	1,200	1,200	NA	887 - 1,189	Open interval 887 - 1,189 ft bgs
WW-5A	3,093.73	910	877	NA	697 - 877	Open interval 697 - 877 ft bgs

ft bgs - Feet below ground surface
amsl - Above mean sea level
NA - Not applicable

data were obtained to confirm whether this was the case, or whether a declining background water-level trend in the region was occurring through the testing and recovery period.

The short duration of the pretest monitoring period (Table 1-7) also resulted in insufficient ambient monitoring data to assess barometric efficiency (BE) for each well. However, the correction for BE is generally not important to define a good record for interpretation of hydraulic parameters because responses are substantially larger than barometric corrections.

Also important to note is that the distance-drawdown relationship for the maximum time of pumping indicates heterogeneous or anisotropic hydraulic conductivity, both horizontally and vertically in the AA. There are drawdown

Table 1-7
Summary of RNM-2s MWAT Activities

Activity	Start Date	Finish Date
Install PXDs in observation wells.	4/10/2003	4/25/2003
Install bridge plug with PXDs in ER-5-4.	4/17/2003	4/17/2003
Test function of RNM-2s pump.	4/21/2003	4/21/2003
Start RNM-2s MWAT: begin pumping and monitoring responses in observation wells.	4/26/2003	7/10/2003
Pump stops, restarted ~ 1-hour later.	4/29/2003	4/29/2003
Pump stops, restarted ~ 1-hour later.	5/13/2003	5/13/2003
Pump stopped for 2.5 hours.	6/6/2003	6/6/2003
Pumping stopped. Monitoring recovery in observation wells begins.	7/10/2003	Through PXD removal dates shown below
Remove PXD from ER-5-3#3.	7/21/2003	7/21/2003
Remove PXDs from remaining observation wells.	9/10/2003	9/13/2003
Remove bridge plug from ER-5-4.	9/10/2003	9/24/2003
Install dedicated sampling pump in ER-5-4.	9/25/2003	9/25/2003
Demobilize.	9/26/2003	9/29/2003

MWAT - Multi-well aquifer test
PXD = Pressure transducer

values for three distances from RNM-2s (314 ft to RNM-2, 707 ft to RNM-1, and 1,192 ft to ER-5-4), and the respective maximum drawdowns for each distance are similar (3.5, 3.9, and 3.8 ft).

1.4 Document Organization

The document is organized into five main sections. Section 1.0 presents the introduction to the development and testing of wells within Well Cluster RNM-2s. Section 2.0 describes the hydraulic tests conducted at each well and presents the methods of data preparation for their use in subsequent analysis and interpretation. The analysis and interpretation of the hydraulic data are presented in Section 3.0, which primarily includes the hydraulic property estimation of the HSUs tested. The analyses are complete with an uncertainty analysis of hydraulic property estimates. Section 4.0 presents a summarized interpretation of the single-well tests conducted at ER-5-4 and ER-5-4#2, and the RNM-2s MWAT. A comprehensive summary table of hydraulic property estimates, at each well and for each HSU tested, is presented. Section 4.0 also includes a comparison of results with those derived from an independent analysis of the RNM-2s MWAT that was performed by the USGS in *USGS Memorandum from M. Pavelko and K. Halford to D. Galloway.* A copy of the memorandum is attached as Appendix A.

2.0 Description of Hydraulic Testing

The hydraulic testing activities and testing data collected at wells within the RNM-2s well cluster are presented in this section. The quality of the measured data is assessed, relative to their use in subsequent interpretation and analyses, and corrective measures are described when appropriate.

In general, a well-test analysis consists of the interpretation of the formation pressure response, over some depth-interval of contributing formation, to well production. The measured drawdown in the well, in response to well production or recovery, often contains components that are not attributed to the formation response alone. These primarily include barometric effects, well loss, and thermal volume effects of groundwater in the well. The influence of each of these factors on the measured response is assessed in this section. Further, the formation thickness, or depth interval of the formation that contributes groundwater to the well, is identified for each well when possible. Altogether, this section presents the testing data and their preparation for interpretation and analysis in Section 3.0.

2.1 Well ER-5-4 Single-Well Test

Measurement of hydraulic data at Well ER-5-4 during ambient and pumping wellbore conditions included water-level measurements from the predevelopment through testing period, two step-drawdown tests, flow logging under ambient and pumping conditions, a constant-rate production test in the main completion, and a slug test of the piezometer string. This section presents these data and reduces them for analysis and interpretation.

2.1.1 Depth-to-Water Measurements and Hydraulic Gradients

The discrete intervals of blank and slotted casing in the Well ER-5-4 completion permit the measurement of three different formation intervals of the AA HSU. The piezometer casing is slotted from 723 to 813 ft bgs. The main completion casing is slotted over two intervals, between 1,170 and 2,113 ft bgs, and between 3,136 and 3,350 ft bgs. Water levels in the production string represent a composite of both completion intervals (Figure 1-3); those in the piezometer are representative of a single completion.

Depth-to-water measurements for the Well ER-5-4 production string and piezometer are presented in Table 2-1. Measurements prior to May 24, 2001, represent predevelopment conditions. Measurements on or after July 10, 2001, represent well conditions after recovery from the constant-rate pumping test, although recovery may not have been fully completed. Similarly, measurements

Table 2-1
Well ER-5-4 Depth-to-Water Measurements

Date	Time	Depth-to-Water (bgs)		Barometric Pressure (mBar)	Head[a]	
		Feet	Meters		Feet	Meters
Well ER-5-4 Production String						
5/4/2001	14:45	728.37	222.01	906.20	2,398.63	731.10
5/6/2001	08:45	728.31	221.99	908.20	2,398.69	731.12
5/9/2001	09:08	728.15	221.94	905.60	2,398.85	731.17
5/13/2001	08:48	730.52	222.66	908.70	2,396.48	730.45
5/15/2001	14:26	730.19	222.56	906.10	2,396.81	730.55
6/5/2001	11:43	725.89	221.25	902.08	2,401.11	731.86
6/8/2001	09:13	737.97	224.93	906.86	2,389.03	728.18
6/21/2001	11:20	733.10	223.45	910.00	2,393.90	729.66
7/10/2001	13:23	727.66	221.79	905.74	2,399.34	731.32
Well ER-5-4 Piezometer						
5/6/2001	08:25	722.95	220.36	908.20	2,404.05	732.75
5/9/2001	09:28	723.57	220.54	905.40	2,403.43	732.57
5/13/2001	09:03	724.04	220.69	908.70	2,402.96	732.42
5/15/2001	14:48	724.23	220.75	906.10	2,402.77	732.36
6/5/2001	16:00	725.05	221.00	900.82	2,401.95	732.11
7/10/2001	10:43	725.85	221.24	906.82	2,401.15	731.87
7/16/2001	10:53	725.19	221.04	901.72	2,401.81	732.07
7/16/2001	15:31	725.43	221.11	900.99	2,401.57	732.00

[a]Reference Datum: meters (feet) above mean sea-level datum
bgs - Below ground surface
mbar - Millibar

collected during development and testing activities may not be representative of static and equilibrium conditions.

It is uncertain whether any of the production well depth-to-water measurements are representative of the SWL. Following installation of the testing pump and access line in ER-5-4, PXDs were installed in the access line and the piezometer. The water levels (and barometric pressure) were measured for a period of five days, in part to test for and measure the static, equilibrium water level. Figure 2-1 shows the predevelopment water-level monitoring during this period. Static conditions were not achieved; it appears that the water level was slowly recovering from completion activities. Therefore, the Well ER-5-4 SWL was not measured during the period from predevelopment through recovery from testing.

It was anticipated that the vertical hydraulic gradient within the completed section of the AA could be estimated from a comparison of water-level measurements between the main string and piezometer string. Unfortunately, it was discovered following the testing period that the piezometer was plugged with drilling fluid

through development and testing. As would be expected given this observation, the piezometer water level did not respond to production in the main completion through well development and testing.

The vertical hydraulic gradient was not discernible from water-level measurements in the main completion because the water level is representative of the composite formation head at the upper and lower slotted casing intervals. However, as part of the RNM-2s MWAT conducted in FY 2003, a bridge plug was installed in the Well ER-5-4 main completion at 2,290 ft bgs, isolating the upper and lower slotted casing intervals. Completion pressures, measured using *in situ* pressure transducers located in both isolated completion intervals, were recorded from April 17, 2003 (Julian Day [JD] 107) through September 24, 2003 (JD 267). After pressure equilibration following the setting of the bridge plug, a pressure differential of 1.723 pounds per square inch (psi) was measured between the upper and lower (upper minus lower) completions. The transducers have rated measurement accuracies of 0.025 percent of full scale (827 pounds per square inch gauge [psig]) with a precision of 0.01 percent. The maximum possible combined measurement error between the transducers is 0.414 psi; therefore, the 1.723 psi pressure differential is significant. Conversion of pressure to head, incorporating groundwater density as a function of temperature, corresponds to a head differential of 3.99 ft. Relative to the midpoints of the upper and lower slotted casing intervals, measured respectively at 1,941.67 and 3,243.19 ft bgs, the downward vertical gradient is 0.0031. This result is discussed further, in context to the local hydrogeology at a larger spatial (well cluster) scale, in Section 4.1.

2.1.2 Constant-rate Test

A constant-rate pumping test was conducted at Well ER-5-4 following well development to collect hydraulic response data for determination of AA hydraulic properties. Prior to the test, the water level in the access line and the piezometer were monitored to observe recovery from development pumping to the static formation pressure under ambient conditions, and to establish baseline pretest conditions. Pumping for the test commenced on June 26, 2001 (JD 177), and continued without interruption until the pump was turned off on July 5, 2001 (JD 186), ten days later. Prior to ending the constant-rate test, composite groundwater samples were collected at the wellhead sampling port. In addition to providing data for determining hydraulic parameters, the pumping during the constant-rate test served to continue and complete the development process to restore natural groundwater quality for sampling purposes. The recovery of the well was monitored for an additional five days to July 10, 2001 (JD 191).

2.1.2.1 Measured Formation Response

A continuous data logger record was captured for the PXD pressure and temperature in both strings (main completion access line and piezometer string), the barometric pressure, and the production rate during the constant-rate test. Water quality was monitored during the constant-rate test with the in-line system and from field analyses of grab samples that were taken about every two hours during day shifts.

A pumping rate of 160 gallons per minute (gpm) was chosen as the optimal rate for the test. This pumping rate was less then the maximum rate of 175 gpm used during the development phase, but provided continued development of both completion zones. A 0 to 50 psig PXD was installed in the access line on June 21, 2001 (JD 172), at a calculated set depth of 868.44 ft bgs. The PXD in the piezometer string was not removed during development; the installation set depth, 779.84 ft bgs, remained the same.

Figure 2-2 shows the ER-5-4 data logger record of the pumping rate and measured pressure in the access line during pretest (recovery from development) monitoring, the constant-rate test, and the recovery monitoring that occurred following the test. The piezometer did not respond to constant-rate production; those data are not shown. Well drawdown was still increasing in the access line at the end of the test at which time a drawdown of 117.48 ft was observed.

The following sections discuss the influence of and correction for barometric effects, well loss, and thermal volume effects on the measured formation pressure response. Although in some cases a measurement correction is not able to be performed, each is presented for completeness.

Barometric Effects

In an effort to determine the barometric efficiency in the production string, the predevelopment water-level monitoring record was reviewed. The following considerations were made to select the best possible record:

- The record should be sufficient to determine that the SWL is achieved and that the wellbore water column is in thermal equilibrium.
- A continuous barometric variation of 10 millibar (mbar) should be observed, a magnitude sufficiently large to distinguish the components of earth tides.
- The frequency of the barometric pressure variation should equal that of the fluctuations in the water level. Time lags in the measured formation pressure response indicate that other effects are occurring.

The attempts to derive barometric efficiency from the production string data were unsuccessful due to all three factors. Primarily, the predevelopment water-level record contained a distinct trend due to recovery from prior functional testing of the pump. Regardless, the magnitude of the barometric fluctuations is approximately 0.1 percent of the maximum drawdown observed during the constant-rate test and proves to be a negligible component.

Well Loss

The partitioning of the total measured drawdown into its components provides better understanding of the hydraulics of water production and more accurate estimates of formation properties. The drawdown observed in the well is comprised of aquifer drawdown and well losses that result from flow of water into

the well and up the well casing to the pump. Formation drawdown can be observed directly in observation wells near a pumping well; however, observation wells were not utilized during the ER-5-4 single-well test, and the shallow piezometer was plugged.

Two step-drawdown tests were performed during well development. It was anticipated that analyses of the test data be used to determine the laminar and turbulent components of drawdown. The laminar component of well drawdown is attributed to aquifer drawdown via Darcian flow. The turbulent component, considered well loss, is attributed primarily to wellbore skin losses and flow losses due to friction along the casing up the well. In other words, the drop in water level from increasing production rates is larger than would be expected from resistance to Darcian inflow from the formation alone. Turbulent head loss, both in the well and the near-well environment (e.g., gravel pack, formation skin, near-well fractures) are assumed to increase with the square of the pumping rate. Some researchers allow the power of the turbulent loss component to exceed two, reaching as large as three. However, in this analysis it is assumed that nonlinear well losses vary according to the second power of the production rate. Therefore, the Hantush-Bierschenk methodology (Kruseman and de Ridder, 1990) is applied to determine the component of drawdown that is well loss. The equation for drawdown with nonlinear well losses is given as:

$$S_w = BQ_n + CQ_n^2 \qquad (2\text{-}1)$$

where

S_w = the drawdown in the well

Q_n = the production rate at step *n*

B = the linear coefficient

C = the nonlinear coefficient

Dividing both sides of Equation 2-1 by Q_n produces an equation suitable for linear regression, providing the inverse solutions for the linear and nonlinear coefficients.

During the two step-drawdown tests, conducted on June 13 (JD 164) and June 15, 2001 (JD 166), the well was pumped for one hour at each of four progressively higher pumping rates. The approximate pumping rates were 70, 105, 140, and 175 gpm. The calculated drawdown values, respective of the time just prior to stepping up to the next highest rate, are presented in Table 2-2. A comparison between the two tests indicates that the well efficiency remained similar through the development period (i.e., surging of the well did not significantly improve the efficiency).

Application of the Hantush-Bierschenk method to the step-drawdown data resulted in a negative well loss coefficient (C). The method, applied to the data for the second step-drawdown test, is shown graphically in Figure 2-3. A negative

Table 2-2
Step-Drawdown Results for Well ER-5-4 Single-Well Test

Date of Step-Drawdown Protocol	Drawdowns at Pumping Rates (in feet)			
	70 gpm	105 gpm	140 gpm	175 gpm
6/13/01	53.49	72.28	98.97	123.54
6/15/01	53.43	76.52	99.46	122.37

Each pumping step lasted one hour. Readings of drawdown were taken at the end of each step.

well loss coefficient could indicate that the well efficiency improves with an increase in well production. This would result from a transient wellbore condition that reflects an increase in flow through the gravel pack (Figure 1-3) with an increase in production (i.e., improved borehole wall and well skin permeability). The negative well loss coefficient could also indicate that thermal volume expansion of the water column occurs as larger percentages of high temperature groundwater from the lower completion interval enter the well at the higher production rates. That is, the apparent improvement in well efficiency could reflect expansion of the water column. Regardless of the cause of the apparent increase in efficiency, a well loss correction is not applied to the measured formation pressure response at Well ER-5-4.

Temperature Effects

The transient borehole temperature profile through well production and recovery periods, coupled with the shallow placement of the pressure transducer in the wellbore, may have a considerable influence on the measured formation response to pumping. During pumping, higher temperature groundwater enters the wellbore from the formation and undergoes thermal volume expansion. Similarly, thermal volume contraction occurs during well recovery as the water column cools. The thermal effect on the measured pressure response can be particularly significant during early periods of pumping before the temperature profile in the water column becomes steady. During recovery, thermal effects persist for a longer duration than under pumping conditions, and end when the temperature profile cools to the equilibrium condition.

Conceptually, when thermal expansion of the water column occurs below the pressure transducer during a pumping (drawdown) period, the measured decrease in the pressure transient will be erroneously lowered, or slowed. That is, the water column below the transducer expands as the water level is coincidently lowered from pumping (assuming that the pumping rate exceeds the effect of thermal expansion). Once the temperature profile in the water column below the transducer achieves a steady-state during well production, volume expansion no longer affects the pressure measurement; the thermal expansion offset remains in the measured pressure response, but the rate of pressure change through time no longer reflects the influence of thermal expansion (or contraction). The pressure response reflects only the influence of well boundary conditions. Note that

thermal volume expansion that occurs above the transducer is invisible to the measurement; the resulting increase in water level is offset by the decrease in density.

In order to assess the influence of thermal volume expansion and contraction on the formation response to production and recovery through the constant-rate test, three critical datasets are necessary. These are the initial wellbore temperature profile prior to pumping (initial condition), the temporal rate of temperature change along the profile (transient condition), and the steady-state wellbore temperature profile that is achieved during constant-rate well production (steady condition).

Prior to the start of the constant-rate test, at the end of a five-day recovery period following development activities, the vertical wellbore temperature profile is assumed to correspond to the (near-) equilibrium condition. A near-equilibrium profile was logged on July 13, 2001 (JD 194), using the DRI ChemTool, eight days into the recovery period following completion of the constant-rate test. The profile is shown in Figure 2-4.

At the start of constant-rate test production on June 26, 2001 (JD 177), higher temperature formation groundwater entered the well through the lower and upper slotted casing intervals, from 3,136 to 3,350 ft bgs and from 1,770 to 2,113 ft bgs, respectively. The PXD was placed at 868 ft bgs. Therefore, a thermal volume-effect offset in the measured pressure response resulted from the expansion/contraction of groundwater that occurred over a 2,482-ft interval, the length between the PXD and bottom of the lower slotted completion interval. Through heating (and cooling) of the water column during production (and recovery), the PXD temperature provides the only temporal measurement of the transient temperature profile. Although the transient profile reflects the temperature variation at the PXD set depth, it is assumed that the time-rate of temperature change along the entire wellbore is equal to that measured at the PXD depth.

The steady temperature profile attained during the constant-rate test is assumed to follow a trend equivalent to the profile logged on June 19, 2001 (JD 170) during an impeller flow-log survey. This was the final log run over a two-day period of nearly continuous pumping. The temperature profile was measured from 1,610 to 3,360 ft bgs. Recall that the PXD was set at 868 ft bgs. Although the log was discontinued above 1,610 ft because the pump intake was set directly above at 1,592 ft bgs, the stainless steel pump string runs across the full extent of the interval between the top of the temperature log (1,610 ft) and the PXD (868 ft). It is well known that the temperature of the water column in the casing that is adjacent to the access line approaches a uniform temperature during well production, equal to the temperature of the access line that is heated by both the pump and inflowing groundwater. The steady PXD temperature is used to define this uniform temperature (83°F). The full extent of the steady-state wellbore temperature profile achieved during production is shown in Figure 2-4.

To correct the measured formation pressure response for thermal effects, the equilibrium (initial condition) and steady-state temperature profiles, for the

interval between the PXD and lower end of the slotted casing interval, are discretized into 1-ft intervals. Using the temporal rate of temperature change measured by the PXD, assumed to represent the rate at all depth intervals, the temperature profile is modeled through production and recovery time. Time-steps are defined as the time resolution of the PXD measurements (on the order of seconds). At each time-step and over each 1-ft interval, the volume differential dV that results from thermal expansion or contraction is calculated using $dV = V_o \alpha dT$, where V_o is the 1-ft interval casing volume and dT is the change in temperature per time-step. α is the coefficient of thermal expansion [$°F^{-1}$], expressed as:

$$\alpha = \angle\rho^{\angle 1}\frac{\partial \rho}{\partial T} \qquad (2\text{-}2)$$

The coefficient incorporates density (ρ [$M\ L^{-3}$]) as a function of temperature (T [°F]) at each 1-ft interval. The interval volume differentials are converted to interval pressure differentials, incorporating the interval temperature at each time step to calculate the density applied for the conversion. Finally, at each time step the interval pressure differentials are summed over the entire column and are appropriately incorporated into the measured formation pressure response. The summed pressure differentials, through both production and recovery periods, are shown in Figure 2-5. The thermal effects, prominent in the early periods of production and recovery, are accounted for in the temporal pressure correction. The uncorrected and corrected constant-rate test pressure records are shown in Figure 2-6.

The maximum corrective pressure datum during production is 1.24 psi. The offset accounts for 2.4 percent of the maximum measured pressure drawdown, 50.7 psi. Therefore, despite the large variation observed in the wellbore temperature profile through production, the correction for thermal effects is not significant because of the large drawdown measured. Regardless, the corrected formation response to constant-rate test pumping and recovery is applied in the subsequent analyses of the testing data.

2.1.2.2 Formation Thickness

To briefly review, Well ER-5-4 is cased to a total depth of 3,438 ft bgs. The cased well completion is slotted over two discrete sections of the AA, vertically separated by a 1,023-ft interval of blank casing. The total measured thickness of the AA at the well site is 3,676-ft; the upper bound of the AA is at the ground surface.

It is possible that producing intervals of the formation represent a fraction of the extent of both slotted intervals. This contributing fraction is defined as the formation thickness and is a necessary datum for further analyses. The interpretation of continuous wellbore flow-rate measurements that were logged under pumping conditions permits the identification of discrete-interval formation responses to pumping. The composite length of formation intervals that contribute groundwater to the well are defined as the formation thickness.

Discrete flow in the well as a function of depth was recorded using the DRI impeller flowmeter during multiple periods of constant-rate pumping. The flowmeter impeller spins in response to water moving through the meter. The rate of revolution is related to water velocity and flow via an equation which accounts for wellbore diameter and the trolling speed of the flowmeter. The coefficients of the equation relating the impeller response to the discharge are determined via calibration. In theory, the meter could be calibrated in the laboratory using the same pipe as the wellbore casing, and no further calibration would be necessary. In reality, the flowmeter response is influenced by a large number of factors specific to an individual well including temperature, pumping rate variation, hole condition, entrained air, and sediment load. Therefore, it is advantageous to perform a calibration in the well to use for interpretation. At Well ER-5-4, the calibration of the flowmeter response is determined using flowmeter data collected in the blank casing above the slotted interval. The flowmeter response is calibrated against the measured surface discharge to provide the necessary coefficients to calculate the discharge at any depth in the well as a function of impeller response and logging speed.

A total of nine flow logs, performed at three trolling speeds and three production rates in both vertical directions, were completed on June 18 and 19, 2001, to identify the source(s) and distribution of water production into the well. A complete listing of the different logging runs is presented in Table 2-3. All logging runs were completed across the entire extent of both slotted casing intervals, between approximately 1,610 and 3,370 ft bgs. Neither the borehole formation pressure nor depth to water were measured during this period. At each production rate, logs were calibrated individually. DRI provided the calibrated data at 0.2 ft resolution. A description of the calibration, methods, and raw data manipulation, through the conversion of the measured spinner rate (revolutions per second) to interval flow rates, is reported by DRI (Oberlander and Russell, 2003).

The trolling logs indicate that approximately 82 to 90 percent of the flow into the wellbore is supplied by the upper slotted interval, depending on the production rate and trolling speed. Because the constant-rate test was performed at 160 gpm, the borehole flow rates logged during production at 175 gpm are used to define the formation thickness. This permits the (nearly) direct correlation between data derived from flow logging and the constant-rate test. In particular, the log measured at a line speed of 20 feet per minute (fpm) and 175 gpm production provide the best representation of actual flow conditions across all of the pumping rates, reporting the most sensitivity with the least induced disturbance. This log (ER54MOV07) is shown in Figure 2-7.

Conceptually, the vertical flow rate at the bottom of the well casing should equal zero; this is a no-flow boundary. As the impeller tool moves up the well, the flow rate should smoothly increase across sections of the slotted casing intervals. Under ideal conditions of radial flow through a porous formation, the flow rate would increase linearly up the wellbore. Intervals over which the flow rate increase is nonlinear or discontinuous could indicate a fracture/fault flow zone, an anomaly in the wellbore cross-section area, and/or a preferential flow path through

Table 2-3
Listing of Trolling Flow Logs at Well ER-5-4

Run Number	Date	Direction of Run	Line Speed (fpm)	Surface Discharge (gpm)	Start - Finish (ft bgs)
ER54MOV01	6/18/01	Down	20	70	1,611.0 - 3,371.5
ER54MOV02		Up	60		2,115.3 - 3,370.4
ER54MOV02B		Up	60		1,619.7 - 2,500.3
ER54MOV03		Down	40		1,611.1 - 3,371.7
ER54MOV04		Down	20	125	1,611.1 - 3,370.0
ER54MOV05		Up	60		1,618.3 - 3,370.4
ER54MOV06		Down	40		1,611.0 - 3,370.4
ER54MOV07	6/19/01	Down	20	175	1,611.1 - 3,370.5
ER54MOV08		Up	60		1,619.6 - 3,371.0
ER54MOV09		Down	40		1,610.1 - 3,370.5

fpm - Feet per minute
ft bgs - Feet below ground surface
gpm - Gallons per minute

the gravel pack or well skin. Across sections of blank casing, the flow rate should remain constant with depth if volume is to be conserved.

The flow log shown in Figure 2-7 displays several of the features discussed above. Beginning at the bottom of the casing, just below the lower slotted casing interval, the flow rate is approximately zero. Over the bottom 30-ft of the lower slotted interval the flow rate increases about 12 gpm, and remains constant up across the remainder of the lower slotting casing. That is, of the 175 gpm well production rate, the lower completion zone contributes approximately seven percent of the flow, all of which is produced from the bottom 30 feet of the 214-ft lower slotted casing interval. The flow rate across the blank casing interval is constant; the small scale variability reflects impeller tool noise that increased due to higher line speeds used while logging the blank casing between the two screened intervals. The anomaly at 2,730 ft bgs reflects a sudden deviation in the line speed and does not reflect a change in wellbore or casing conditions. Up and across the entire extent of the upper slotted casing interval, the flow rate increase is nearly linear. Appropriately, the flow rate measured in the blank casing above the upper completion zone is equal to the well production rate (175 gpm).

Both slotted casing intervals contribute flow into the well during constant-rate production, although the lower interval contributes less than ten percent of the total. Across the upper interval, the formation inflow appears vertically constant and indicates horizontal flow. Across the lower interval, inflow was measured only over a 30-ft subsection of the 214-ft interval. The lack of inflow from the lower completion primarily reflects the lower hydraulic conductivity formation relative to that of the upper completion. The difference in conductivity between the completion intervals is discussed in detail in Section 3.1.4.

In defining the formation thickness, it is assumed that the entire extent of the formation tested, in both slotted completion intervals, contributes to wellbore flow. Therefore, formation properties derived from the analysis of the constant-rate test data are representative of the composite 557-ft thick section of the AA. Post-processing of the composite properties are performed (in Section 3.1.4) to account for the proportionate flow that was observed from the upper and lower slotted casing intervals.

2.1.3 Slug Testing of the Piezometer

Slug testing of the piezometer was performed on July 16, 2001, 11 days after the completion of the constant-rate test. An evaluation of the data was not completed because the piezometer was discovered to be plugged with drilling fluid. The high density of the fluid, relative to that of groundwater, alters the measured pressure response. There is sufficient uncertainty in the measured piezometer data (e.g., the concentration of the fluid with depth, the temperature variation with depth, and the unknown hydraulic efficiency of the undeveloped completion in general) that the data are deemed unsuitable for analysis.

2.2 Well ER-5-4#2 Single-Well Test

Measurement of hydraulic data at Well ER-5-4#2 during ambient and pumping conditions included water-level measurements from the predevelopment through testing period, a constant-rate production test in the main completion, two step-drawdown tests, and borehole flow logging. This section presents these data and reduces them for analysis and interpretation, the results of which are presented in Section 3.2.

2.2.1 Depth-to-Water Measurements and Hydraulic Gradients

Depth-to-water measurements for Well ER-5-4#2 are presented in Table 2-4. Refer to Figure 1-6 for completion and slotted casing interval information. All of the measurements are associated with the installation or removal of the PXDs. Further, the measurements are not representative of static and equilibrium well conditions. The final depth-to-water measurement during the recovery period was made on February 7, 2003 (JD 38). Since the final measurement time, the ER-5-4#2 water level has risen approximately 40 ft and appears to be currently (July 2004) approaching the static level (USGS, 2004).

In general, the water level in ER-5-4#2 was affected by equilibration of the water column temperature profile following any production of water from the deep completion interval. The effect of the transient temperature profile is discussed in detail in Section 2.2.2.1. In addition, the well recovered slowly from drawdown and was generally far from the static condition. Measurements made prior to October 18, 2002 (JD 291), reflect predevelopment conditions. Measurements made after November 4, 2002 (JD 308), reflect conditions after well development, although recovery was not fully completed. These measurements are referred to in Section 4.1 in the analysis of horizontal and vertical hydraulic gradients across the local RNM-2s well cluster site.

Table 2-4
Well ER-5-4#2 Depth-to-Water Measurements

Date	Time	Depth-to-Water (bgs)		Barometric Pressure (mbar)	Head[a]	
		Feet	Meters		Feet	Meters
Well ER-5-4#2 Production String						
9/29/2002	10:15	702.79	214.21	903.11	2,424.2	738.9
10/14/2002	11:15	694.34	211.63	910.25	2,432.7	741.5
10/18/2002	11:20	694.31	211.63	905.29	2,432.7	741.5
10/26/2002	8:40	705.65	215.08	901.09	2,421.4	738.0
11/6/2002	13:30	697.20	212.51	911.01	2,429.8	740.6
12/2/2002	9:59	740.53	225.71	909.75	2,386.5	727.4
12/14/2002	12:15	727.55	221.76	909.47	2,399.5	731.4
2/7/2003	10:40	696.59	212.32	911.28	2,430.4	740.8

[a]Reference Datum: 953.1 meters (feet) above mean sea-level datum

bgs - Below ground surface
mbar - Millibar

2.2.2 Constant-rate Test

A constant-rate pumping test was conducted at Well ER-5-4#2 following well development to collect hydraulic response data for determination of the local LTCU hydraulic properties. Prior to the test, the water level in the access line and the piezometer were monitored to observe recovery from development pumping to the static formation pressure under ambient conditions, and to establish baseline pretest conditions. Pumping for the test commenced on November 12, 2002 (JD 316). A production rate of 170 gpm was chosen as the optimal rate for the test. Control problems with the pump resulted in varying production rates from 168 to 189 gpm during the first two days of constant-rate production. The rate was reduced to 125 gpm after six days from the start of the test to limit the drawdown, which was approaching the range of the PXD. Upon correction, well production was continued without interruption until the pump was turned off on November 23, 2002 (JD 186), ten days after the start of the test. The recovery of the well was monitored for an additional nine days until December 2, 2002 (JD 336).

2.2.2.1 Measured Formation Response

A continuous data logger record was captured for the PXD pressure and temperature in the main completion access line, the barometric pressure, and the production rate during the constant-rate test. Figure 2-8 shows the data logger record of the pumping rate, PXD pressure, and PXD temperature for the access line during pretest (recovery from development) monitoring, the constant-rate test, and the recovery monitoring that occurred following the test. A Design Analysis (DA) 0-75 psig PXD was installed in the access line on November 6, 2002 (JD 310), at a calculated set depth of 855 ft bgs, 208 ft above the pump intake at 1,063 ft bgs. During pumping, inflow from the formation occurred through the slotted

casing interval, between 6,486 and 6,658 ft bgs. Therefore, a large (5,631-ft) interval of blank casing extends between the interval of formation inflow and the PXD, the influence of which on the measured pressure response is discussed in detail below.

The following sections discuss the influence of and correction for barometric effects, well loss, and thermal volume effects on the measured formation pressure response. Although in some cases a measurement correction is not able to be performed, each is discussed for completeness.

Barometric Effect

Prior to setting the testing pump for well development, the water level in the production string and barometric pressure were monitored for a period of 15 days. The predevelopment record is shown in Figure 2-9. The data show that the water level rose substantially during this period, most likely reflecting recovery from drawdown during production from drilling, which ended nine days prior to the start of monitoring (on September 16, 2002). The well was also not in thermal equilibrium when these water-level measurements were made; the water-level recovery was reduced in response to cooling to the equilibrium condition (geothermal gradient).

A second ambient water-level record was measured following the constant-rate test during recovery (Figure 2-8). Neither of the ambient monitoring records is suitable for determining barometric efficiency. Both records show temporal trends that reflect recovery from prior periods of production (increasing water levels) and cooling to the geothermal gradient (decreasing water levels). Regardless, the barometric response was sufficiently small relative to the effects of changing wellbore conditions that a correction term for the barometric effect is assumed negligible (less than 0.5 percent of the maximum drawdown observed through constant-rate production).

Well Loss

A theoretical introduction to well losses was presented in Section 2.1.2. These concepts are discussed further in this section, with a focus on the flow loss component of total well loss. It is important to assess flow losses because of the large, 5,423-ft blank casing interval between the slotted casing and the pump intake.

The drawdown observed in the well is comprised of aquifer drawdown and well losses that result from the flow of water into the well and up the borehole to the pump. Aquifer drawdown, or the linear component of drawdown, can be observed directly in observation wells near a pumping well; however, no such wells were available near Well ER-5-4#2. Therefore, it was anticipated that the step-drawdown test conducted during well development would provide data that could be analyzed to determine the linear (aquifer) and nonlinear (well loss) components of drawdown. The linear component of well drawdown is attributed to aquifer drawdown via Darcian flow. The nonlinear, or turbulent, flow component is attributed primarily to wellbore skin losses and flow losses due to

friction along the casing up the well. Again, note that flow loss comprises a component of the total well loss. At Well ER-5-4#2, it would be expected that flow losses represent a large component of the measured drawdown due to the large vertical interval of blank casing between the slotted completion and the pump intake.

Two step-drawdown tests were performed during well development. The protocol for both tests included one hour of pumping at each of three successively higher steps (pumping rates). The target pumping rates were 75, 125, and 175 gpm. Problems with the production rate control system occurred during the first test and resulted in erratic data that cannot be interpreted. Furthermore, during both tests, effects of increasing temperature in the wellbore during pumping complicated reduction of the data. The method by which the thermal effect is included in the measured formation response to production is discussed in detail below. However, it is simply stated at present that the thermal volume expansion of groundwater in the wellbore significantly convolutes the measured response to step-drawdown pumping. For example, during the first step (75 gpm) of the second step-drawdown test, the measured water level decreases and then increases through the 1-hour step. That is, the effect of thermal expansion as heated groundwater enters the well gradually becomes greater than the drawdown response. The lack of sufficient data on the rate of change of the temperature profile through step-drawdown production does not permit a temporal correction term to be applied to the data; therefore, the step-drawdown test data do not permit the estimation of the linear and nonlinear components of the total drawdown measured.

However, flow losses, which are expected to comprise a significant portion of the measured drawdown, can be assessed. During well production, flow losses represent the averaged component of energy in the completion, over some interval, that is lost as a result of the friction against flow, both from the formation into the borehole across the slotted casing, and against flow up the casing. The amount of friction is primarily a function of the fluid viscosity, flow velocity, material surface (casing roughness), and geometry of the flow system. Although flow losses themselves are not necessarily the result of a turbulent flow system, they are traditionally grouped with the nonlinear, or turbulent, component of well losses, e.g., the Hantush-Bierschenk method. It is difficult to partition the fraction of well losses that are attributed to turbulence versus flow loss. This is a particularly difficult task along the length of the slotted well casing, where the divergence and convergence of flow through the casing slots results in an unknown flow dynamic.

Head losses h_f, attributed to flow losses inside the well casing, are computed based on the standard theory of flow in a pipe using the Darcy-Weisbach equation (Weisbach, 1845),

$$h_f = \frac{fL}{2Dg}u^2 \tag{2-3}$$

where

L = interval length

D = pipe (casing) diameter

f = friction factor

u = interval flow rate (from flow logging)

The head (flow) loss terms are calculated for the composite length intervals of two sections of the well casing. These are the 5,424-ft blank casing interval between the slotted completion and the pump intake, and the 171-ft slotted casing interval below the blank casing. The vertical flow rates (u) within these sections of casing are determined from impeller flow logging that was conducted during pumping of the well at 175 gpm. Although discussed in detail in the following section, the flow-rate data are depth integrated over the two intervals of casing to provide the average vertical velocity across each interval. Use of these data permit the (nearly) direct comparison of results to those derived from the 160 gpm constant-rate test analysis.

The calculation of interval head loss is straightforward with the exception of the estimation of interval friction factors. The friction factor along the blank casing is estimated from the Moody diagram (Moody, 1944) assuming a smooth, straight pipe. Estimation of the friction factor along the slotted casing interval is difficult. Due to the possible presence of turbulence along the slotted interval, in addition to convergent and divergent flow, friction factors are unknown. In particular, there is a 4.1-centimeter (cm) thick open annulus between the outer casing wall and the borehole wall at ER-5-4#2 that is shown to have a significant effect on inflow to the well from the formation (see Section 2.2.2.2). It has been suggested in the literature from empirical investigation that losses through the slotted sections be assigned friction factors double those of blank pipe (Roscoe Moss Company, 1990). This recommendation is used in the analysis (Table 2-5).

The estimated composite interval head (and pressure) losses across the two casing intervals are presented in Table 2-5, along with the Darcy-Weisbach flow parameters applied in the method. The head loss across the 5,424-ft interval of blank casing is estimated at 19.11 ft, equivalent to 8.15 psi at 120°F, and accounts for approximately 13 percent of the maximum measured drawdown during the constant-rate test. The head loss across the slotted casing is less than one-tenth of a foot. A temperature of 120°F was applied in the conversion of head to pressure because the uniform wellbore temperature profile through constant-rate production approached this temperature; the temperature profile variability through production and recovery is discussed in detail in the following section.

As discussed (Section 2.1.2.1), the drop in water level from the 160 gpm production rate is larger than would be expected from resistance to Darcian flow in the formation alone. To correct for the flow loss component in the measured drawdown, the sum of the pressure (converted from head) losses across the blank and slotted casing (Table 2-5) are added to the measured drawdown. The corrected response, in relation to the measured response, is shown in Figure 2-10.

Note that the corrected response includes a temperature correction component, the derivation of which is discussed next in the document.

Table 2-5
Well ER-5-4#2 Head Loss Parameters

Casing Interval	RMS*Q (gpm)	RMS* u (ft s^{-1})	Axial Length (ft)	Casing Radius (ft)	Kinematic Viscosity (ft^2 s^{-1}) at 120°F	Re (-)	f (-)	h_f (ft)	Density Conversion Factor (ft psi^{-1}) @ 120°F	P_f (psi) at 120°F
Slotted	42.11	0.56890	171	0.22917	0.00000609	21408	0.0370	0.07	2.347	0.030
Blank	175.38	2.36939	5,424	0.22917	0.00000609	89160	0.0185	19.11	2.347	8.145

*Root Mean Squared

Temperature Effects

A substantial temperature gradient from the top of the water column to the completion interval was observed at Well ER-5-4#2. The large temperature variation is a result of the deep well depth (7,000 ft bgs). During constant-rate test pumping, higher temperature formation groundwater enters the well through the slotted casing interval, between 6,486 and 6,658 ft bgs. The pressure transducer that measures the formation response to groundwater was set at a depth of 855 ft bgs. As water from the pump intake (at 1,063 ft bgs) down to the completion interval is replaced with higher temperature water produced from the formation, thermal volume expansion occurs across this section of the well casing. Further, the water column along the pump production tubing is heated by conduction. Therefore, a 5,803-ft water column, from the transducer depth down to the bottom of the slotted casing interval, undergoes thermal volume expansion and produces a positive offset in the measured formation pressure response. The process by which this occurs was discussed in detail in Section 2.1.2.1. The effect of a time-varying temperature profile in the wellbore, through both constant-rate test production and recovery, was also discussed in Section 2.1.2.1.

As discussed, three datasets are necessary to correct for the influence of thermal volume expansion and contraction on the measured formation pressure response to production and recovery. These are the initial wellbore temperature profile prior to pumping (initial condition), the temporal rate of temperature change along the profile (transient condition), and the steady-state wellbore temperature profile that is achieved during constant-rate well production (steady condition).

The constant-rate test was started at the end of a 5-day recovery period following development activities. For the purpose of the correction, it is assumed that the vertical temperature profile was near equilibrium at this time; no data were collected to either verify or contradict this assumption. A temperature log taken on March 22, 2003 (JD 81), approximately three months after the end of pumping at Well ER-5-4#2, best reflects the equilibrium temperature profile in the well. A plot of this log is shown in Figure 2-11. At (near-) equilibrium, the water level is approximately 700 ft bgs (696.54 ft, on February 7, 3002), where the temperature is about 74°F. The temperature at the pump intake at 1,063 ft bgs is 75°F. The

temperature across the slotted casing interval, from 6,486 to 6,658 ft bgs, ranges from 106 to 120°F. Upon constant-rate production, hotter water from the formation enters the well and flows up to the pump intake. The water column above the intake is heated more gradually by conduction from the production string. During the constant-rate test, the temperature at the PXD (855 ft bgs) stabilized at approximately 120°F. This information suggests that the entire water column in the well was heated to 120°F during production and represents the steady temperature profile achieved during the constant-rate test. The steady profile, shown with the initial temperature profile before the start of pumping, is shown in Figure 2-11.

The PXD temperature (Figure 2-8) provides the only temporal measurement of the transient temperature profile. Although the transient profile reflects the temperature variation at the PXD set depth at 855 ft bgs, it is assumed that the time-rate of temperature change along the entire wellbore is equal to that measured at the PXD location.

To correct the measured formation pressure response for thermal effects, the change in the temperature profile through pumping and recovery is modeled through time using the initial condition profile (Figure 2-11), the steady-state profile (Figure 2-11), and time-rate of change derived from the PXD measurement (Figure 2-8). The wellbore temperature profile is discretized into 1-ft intervals, and the PXD time-rate of temperature change is assumed to represent the rate at all depth intervals. The method of correction is identical to that presented in Section 2.1.2.1 for the Well ER-5-4 corrective analysis.

The corrective terms for thermal volume effects through constant-rate test production and recovery, expressed as pressure offset time series, are shown in Figure 2-12. The measured formation response, corrected for both temperature effects and well losses, is shown in Figure 2-10.

2.2.2.2 Formation Thickness

At Well ER-5-4#2, the slotted casing interval length is not representative of the formation thickness that contributes groundwater to the well. There is a 4.13-in. thick open annulus between the well casing and borehole that extends from 4,848 to 6,658 ft bgs (Figure 1-6). The borehole is open below the casing to 6,966 ft bgs. The entire extent of the formation exposed across the borehole is the Bullfrog Tuff, a stratigraphic unit of the LTCU HSU, composed of bedded and nonwelded to welded tuffs. Flow logging conducted during pumping of the well showed that the majority of inflow to the well occurred within the upper 20-ft section of the 172-ft slotted casing length, or more exactly, between 6,486 and 6,500 ft bgs. It is unknown where inflow may be occurring into the borehole behind the casing above 6,486 ft bgs. Table 2-6 lists the 12 trolling flow logs that were run at Well ER-5-4#2, and also shows a tabulation of the flow rate and percentage of total flow produced from below 6,500 ft bgs for each log. The percentages become more consistent for the logs run at higher production rates as interval flow rate variability is reduced. Below 6,500 ft bgs, the flow rates are relatively constant to 6,555 ft bgs, and then decline to zero flow near the casing bottom.

Table 2-6
Trolling Flow Logs at Well ER-5-4#2

Run Number	Direction of Run	Line Speed (fpm)	Surface Discharge (gpm)	Start - Finish (ft bgs)	Mean flow rate From Below 6,500 ft (gpm)	Percent Flow From Below 6,500 ft
er542mov01	Down	20	75	4,663 - 6,639	7	9
er542mov02	Up	20		6,644.8 - 6,266.6	22	29
er542mov03	Down	40		6,263.6 - 6,639	12.5	17
er542mov04	Up	40		6,645.8 - 4,691.6	29	39
er542mov05	Down	20	125	4,648.6 - 6,638.8	36	29
er542mov06	Up	20		6,643.6 - 6,390.4	34	27
er542mov07	Down	40		6,388.2 - 6,640	27	22
er542mov08	Up	40		6,644.8 - 4,694	44	35
er542mov09	Down	20	175	4,636.4 - 6,637	42	24
er542mov010	Up	20		6,642.8 - 6,439.2	39	22
er542mov011	Down	40		6,436 - 6,639.6	43	25
er542mov012	Up	40		6,645.4 - 4,632.4	43.5	25

fpm - Feet per minute
ft bgs - Feet below ground surface
gpm - Gallons per minute

The data suggest that there is significant inflow from the open annulus and imply that a larger section of the formation than is exposed across the slotted casing contributes to well production. The flow-rate profile er543mov012 logged during pumping at 175 gpm is shown in Figure 2-13. Logging at this rate permits the nearly direct comparison of data to those collected during the 170 gpm constant-rate test. The majority of groundwater inflow to the casing occurs in the uppermost section of the slotted interval. The flow-rate data suggest inflow from the annulus above the slotted interval. There is no information to constrain the upper depth at which the formation exposed in the borehole ceases to contribute to production; therefore, the upper bound of the formation thickness is defined as the depth above which the borehole is first cemented off at 4,848 ft bgs (Figure 1-6). The corresponding temperature log (Figure 2-13), measured at the time of flow logging, confirms this assumption. The temperature across the slotted interval increases up the casing above 6,600 ft bgs, although less than 1°F, with increasing inflow. Below 6,600 ft bgs, slightly cooler water enters the well. Over the upper 20-ft section of the slotted casing, the temperature profile undergoes a step increase, from 120.25 to 120.33°F, with the step increase in inflow. This is the maximum temperature observed across the slotted interval and confirms that (higher temperature) groundwater from the formation above the slotted casing contributes to production.

The lower bound of the formation thickness is defined as the depth of the slotted casing interval. Flow at the casing bottom is approximately zero. The large step-increase from a negative to positive flow-rate over the bottom 10-ft interval, shown in Figure 2-13, reflects the lower casing boundary and deviation of the flow

geometry from radial inflow and vertical flow up the wellbore. The data show that casing inflow did not occur at or near the base of the slotted interval; therefore, the formation does not contribute to pumping below 6,658 ft bgs.

In summary, the formation thickness is defined as the 1,810-ft interval below the cemented borehole and above the base of the slotted casing interval. While it is possible that the formation thickness is less, no data are available that can be used to constrain the upper bound that is located at an unknown point between the blank casing and borehole wall. DRI impeller flow-rate and temperature logs were used to define the formation thickness. Interval-specific flow rates were not presented in the discussion above; only profile features used to define the formation thickness were discussed. The reader is referred to Oberlander and Russell (2003) for a detailed analysis of the Well ER-5-4#2 flow logging data.

2.3 RNM-2s MWAT

This section presents the production and observation well testing data collected during the FY 2003 RNM-2s MWAT. Measurement of hydraulic data included the pumping rate at RNM-2s and the measured formation response to pumping at the production well and at nine observation wells. A list of wells monitored was provided in Table 1-2. Measurement of well conditions during the testing period (e.g., step-drawdown testing, wellbore temperature profiles, impeller flow logging) were not completed at any wells as they were during the single-well testing of ER-5-4 and ER-5-4#2. This section presents the measured response data and reduces them for analysis and interpretation, the results of which are presented in Section 3.3.

2.3.1 Summary of Field Activities

PXDs were installed in the RNM-2s MWAT wells between April 10 and 25, 2003 (JD 100 and 115), for pre-test monitoring. A bridge plug was installed in ER-5-4 to isolate the lower completion zone from the upper completion zone on April 17, 2003 (JD 107). Work to clear an obstruction in RNM-2 was performed on April 18, 2003 (JD 108). The MWAT constant-rate pumping began at RNM-2s on April 26, 2003, and continued for a period of 75 days (JD 116 through 191). On June 6, 2003 (JD 157), the RNM-2s piezometer was pressurized to test its connection with the formation. Constant-rate pumping ended on July 10, 2003 (JD 191), and recovery monitoring was initiated. Recovery monitoring ended on September 10, 2003 (JD 253), at all wells with the exception of ER-5-3#3, which ended on July 21, 2003 (JD 202). A summary of these and other MWAT activities was presented in Table 1-7.

2.3.2 Depth-to-Water Measurements and Hydraulic Gradients

Water-level (depth-to-water) measurements were obtained during PXD installation and removal at each well. The PXDs were installed in April shortly before the start of the MWAT and were removed, for the most part, in September at the end of the MWAT. The resulting data are presented in Table 2-7.

Based on review of the limited premonitoring records, all of the wells with the exception of ER-5-4#2 appeared to be in equilibrium with the formation head prior to the start of pumping at RNM-2s. The later water-level measurements reported in Table 2-7, taken when the PXDs were removed after testing, reflect recovering water levels from constant-rate pumping. Prior to testing, Well ER-5-4#2 was still equilibrating from the single-well test performed in the last quarter of FY 2002. Also, there is uncertainty in defining the static and equilibrium pressure at RNM-1. RNM-1 was drilled at an average angle of 21° from the vertical into the CAMBRIC test cavity. For the MWAT, the well casing was perforated between 858 and 884 ft bgs, reported as the true vertical depth interval. The test working point was at 968 ft bgs; therefore, the cavity is located about 100 feet below the completion zone. The hydraulic continuity between the cavity and well completion zone is uncertain. The steady (assumed equilibrium) formation head measured in RNM-1, corrected for the deviation from the vertical, is approximately 2,397.4 ft (Table 2-7). This datum is approximately 8.5 ft below other heads observed in the well cluster during the same time period. The head differential is thought to reflect uncertainty in the true completion interval depth resulting from the lack of a borehole deviation survey. For example, an actual deviation between the RNM-1 wellhead and completion zone of 22.78°, less than 2° different from the 21° average, would result in a corrected water level at RNM-1 that is within one-hundredth of a foot of the static water level measured at RNM-2. While it is possible that local deformation of the alluvium from the nuclear test altered the hydraulic continuity between the RNM-1 completion zone and the alluvium outside of the blast radius of influence, the RNM-1 response data to pumping at RNM-2s indicate that this is unlikely. This supposition is discussed in greater detail during the analysis of the RNM-1 test response in Section 3.3.2.

Table 2-7
Depth-to-Water Measurements
(Page 1 of 3)

Date Activity	Time	Depth-to-Water (bgs)		Barometric Pressure (mbar)	Water-Level Elevation[a]	
		Feet	Meters		Feet	Meters
RNM-2s						
2/18/2003	13:25	723.80	220.61	908.40	2,406.65	733.55
4/12/2003	08:10	723.51	220.52	902.68	2,406.94	733.64
9/12/2003	11:35	724.55	220.84	907.13	2,405.90	733.32
RNM-2s Outer West Piezometer						
2/18/2003	12:50	723.80	220.61	908.9	2,406.65	733.55
4/18/2003	14:15	723.57	220.54	900.16	2,406.88	733.62
6/6/2003	15:07	868.27	264.65	900.26	2,262.18	689.51
9/12/2003	10:00	738.86	225.20	908.40	2,391.59	728.96
RNM-2						
4/18/2003	11:00	721.87	220.03	NR	2,406.93	733.63
4/18/2003	11:55	722.04	220.08	NR	2,406.76	733.58
4/21/2003	13:27	722.04	220.08	898.16	2,406.76	733.58
9/12/2003	16:25	722.85	220.32	901.92	2,405.95	733.33

Table 2-7
Depth-to-Water Measurements
(Page 2 of 3)

Date Activity	Time	Depth-to-Water (bgs)		Barometric Pressure (mbar)	Water-Level Elevation[a]	
		Feet	Meters		Feet	Meters
RNM-1[b]						
2/13/2003	10:50	737.19	224.70	902.9	2,397.98	730.90
4/11/2003	15:50	737.71	224.85	902.16	2,397.46	730.75
9/12/2003	10:30	738.30	225.03	908.12	2,396.87	730.56
ER-5-4 #2						
4/22/2003	14:30	677.14	206.39	897.15	2,454.56	748.15
4/24/2003	09:35	676.97	206.34	903.19	2,454.73	748.20
4/24/2003	13:45	676.82	206.29	900.54	2,454.88	748.25
9/13/2003	09:25	663.30	202.17	908.89	2,468.40	752.37
ER-5-4						
4/17/2003	09:30	725.58	221.16	900.11	2,406.12	733.38
4/17/2003	15:10	725.64	221.18	899.05	2,406.06	733.37
9/10/2003	09:30	726.12	221.32	907.49	2,405.58	733.22
9/10/2003	15:20	726.11	221.32	905.91	2,405.59	733.22
9/22/2003	07:45	726.52	221.44	908.10	2,405.18	733.10
9/23/2003	07:45	726.53	221.45	906.30	2,405.17	733.10
9/24/2003	11:55	726.69	221.50	905.70	2,405.01	733.05
ER-5-4 Piezometer						
4/11/2003	12:11	726.51	221.44	905.04	2,405.19	733.10
9/12/2003	18:35	727.82	221.84	901.86	2,403.88	732.70
9/22/2003	07:56	727.66	221.79	908.10	2,404.04	732.75
UE-5n						
2/13/2003	12:58	705.08	214.91	902.70	2,408.28	734.04
4/10/2003	15:00	705.53	215.04	903.62	2,407.83	733.91
7/26/2003	09:20	705.88	215.15	910.07	2,407.48	733.80
8/5/2003	12:00	706.01	215.19	907.15	2,407.35	733.76
8/23/2003	12:05	706.03	215.20	907.52	2,407.33	733.75
8/24/2003	09:30	706.11	215.22	910.59	2,407.25	733.73
9/12/2003	12:40	705.53	215.04	907.82	2,407.83	733.91

Table 2-7
Depth-to-Water Measurements
(Page 3 of 3)

Date Activity	Time	Depth-to-Water (bgs)		Barometric Pressure (mbar)	Water-Level Elevation[a]	
		Feet	Meters		Feet	Meters
ER-5-3 #3						
4/25/2003	12:50	927.48	282.70	894.25	2,409.92	734.54
7/21/2003	15:45	927.53	282.71	898.15	2,409.87	734.53
8/6/2003	08:53	927.64	282.74	906.69[c]	2,409.76	734.49

[a]Water-level elevations in feet and meters above mean sea level. Reference Table 1-1 for datum elevations.
[b]RNM-1 is a slant-angle well deviated 21 degrees from vertical. Depth-to-water measurements and water-level elevations are true vertical depths corrected for the average borehole deviation.
[c]Barometric pressure from ER-5-4 well pad.

bgs - Below ground surface
mbar - Millibars
NR - Not recorded

An estimation of the horizontal hydraulic gradients at the well cluster is performed using the pre-test formation head measurements (Table 2-7). The formation head is calculated from the depth-to-water measurements, and accounts for the influence of the groundwater temperature on density, the set depth of the PXD, and the wellhead elevations amsl (Table 1-1). Although most of the measurements were collected on different days between April 10 and 25, 2003 (JD 100 and 115), it is assumed that the measurements were collected at the same point in time, or equivalently, that water levels did not change over the 15-day period. It is also assumed that the vertical displacement between well completion zones is negligible. This assumption is justified given that the completion zone intervals often overlap, and/or are surrounded by larger-interval gravel packs that make identification of the completion zone depth interval uncertain.

Pre-test monitoring records show measurement variability, on a daily scale, of 0.10 psi. This translates to a head differential of approximately 0.23 ft. The magnitude of the differential may vary slightly, +/- 0.01 ft, depending on the temperature of groundwater in the well. Therefore, a head difference between wells that is less than 0.23 ft is considered within measurement uncertainty and the head gradient is assumed zero, or negligibly small.

The formation head measurements taken at the time of PXD installation are applied in the analysis. In the case that multiple measurements are made on the same day, the average is used. Figure 2-14 shows the horizontal gradients in tabular form and a schematic of the gradient direction between wells. The significance of these results is presented in Section 4.1.

2.3.3 Constant-rate MWAT

This section describes the multiple-well testing data collected that are pertinent to the estimation of local FF HSU hydraulic properties. Of the 11 wells observed

during testing of the cluster (Table 1-1), a distinct response to the production of RNM-2s was observed in only 4 wells: RNM-2s, RNM-2, RNM-1, and the ER-5-4 upper completion zone. No distinct response to MWAT production was observed at the ER-5-4 lower completion zone, ER-5-4#2, UE-5n, ER-5-3#3, and TW-3. Equipment error prevented the certain measurement of the well response at the ER-5-4 piezometer; theoretical inconsistencies in the data result in unquantifiable data error. The RNM-2s piezometer was determined to be plugged during the test; it is thought that a weep-hole in the plugged casing resulted in a time lag (on the order of hours) and signal damping in the measured response, relative to the time and magnitude of production in RNM-2s, that is highly uncertain and difficult to corrected for.

The MWAT responses measured at Wells RNM-2, RNM-1, and the ER-5-4 upper completion zone (CZ) are analyzed to estimate hydraulic properties of the local FF AA. The following sections provide a description of known conditions and the response data collected at each observation well, and also at the RNM-2s production well.

Before presentation of the data, it is important to note that the formation response data measured at each well were minimally manipulated before analysis. That is, either no information or insufficient information was collected to assess BE of the responses, well loss, or thermal effects. The pre-test measurement records are generally short and did not provide sufficient data (a general water-level trend) for analysis of BE. Evaluation of the pre-test records could not clearly establish that the BE was other than 1.0. Well loss and thermal effect components of drawdown should not, in theory, be present in the measured responses in the observation wells. The responses are assumed to be sufficiently gradual that the formation pressure measured in the wellbore is in constant equilibrium with that in the formation. The only manipulations applied to the measured pressure data in the observation wells were the conversion from formation pressure to head (incorporating groundwater temperature) and referencing the head data to a datum, defined as the base of the AA at 3,676 ft bgs. Therefore, the water table (using SWL measurements in Table 2-7) is 2,954 ft bgs. The MWAT response data presented below (Section 2.3.3.1 through Section 2.3.3.4) are in units of pressure and correspond to a BE equal to 1.0. The response conversions from pressure to head were completed for the data analyses and are presented in Section 3.3.4.

2.3.3.1 RNM-2s

The original 17.5-in. borehole was drilled to a depth of 1,156 ft bgs and 9.625-in. casing was installed from the surface to the top of the fill at 1,120 ft bgs. The casing is perforated between 1,038 and 1,119 ft bgs, and the borehole annulus is gravel packed between 690 and 1,120 ft bgs. An unknown amount of fill had accumulated inside the main completion casing at the time of original installation in 1974. The RNM-2s well operated for 16 years after completion, and additional fill could have accumulated inside the well during that time. The level of fill at the time of testing is not known. Fill inside the completion casing could restrict the interval of perforations through which water is produced, increasing the entrance losses. Losses would also occur during vertical flow upward through the fill within the perforated casing. Given the well construction, the completion can be

specified as either the perforated casing interval (1,038 to 1,119 ft bgs) or the larger gravel-pack interval (690 to 1,120 ft bgs). The water table, at about 720 ft bgs, intersects the gravel pack interval, but is about 300 ft above the perforated interval. In the absence of discrete-interval flow and/or temperature logging under pumping conditions, the thickness of the contributing formation is uncertain. It is unlikely that inflow from the AA along the entire extent of the gravel pack contributed to well production given the directional variation of the permeable alluvial deposits. Therefore, the formation thickness is specified as the 81-ft perforated casing interval. Regardless of the formation thickness specified for the well-test interpretation, the large thickness of the AA (2,954 ft) and long duration of the test (75 days) are shown to minimize the influence of the 300-ft discrepancy between the two assumed formation thicknesses. During the data analyses, the simulated magnitude and radial extent of the water table drawdown were equal when either the length of the saturated gravel pack or length of the perforated casing interval are specified as the completion interval.

The MWAT production rate and formation pressure response measured at RNM-2s are shown in Figure 2-15. The well responded very quickly incurring a large drawdown at the (average) production rate of 595.5 gpm, indicating that there are significant losses for production. As reported, the losses cannot be quantified given that a step-drawdown test was not performed, that discrete-interval flow rates were not measured in the casing, and that a section of unknown length of the perforated casing interval may have been filled. The pump intake was at a set depth of 992.75 ft bgs and the deepest possible area of inflow through the casing is at 1,119 ft bgs. Although the casing length along which there are well losses is small, the production rate is high. As a result of the unquantifiable loss component, the drawdown measured at RNM-2s is not applied in the analysis of the local AA hydraulic properties; rather, the analysis is completed using the observation well responses that have a minimal component of uncertainty.

2.3.3.2 RNM-2

The RNM-2 completion consists of tubing installed to a depth of 825 ft bgs in a borehole drilled to 935 ft bgs. The tubing is perforated between 720 and 820 ft bgs. The hole contained fill from the TD up to 755 ft bgs at the time of completion. The borehole was left open and additional fill may have accumulated in the open borehole. Prior to testing, an e-tape was lowered to measure the TD of the well. An obstruction was encountered below the SWL at a depth of 770 ft bgs. Because the obstruction (or tight area) was below the SWL, no attempt to clear the well was made.

The data recorded for the well are shown in Figure 2-16. There do not appear to have been any problems with the data collection. There is little pre-test record from which to determine a general water-level trend. The recovery sequence shows a characteristically slow water-level response that primarily results from the small horizontal gradient across the drawdown cone and also possibly from the delayed resaturation of the drained specific-yield component of drawdown.

2.3.3.3 RNM-1

Well RNM-1 is completed in the AA and drilled at an average angle of 21° from the vertical to re-enter the cavity of the CAMBRIC (U-5e) test. The well completion was designed to allow discrete testing of four intervals defined by external casing packers. The well was successfully plugged back and the casing was perforated in each test interval. The lower formation access interval is defined by an external casing packer installed at a depth of 888.86 ft bgs true vertical depth (TVD). Perforations for the test interval are from 857.96 to 884.10 ft bgs (or measured from 919 to 947 ft) (Figure 1-10). The perforated interval is defined as the completion zone.

The MWAT data recorded for RNM-1 are presented in Figure 2-17. The data record shows an appropriate drawdown response. The response is remarkably similar to that measured at RNM-2 (Figure 2-16). Both show a similar trend and magnitude of drawdown through time, and both show a slow water-level recovery (that is not fully captured). The cause of and implications of such similarity on the interpretation of the groundwater flow dynamic through the AA is discussed in detail in Section 3.3.4.

2.3.3.4 ER-5-4 Upper Completion Zone

The upper ER-5-4 CZ tests the AA and is separated from the lower zone by a bridge plug set at 2,290 ft bgs. The upper CZ is gravel packed from 1,745 ft bgs (top of the 6 to 9-ft sand filter) to 2,192 ft bgs (top of the underlying annular cement seal). The slotted casing interval is between 1,770 and 2,113 ft bgs, which is defined as the completion zone.

The MWAT data recorded at the well are shown in Figure 2-18. The early-time (drawdown and recovery) response is noticeably greater than that observed at RNM-1 and RNM-2. The difference probably reflects the depth of the ER-5-4 completion that may respond as a confined, rather than unconfined, system, and may also reflect heterogeneity related to the nuclear test. The conceptual model (confined system) is discussed in Section 3.3.4.

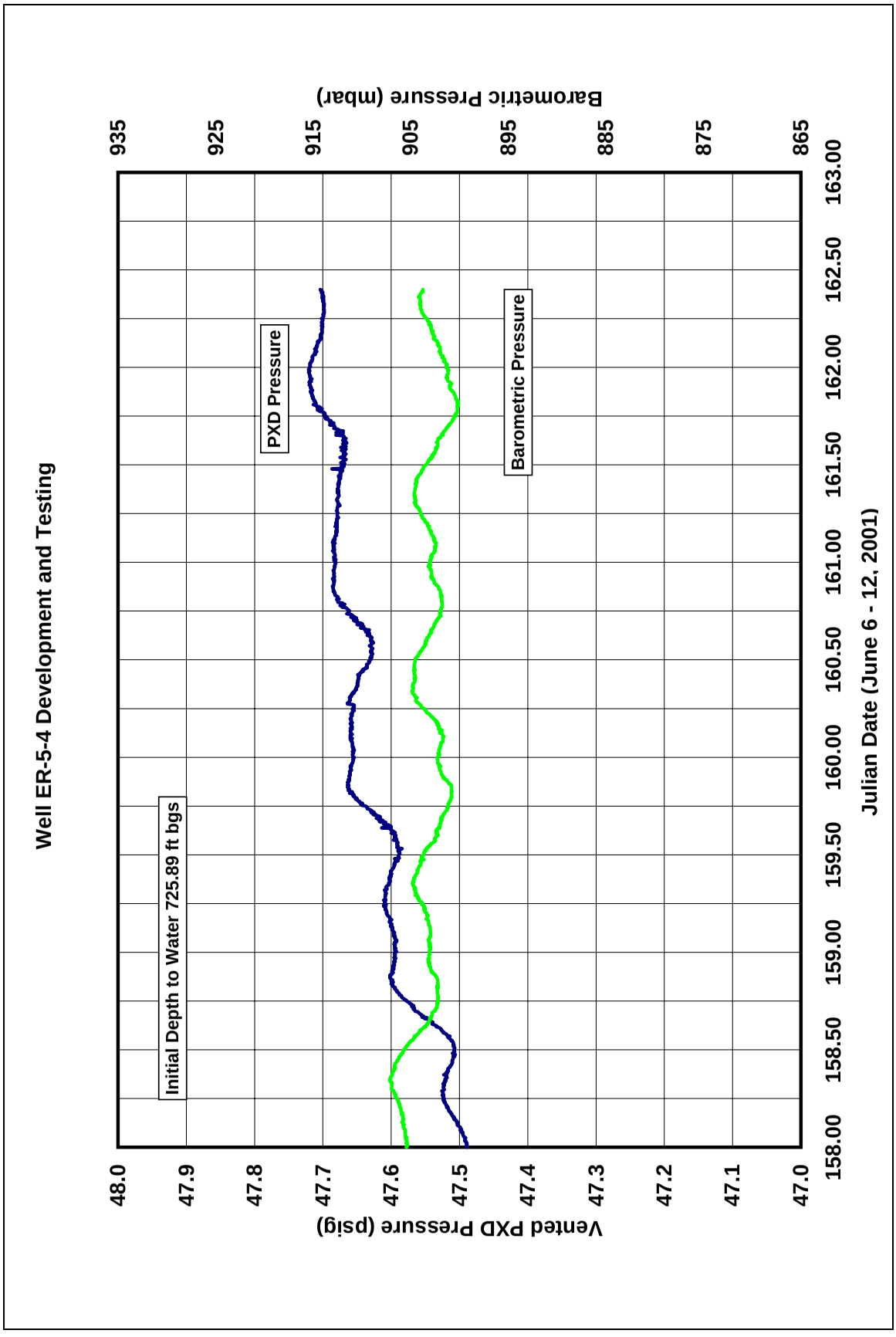

Figure 2-1
Predevelopment Water-level Monitoring in the Well ER-5-4 Access Line

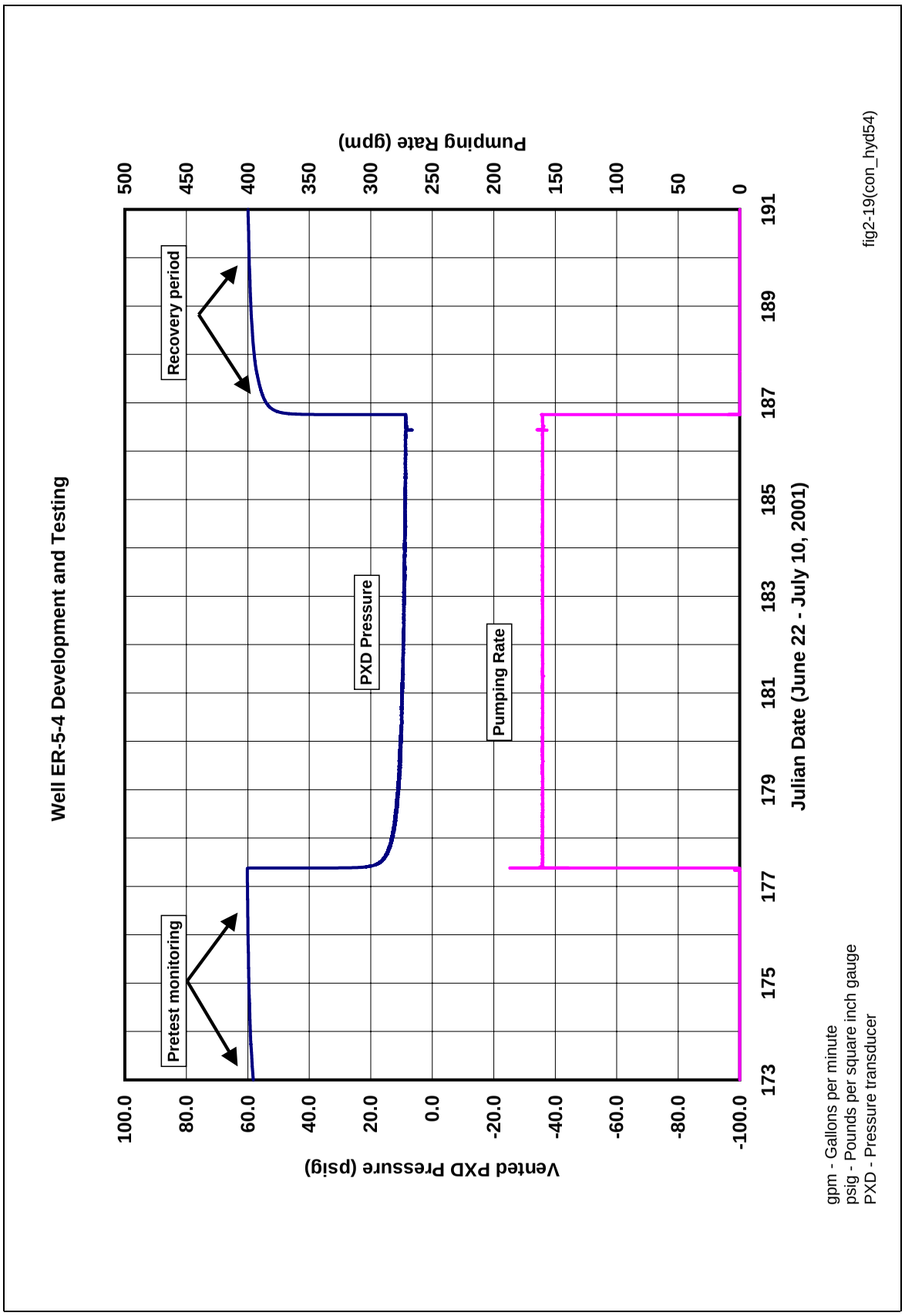

Figure 2-2
Well ER-5-4 Production Rate and Formation Response During the Single-well Constant-rate Test

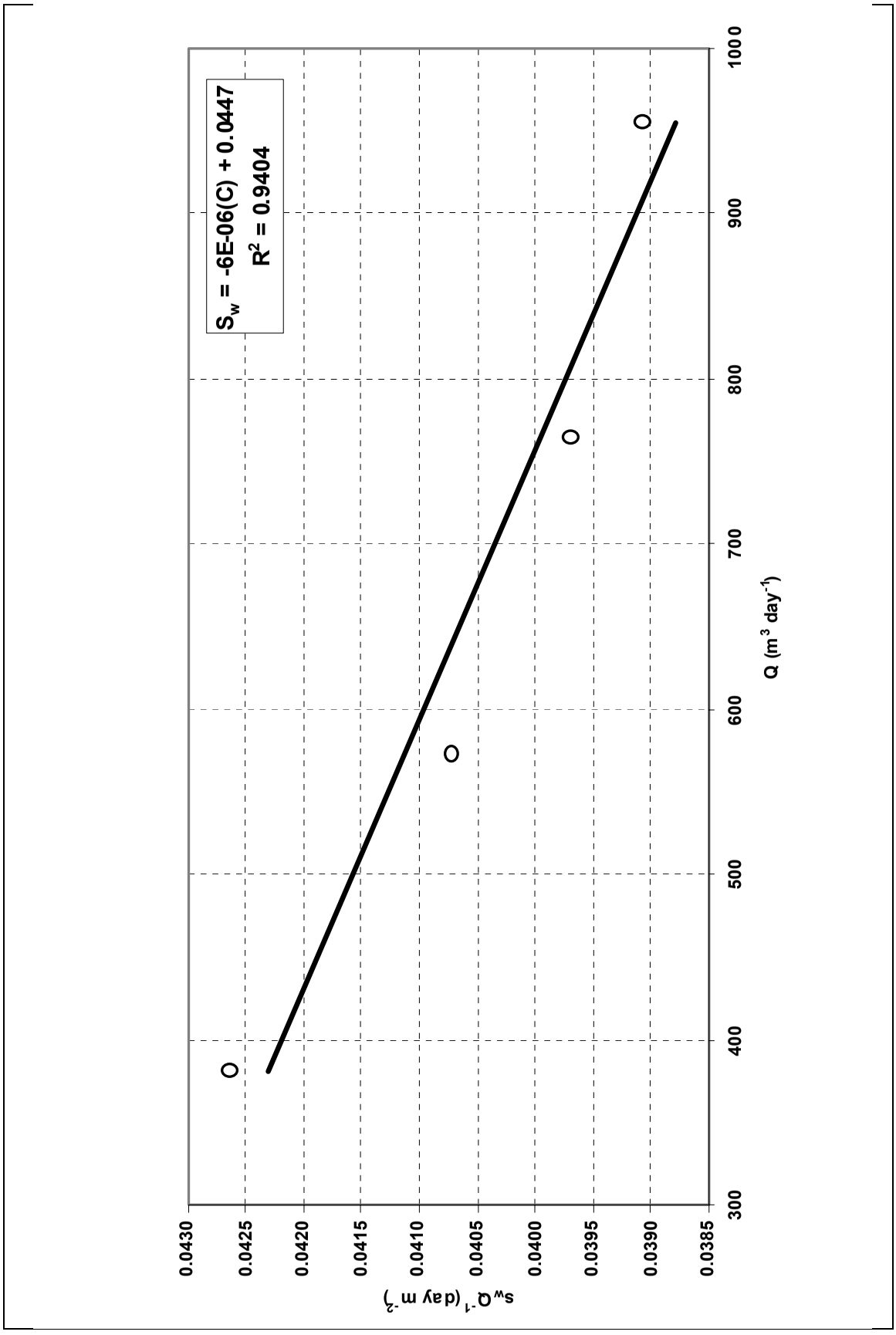

Figure 2-3
Hantush-Bierschenk Analysis of Step-Drawdown Testing Data at Well ER-5-4

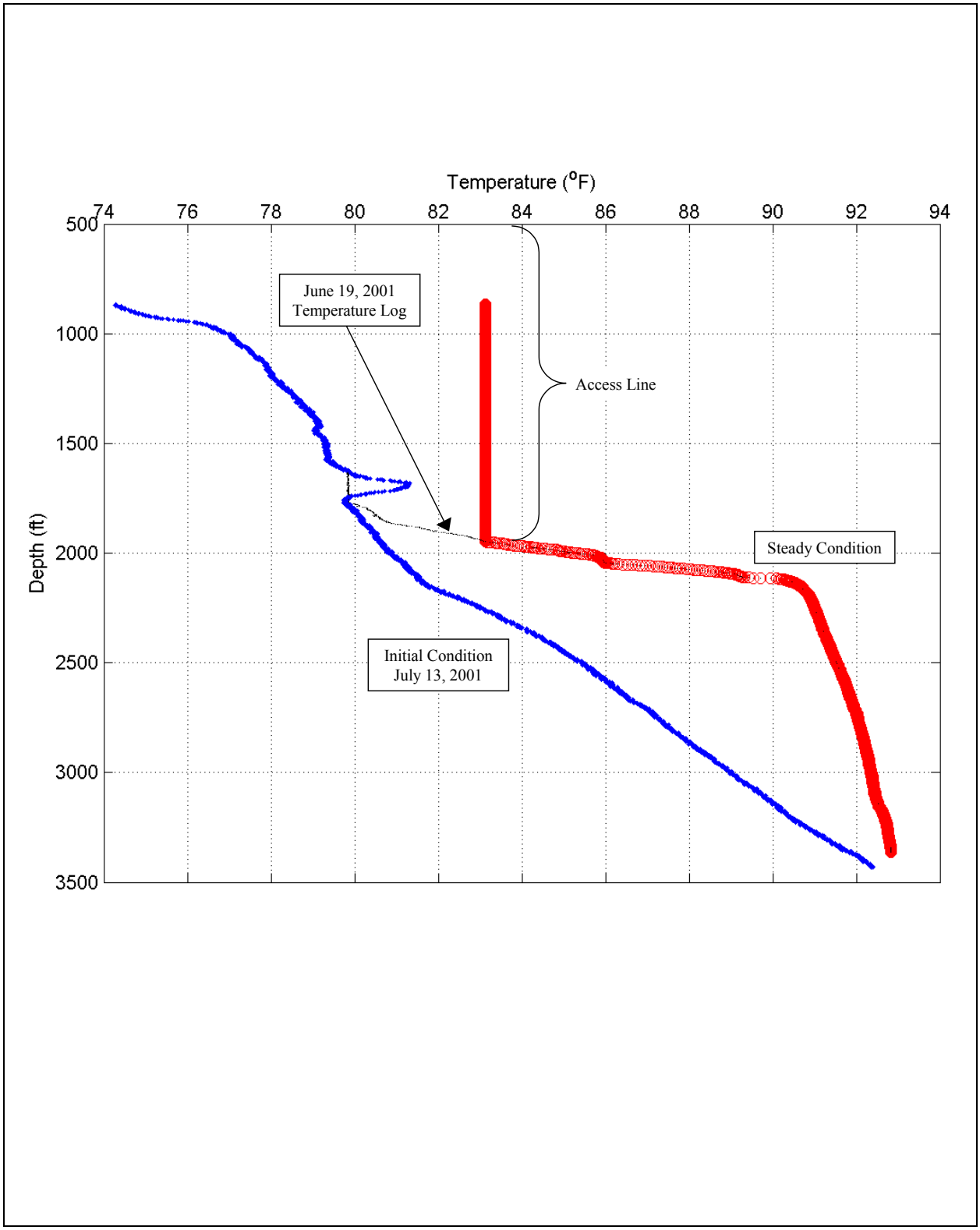

Figure 2-4
ER-5-4 Single-Well Test: Wellbore Temperature Profiles Applied in the Correction for Thermal Effects on Measured Pressure

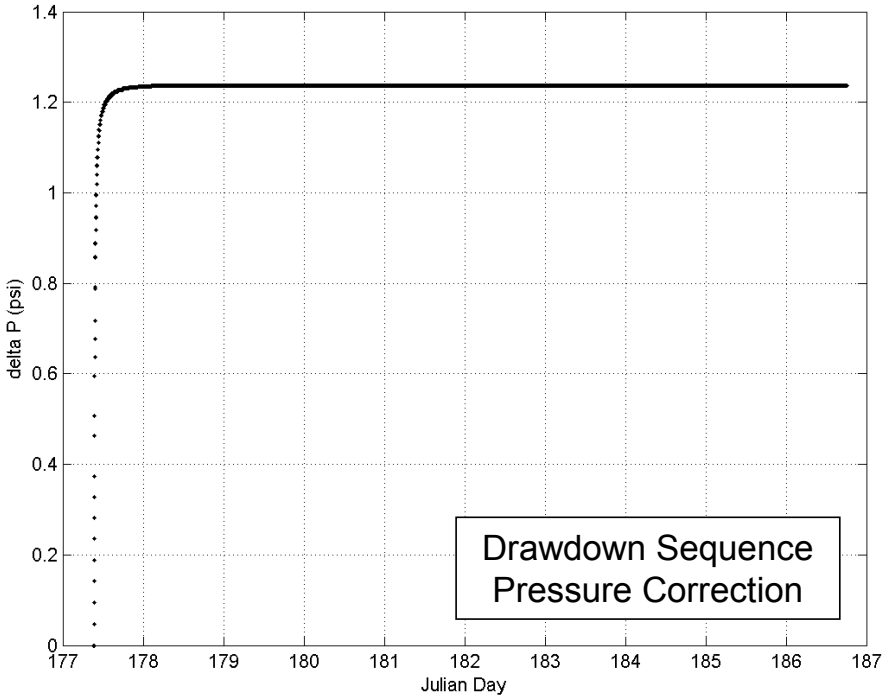

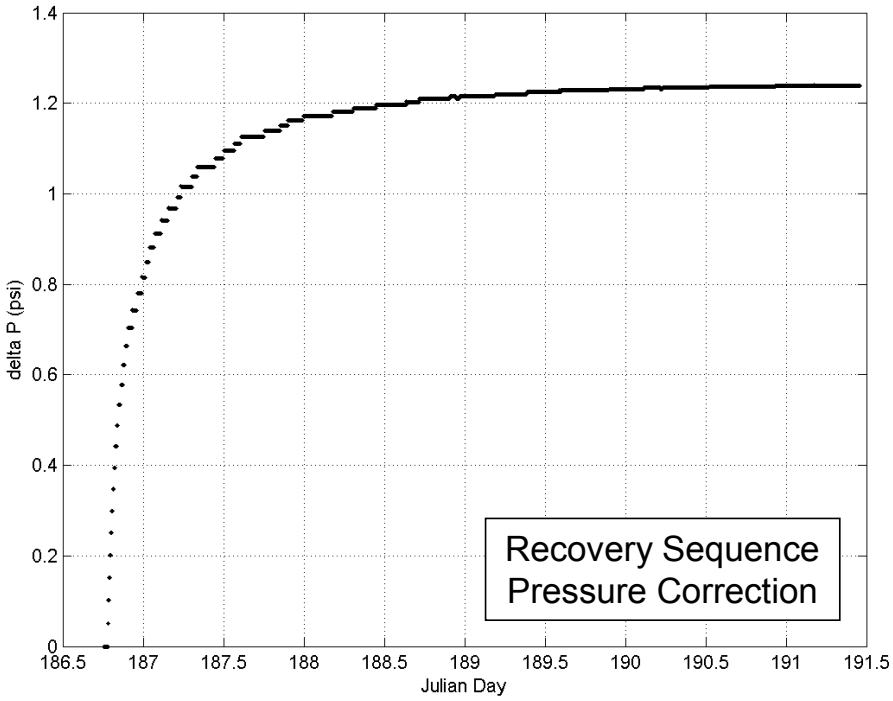

Figure 2-5
ER-5-4 Single-Well Test: Temperature-Corrective Component of Measured Pressure during the Constant-rate Test

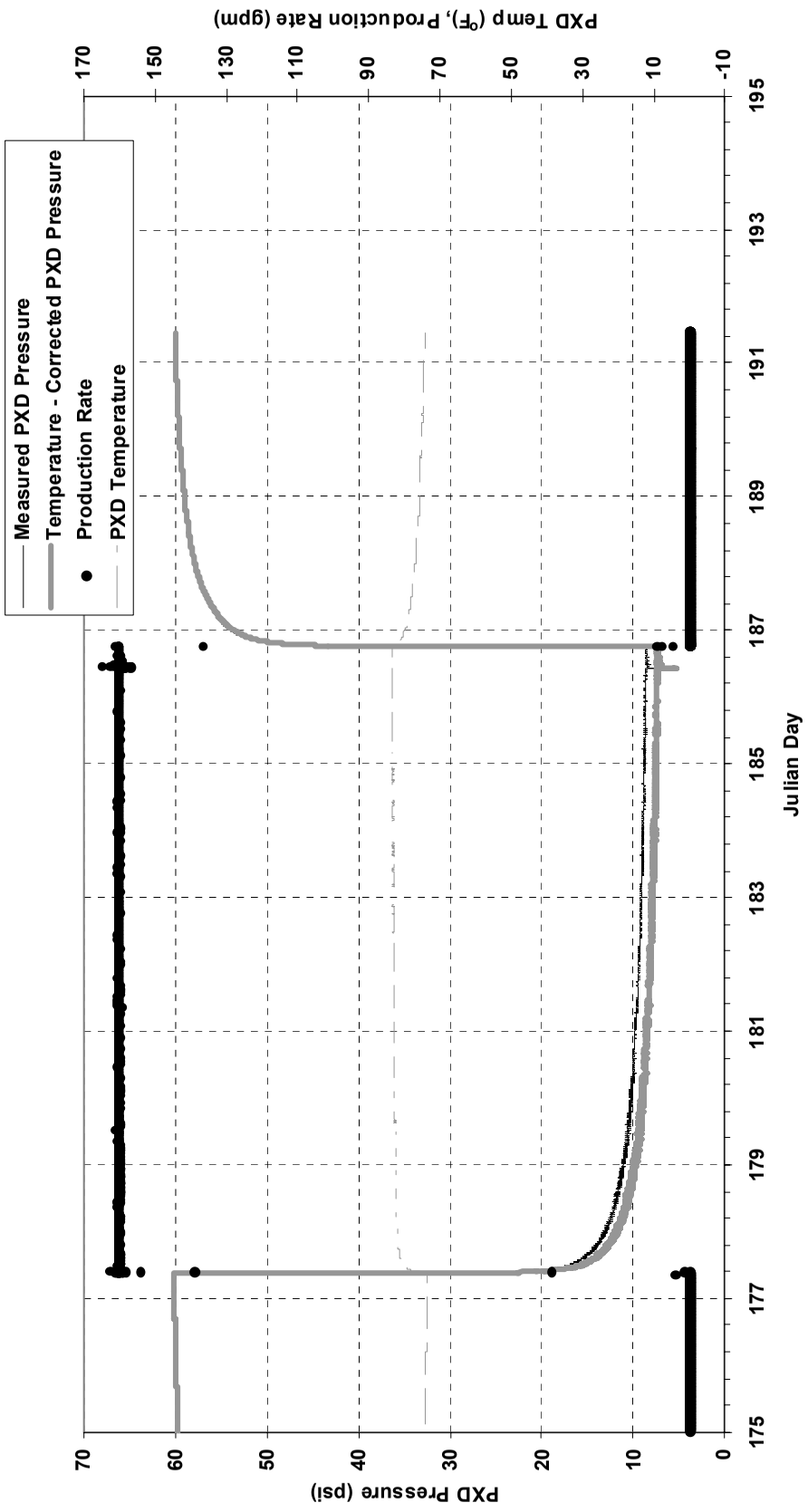

Figure 2-6
ER-5-4 Single-Well Test: Constant-rate Test Measured and (Temperature) Corrected Well Response Data

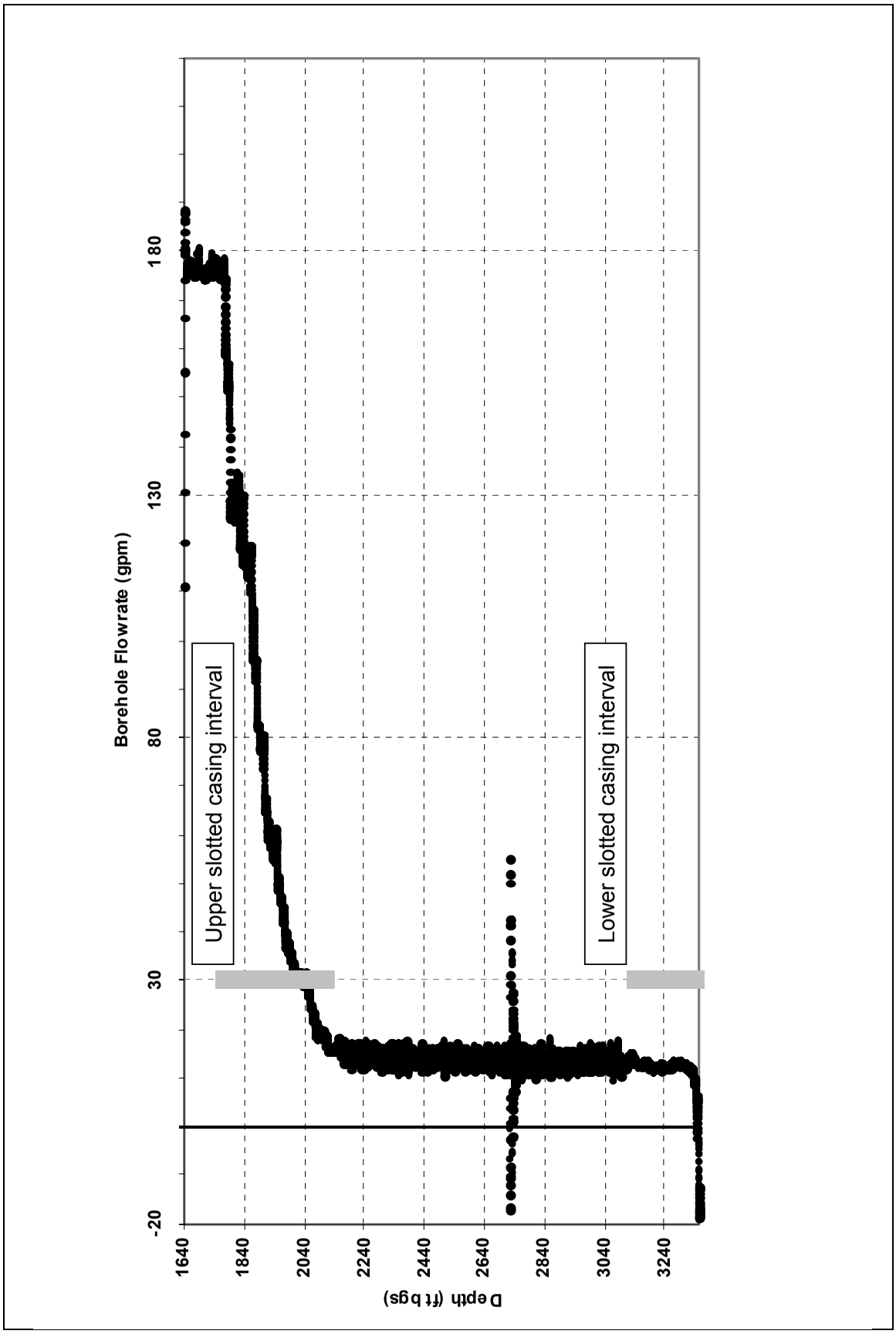

Figure 2-7
ER-5-4 Single-Well Test: Analysis of Impeller Flow Log to Determine Formation Thickness

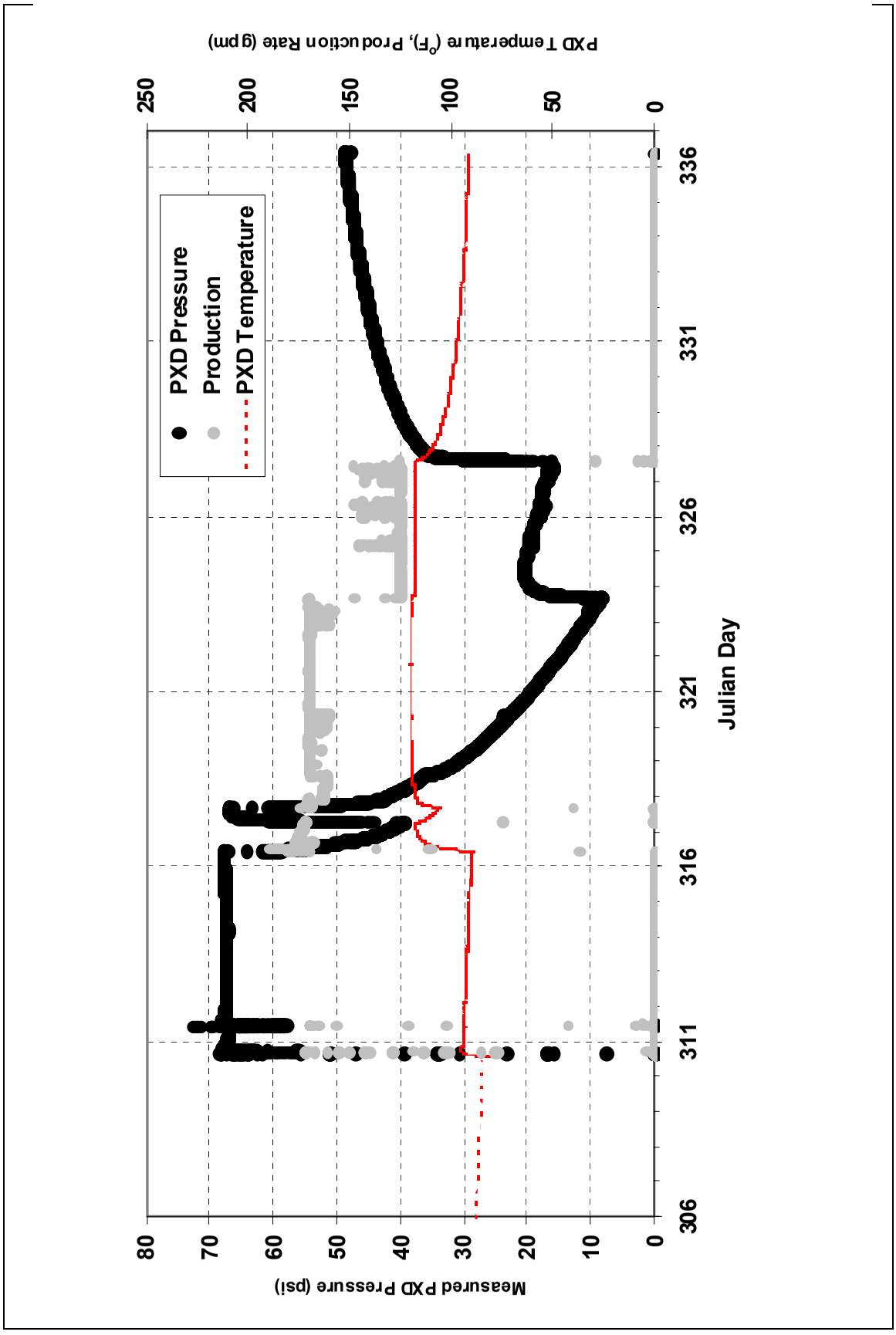

Figure 2-8
ER-5-4#2 Single-Well Test: Measured Constant-rate Test Data

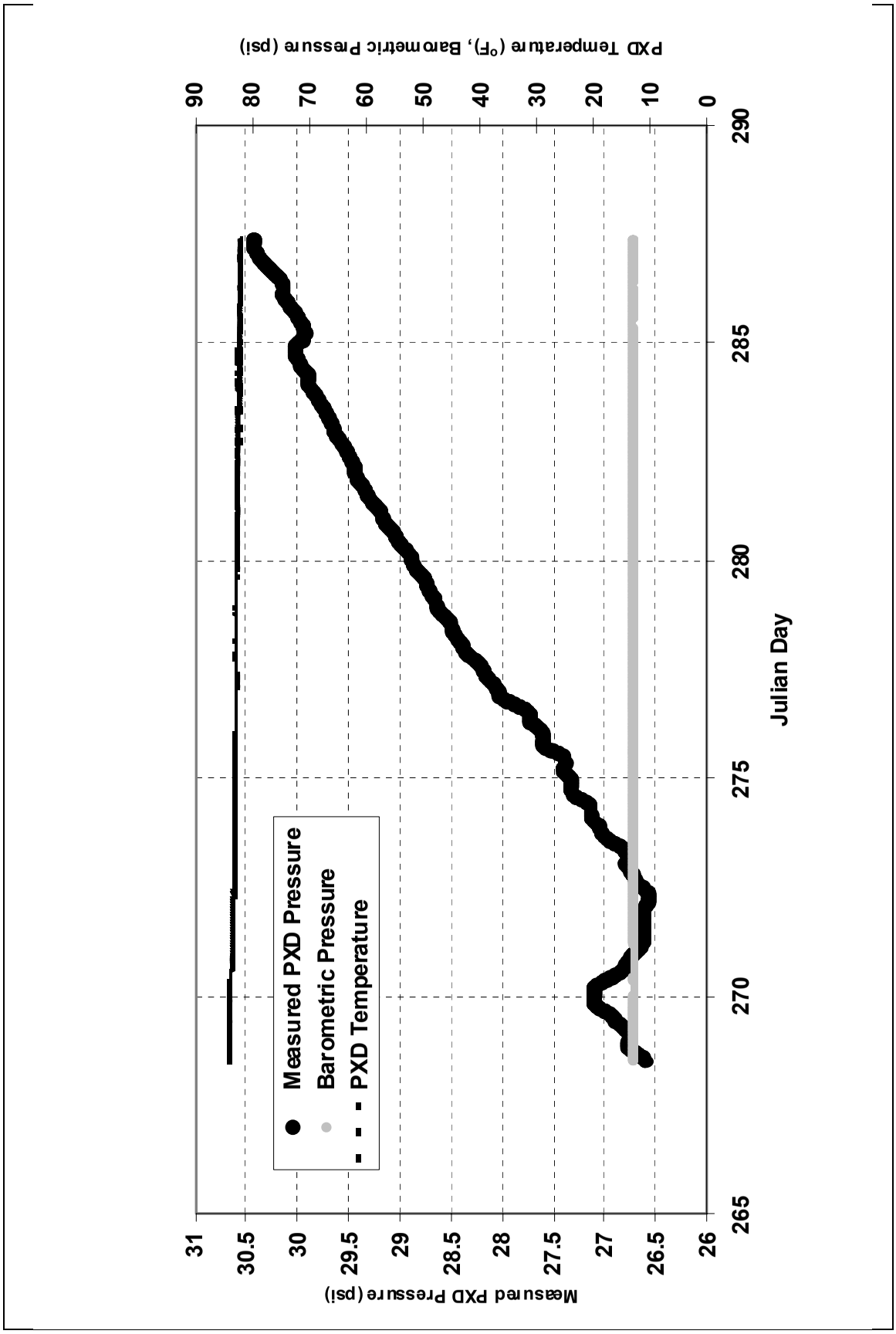

Figure 2-9
ER-5-4#2 Single-Well Test: Predevelopment Well Monitoring

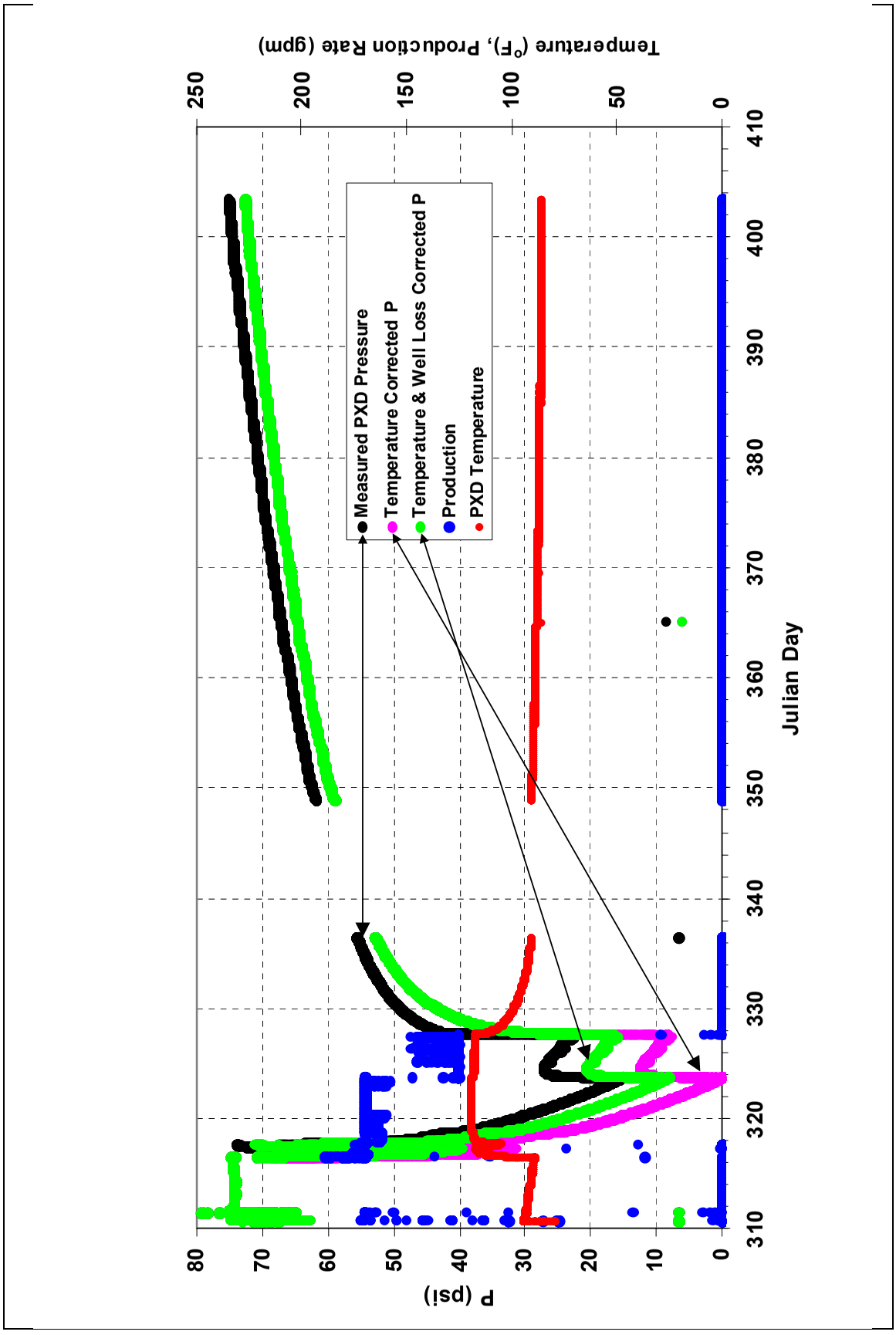

Figure 2-10
ER-5-4#2 Single-Well Test: Constant-rate Test Measured, Temperature Corrected, and Well Loss Corrected Well Response Data

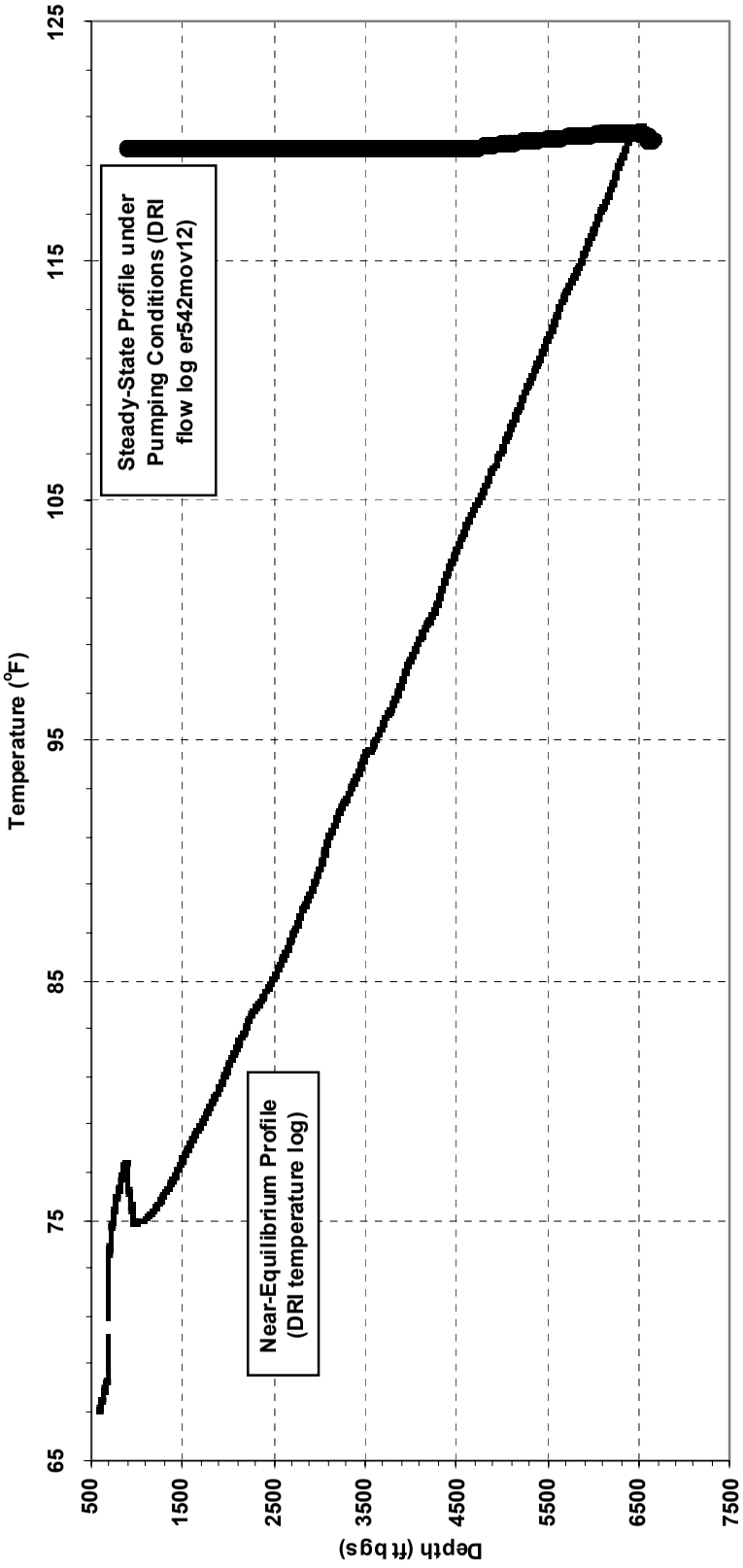

Figure 2-11
ER-5-4#2 Single-Well Test: Wellbore Temperatures Profiles Applied in the Correction for Thermal Effects on Measured Pressure

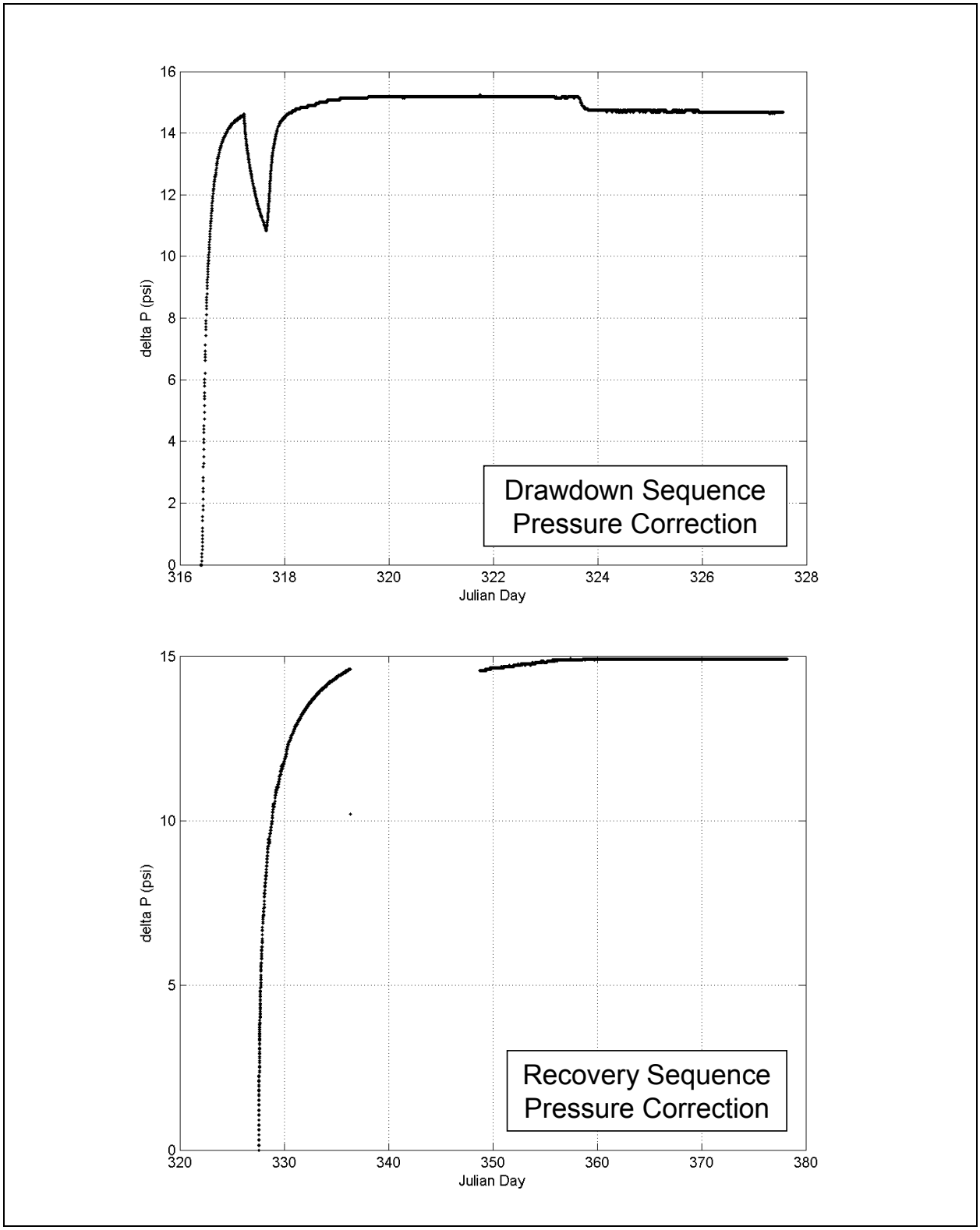

Figure 2-12
ER-5-4#2 Single-Well Test: Temperature-Corrective Component of Measured Pressure during the Constant-rate Test

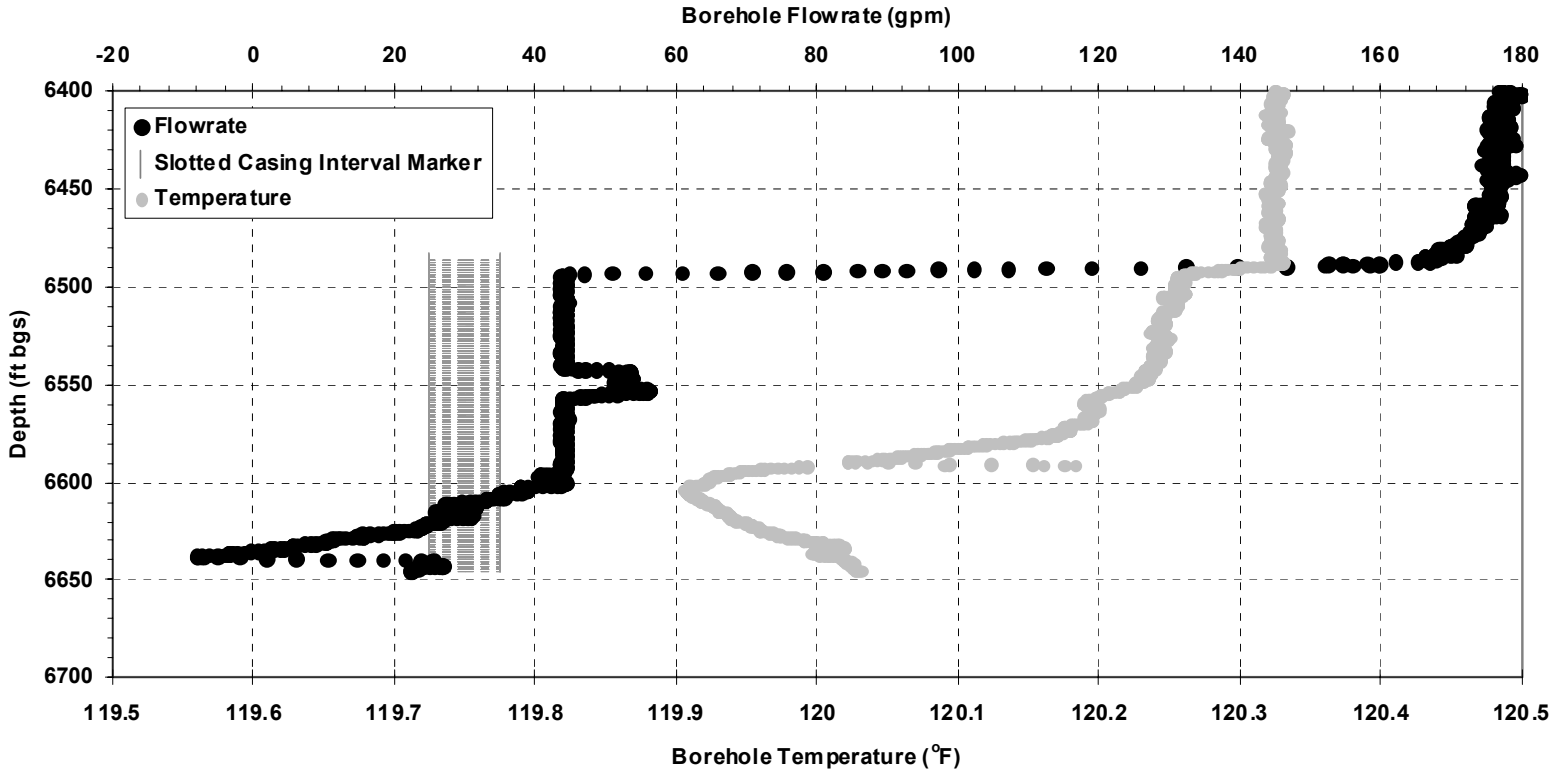

Figure 2-13
ER-5-4#2 Single-Well Test: Analysis of Impeller Flow and Temperature Logs to Determine Formation Thickness

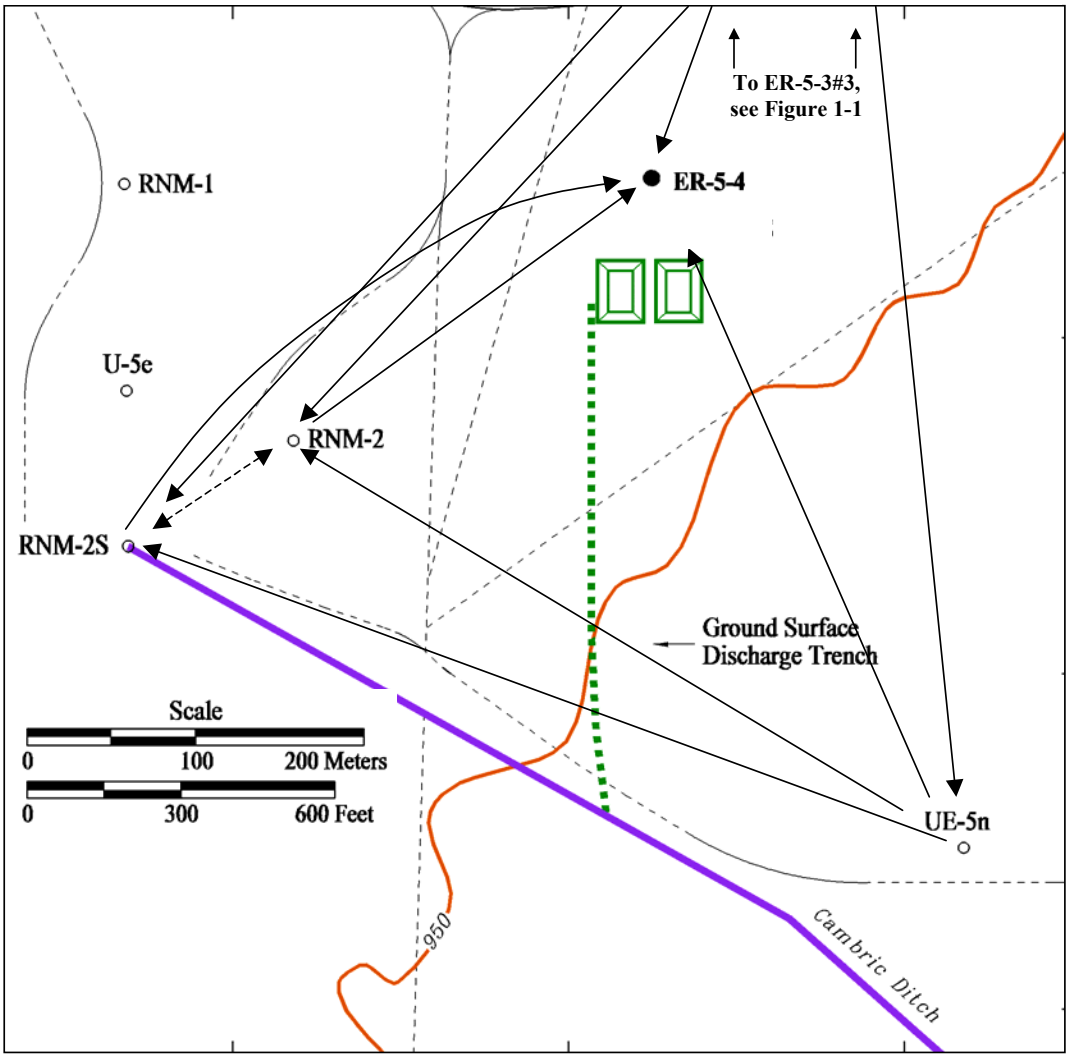

	RNM-2s	RNM-2	ER-5-4	UE-5n	ER-5-3#3
RNM-2s	-	0.00029*	0.00074	-0.00051	-0.00015
RNM-2	-	-	0.00090	-0.00063	-0.00015
ER-5-4	-	-	-	-0.00125	-0.00020
UE-5n	-	-	-	-	-0.00010
ER-5-3#3	-	-	-	-	-
*Head difference between wells is within measurement uncertainty (0.23 ft)					

Figure 2-14
Horizontal Hydraulic Gradients through the RNM-2s Well Cluster Prior to the RNM-2s MWAT

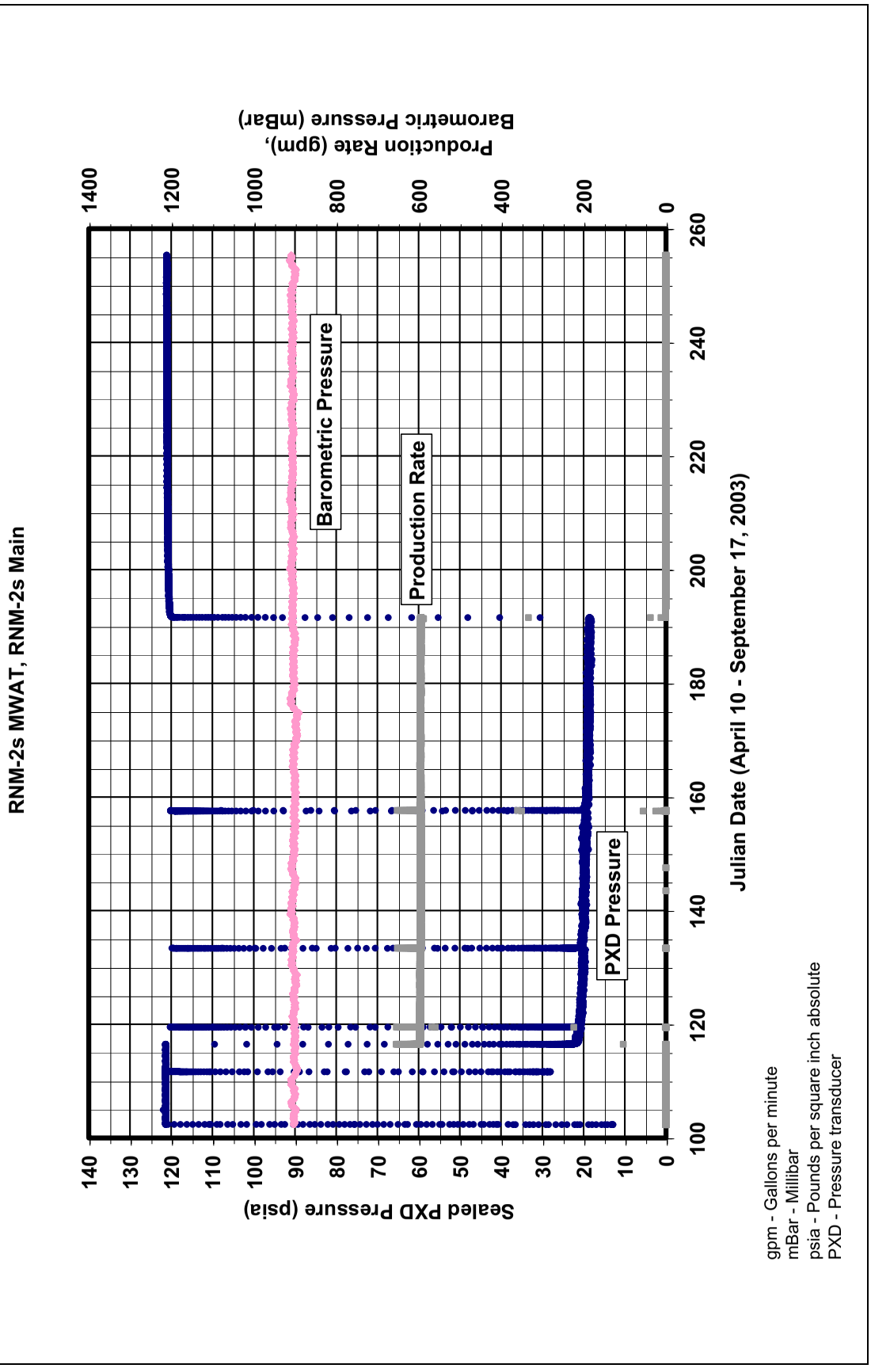

Figure 2-15
RNM-2s MWAT Monitoring Record

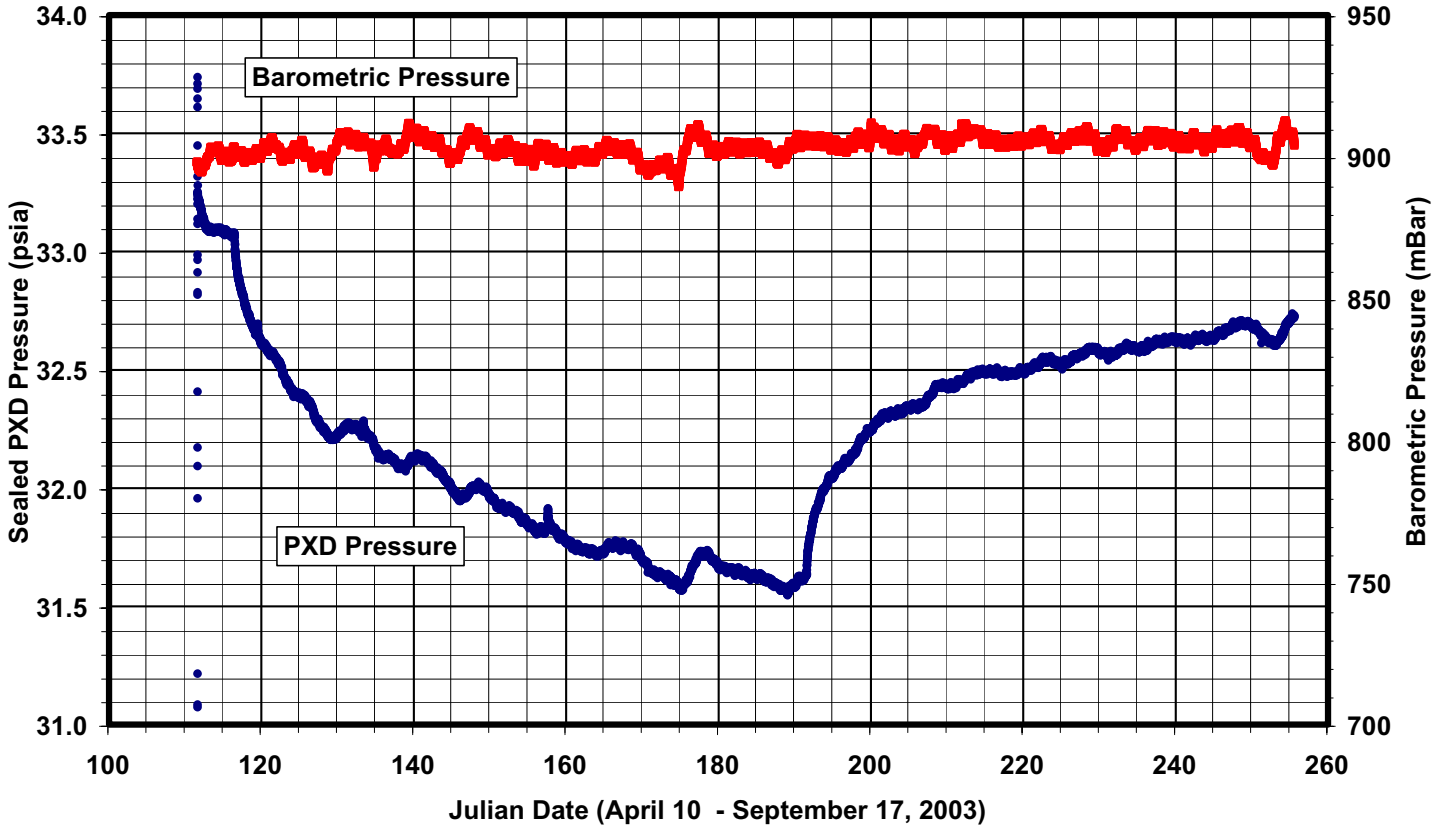

mBar - Millibar
psia - Pounds per square inch absolute
PXD - Pressure transducer

Figure 2-16
RNM-2 Monitoring Record During Pumping of RNM-2s

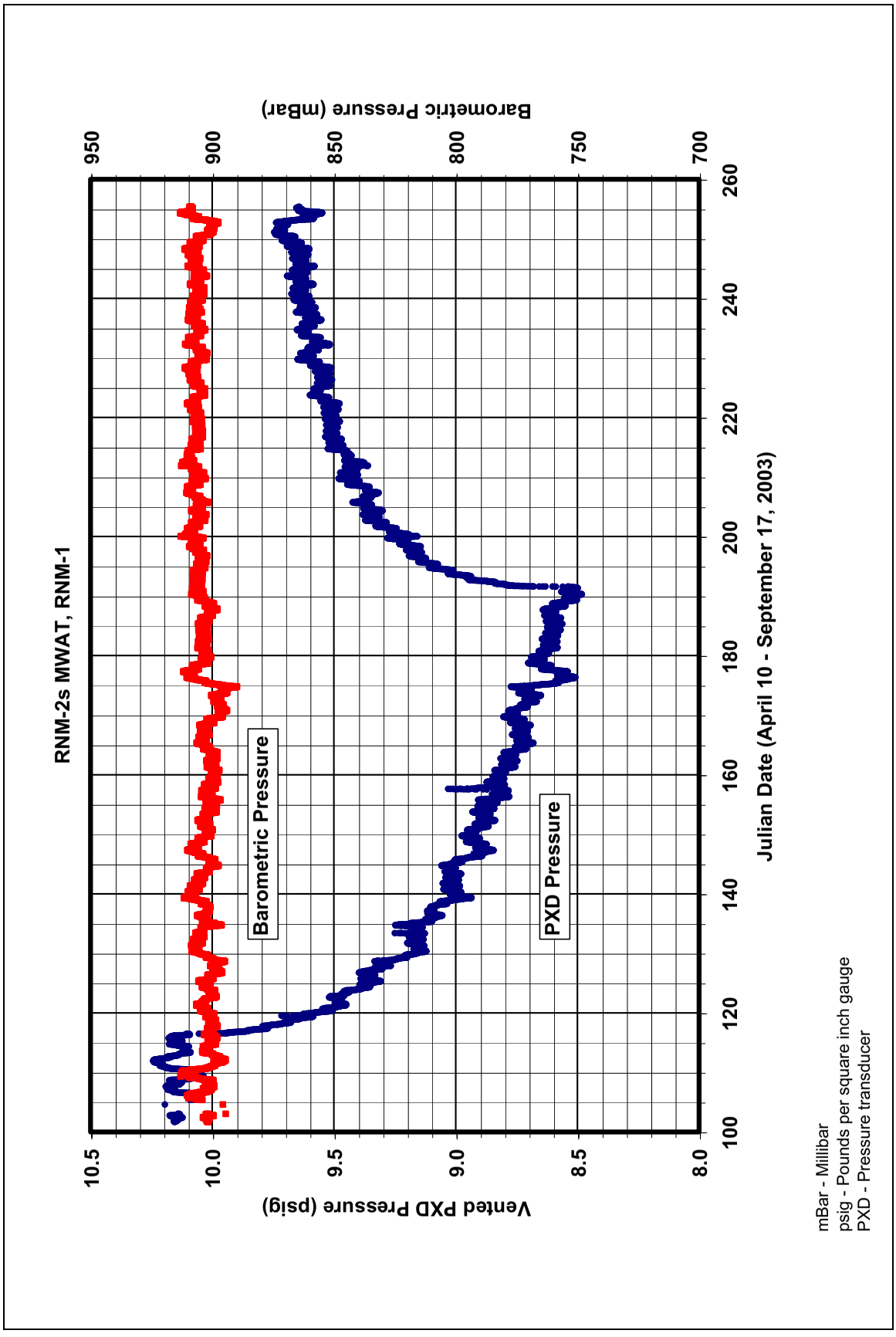

Figure 2-17
RNM-1 Monitoring Record During Pumping of RNM-2s

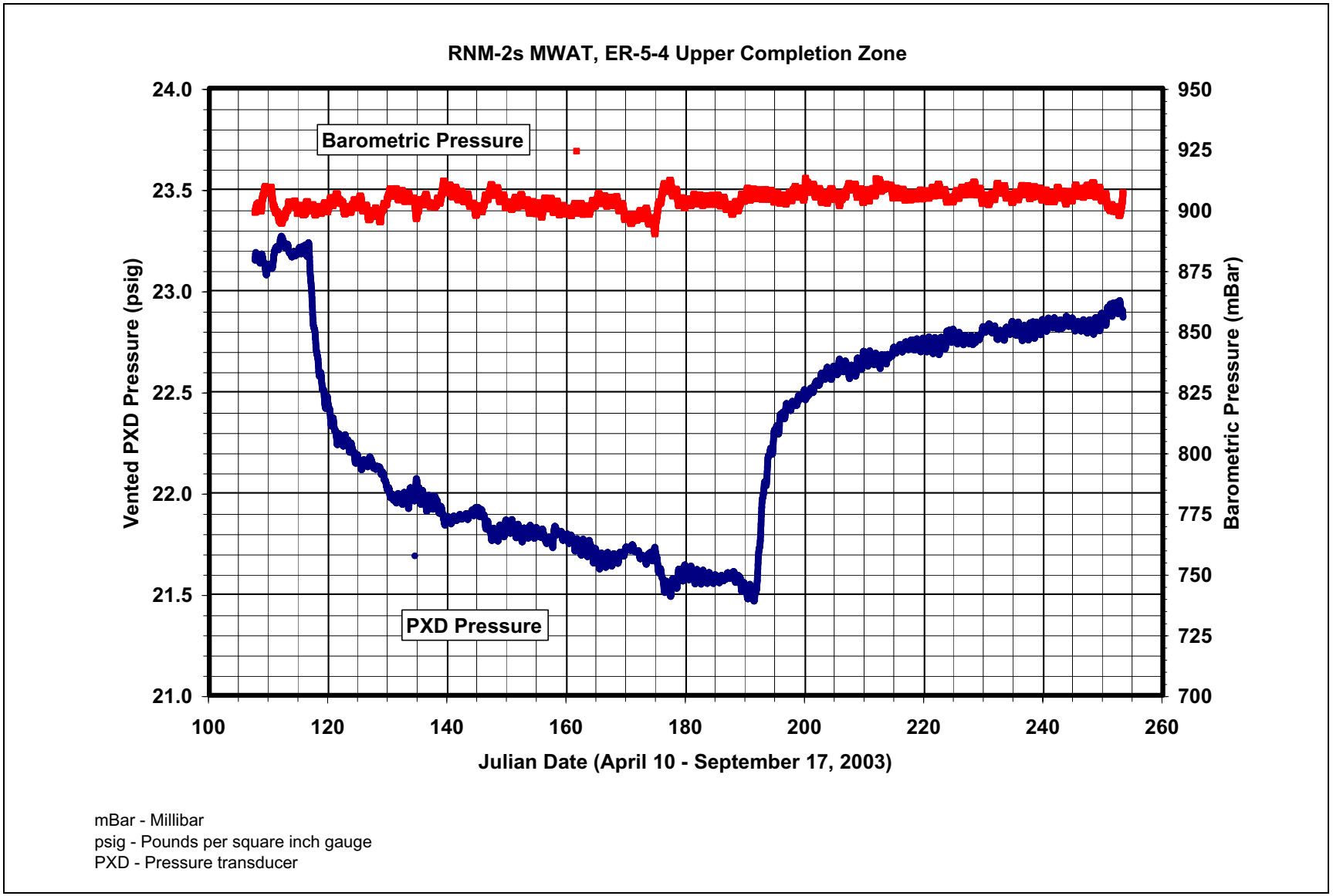

Figure 2-18
ER-5-4 Upper Completion Zone Monitoring Record During Pumping of RNM-2s

3.0 Interpretation of Hydraulic Testing

Hydraulic properties are estimated from single- and multiple-well aquifer tests by fitting formation response model results to observed drawdowns. This section addresses the general method of analysis that is applied to constant-rate hydraulic testing data. The following sections present the analytical details of each well test and the formation hydraulic properties derived.

nSIGHTS

The analysis is conducted using the well-test analysis code nSIGHTS (n-dimensional Statistical Inverse Graphical Hydraulic Test Simulator). nSIGHTS uses a numerical approach to simulate radial/nonradial groundwater flow through a single-phase, one- or two-dimensional flow domain in response to boundary conditions applied at the production well. The simulation of the hydraulic response to the imposed boundary conditions permits a solution to the inverse problem of determining formation (flow domain) hydraulic parameters from measured transient pressure and flow-rate data. The flow domain is discretized into a system of concentric rings centered on the borehole that uses a multiplicative factor to increase the spacing between rings with the increasing distance from the borehole. Each ring is represented by a node, hence the radial symmetry. If warranted, vertical stacking of layers adds a second dimension to the domain discretization. The simulation of flow and pressure through a laterally heterogeneous domain of variable thickness is permitted; however, vertically homogenous hydraulic properties are assumed.

The flow domain for each of the single-well test analyses is specified as a confined, single-porosity, one-dimensional flow system. Justification for these conceptualizations are discussed in the analyses sections. The formation thickness, defined for the ER-5-4 (Section 2.1.2.2) and ER-5-4#2 (Section 2.2.2.2) single-well tests, are used to define the tested formation thickness assumed for the simulation. The flow domain for each of the MWAT observation wells is specified as an unconfined, single-porosity, two-dimensional flow system. Although these conceptualizations are discussed further in the analyses sections below, it is important to note that the formation thickness *tested* is not a clearly defined datum. The formation pressure response is permitted to propagate both horizontally and vertically from the production well and defines the region of the aquifer that is tested. The formation hydraulic properties influence the rate and direction of propagation, but may themselves be dependent (via the inverse optimization method) on the formation thickness if aquifer boundaries are encountered in the pressure response. Therefore, the formation thickness *tested* may be dependent on the specified formation thickness. For the simulations, the well completion zone intervals are discretely specified relative to the entire thickness of the AA (Section 2.3.3, Section 3.3.1).

nSIGHTS was developed for Sandia National Laboratories, founded on the well-test analysis code GTFM (Graph Theoretic Field Model), the precursor to nSIGHTS. A description of the governing equations used in both codes is found

in Pickens et al. (1987). nSIGHTS was verified following Sandia National Laboratories' Nuclear Waste Management Program Procedure NP 19-1, "Software Requirements," Rev. 4 to meet NQA-2 requirements (ASME, 1990). Verification of nSIGHTS was documented through comparison to the analytical solutions for constant-drawdown confined tests (Lohman, 1972), constant-rate unconfined drawdown tests (Barlow and Moench, 1999), slug tests (Cooper et al., 1967), and pulse tests (Bredehoeft and Papadopulos, 1980). Further details on the unconfined aquifer capability, relevant to the RNM-2s interpretation, are presented in Section 3.3.1.

Flow and Pressure History Sequencing

At each well, formation hydraulic parameters are estimated through an inverse procedure that fits the parameter solutions to the measured formation response using the nSIGHTS numerical model. The measured response is the pressure (or drawdown) recorded through the entire constant-rate production period, including the post-production recovery period. In order to solve the inverse problem, constraints must be specified that permit the fitting algorithm to match the simulated response to the measured data. The more numerous the number of constraints, the better constrained the solution or parameter estimate.

nSIGHTS permits sequencing of the drawdown record during constant-rate production. A sequence is a discrete time interval during a testing period that represents a continuous period of consistent wellbore boundary conditions. Sequencing serves to better constrain the problem, allowing the simulation to consider the cumulative effect of changing wellbore boundary conditions. Sequencing further permits the identification and exclusion, if necessary, of discrete pressure intervals from the simulation that may represent measurement error, uncertainty, and or uncharacteristic response.

Unless otherwise specified, the drawdown records are segmented into two sequences that correspond to the periods of constant-rate production and recovery. The sequencing of the data are shown below during the analysis of each well-test. Prior to the start of testing at each well, the records are defined as pressure history sequences for the simulation. These are time periods during which borehole pressures are specified as constant or variable in time to better constrain the formation initial conditions prior to the start of testing. This is necessary because lingering pressure transients from pretest activities can affect the test interpretation (Pickens et al., 1987).

Fitting and Nonfitting Parameters

Parameter values that describe the physical flow domain and flow dynamics of the well and contributing formations must be specified for radial flow simulation of the constant-rate test. These are of two types, nonfitting and fitting. Nonfitting parameters are primarily those physical quantities based directly on field or laboratory measurement (i.e., they are known with a relatively high degree of certainty). Fitting parameters are primarily hydraulic attributes of the flow domain that are known with little certainty. It is the fitting parameters that

comprise the solution to the inverse problem. Accordingly, it is the fitting parameters that are subject to the uncertainty inherent in an inverse problem.

Nonfitting parameters specified in nSIGHTS principally pertain to wellbore dimensions, fluid properties, and formation attributes that are known with confidence. Wellbore dimensions include the wellbore area through the completion interval and the casing. The fluid density and thermal expansion coefficient are specified as constants. As discussed in Section 2.0, the single-well testing data were corrected for temperature/density/volume expansion prior to simulation. The MWAT observation well data did not require correction for these fluid property effects.

Formation parameters denoted as nonfitting are the formation thickness, external boundary radius, flow dimension, and static formation pressure (although when justified, the flow dimension and static formation pressure are specified as fitting parameters). The formation thickness is determined from the composite length of contributing formations in each well. The identification of the formation thickness at each test well was presented in Section 2.0.

The external boundary radius is set sufficiently large that the formation is assigned an apparent infinite horizontal extent. Depending on the simulated radius of influence for each well test, the external boundary radius is set constant at either 10^5 or 10^6 meters (m).

The flow dimension represents the geometrical flow configuration within the formation, ranging from linear (1.0) to spherical (3.0) flow. In most cases, formation flow toward/away from the well can be assumed radial. Unless the testing data provide evidence of a nonradial flow geometry, the flow dimension is defined as a nonfitting parameter and is set constant at 2.0 (radial). When the flow geometry is shown to be other than radial, the flow dimension is defined as a fitting parameter. These definitions are discussed individually below for each well-test analysis.

The static formation pressure at the pressure transducer depth, equivalent to a SWL when the wellbore temperature is at equilibrium, is defined as a nonfitting parameter when data are available for its definition. As a nonfitting parameter, this datum can provide an important constraint to the simulated drawdown. In general, static and equilibrium well conditions are measured during either a long-term predevelopment or recovery sequence. In the absence of these measured conditions, the static formation pressure/water level is defined in the simulation as a fitting parameter.

The fitting parameters used in nSIGHTS are the composite horizontal, and possibly vertical, formation hydraulic conductivity (K_h and K_v) and the composite formation specific storage (S_s). Estimation of the K and S_s parameter solutions comprise the primary motive of the analysis and are necessary for use in later CAU-scale flow and transport modeling. Details of the K and S_s estimation are specified during the individual well-test analyses presented below.

An additional complication that may be considered is the presence of near-wellbore clogging or damage from drilling. This effect is well known in the petroleum industry where it is described as "skin effect." This effect results in an additional pressure drop in a thin zone between the formation and the wellbore. In the most rigorous representation (used by nSIGHTS), both the near-wellbore zone and formation have individual hydraulic conductivity and storage values (Novakowski, 1990). Incorporating skin effects would result in adding two more parameters to be estimated that are completely unknown. Although the simulation of the test may be improved, it is unlikely that the additional parameterization required would contribute any physical validity. The parameters would be arbitrary values used to improve the model fit to the data.

Parameter-Estimate Numerical Uncertainty and Perturbation Analysis

The problem of inferring formation hydraulic parameters from measured pressure response and well production data is an inverse problem. Inherent to any inverse problem is some degree of numerical uncertainty in the parameters estimated that is primarily a result of parameter correlation. nSIGHTS is complete with a suite of statistical routines that support the identification of parameter uncertainty. Estimated parameter uncertainties for the single-well test analyses are addressed from a numerical perspective through a perturbation analysis. Parameter uncertainties for the MWAT are addressed through a comparison of results derived from the analysis of observation well data.

A perturbation analysis is performed using nSIGHTS for the ER-5-4 and ER-5-4#2 single-well test analyses. The method provides a means to test the numerical correlation and uniqueness of the hydraulic parameter solutions. In general, a perturbation analysis is performed by applying random perturbations to the initial (user specified) estimates of the fitting parameters. For each set of perturbations, the fitting parameters are reoptimized. The perturbation range for each parameter is specified by the user. Ideally, the process is repeated until all possible initial parameter estimate combinations, given that the continuous range for each parameter is binned, are specified as initial conditions for the simulation. Further details of the perturbation analyses performed are presented below as appropriate.

3.1 Well ER-5-4 Single-Well Constant-rate Test

Well ER-5-4 is cased to a TD of 3,438 ft bgs. The cased well completion is slotted over two discrete intervals of the AA that are vertically separated by a 1,023-ft blank casing interval (Figure 1-3). The formation thickness tested is defined as the combined 557-ft section comprising both slotted casing intervals (Section 2.1.2.2). The constant-rate test was performed for 10 days between June 26, 2003 (JD 177) and July 5, 2003 (JD 186), and the recovery of the well was monitored for five days to July 10, 2001 (JD 191).

The following sections present the conceptualization of the model flow domain, the AA hydraulic property estimates derived from simulation of the measured formation response at ER-5-4, and the parameter estimate uncertainties.

3.1.1 Formation Flow Model Conceptualization

The production rate and formation pressure response at ER-5-4 through development and constant-rate production are shown in Figure 3-1. The complete response record is discretized into a series of flow and pressure sequences. As reported, the development record is included in the simulation to account for lingering pressure transients in the formation from pre-test pumping. The constant-rate test drawdown and recovery sequences are respectively identified as flow sequences F_03 and F_04 in the figure.

A log-log diagnostic analysis of the drawdown and recovery sequences is used to assist in the identification of a conceptual flow model and geometry for the formation (AA) tested. The typical log-log diagnostic analysis permits the temporal identification of flow regimes within both the wellbore and the formation. These include, for example, production periods of wellbore storage, skin effects, and infinite acting single- and double-porosity flow. The log-log diagnostic plots for flow sequences F_03 and F_04 are shown in Figure 3-2. Beginning at the start time of each sequence, the brief wellbore storage period and approximate $1^{1}/_{2}$ log cycle period during which the pressure response undergoes a transition between wellbore and formation response is shown (Horne, 1995). Following this period, the derivative plot shows a downward trend in both sequences. Purely infinite acting radial flow geometry would be identified as a horizontal line segment (zero slope) on the derivative plot. The downward trend, confirmed in both flow sequences, indicates that the formation pressure response dissipates at a faster rate than it would under Theis-like aquifer conditions. In general, the trends imply that the formation tested is able to contribute flow to/from the well in a greater volume than would be supplied from purely radial flow, e.g., a constant pressure boundary may have been encountered. Conceptually, there are several hydrogeologic scenarios which could produce the observed data.

The AA tested is a poorly consolidated unit comprised predominantly of sand with minor components of silt and gravel. There are no known hydrogeologic boundary conditions within the immediate (tens-of-meters scale) vicinity of ER-5-4 that would produce such a response. Therefore, given the poor consolidation, it is possible that a vertical component of formation flow exists near the well (i.e., a flow geometry that exceeds radial flow), or some other strong change in formation properties occurs. Although speculative, this supposition is addressed further with respect to the flow dimension fitting parameter, discussed and presented in the following sections. Further, information is provided by the response data measured at the ER-5-4 observation well during MWAT pumping, the MWAT being an aquifer test of significantly longer duration, and therefore testing a larger area of the AA, than the ER-5-4 single-well test (see Section 3.3.4).

3.1.2 Simulation of the Formation Response

The Cartesian flow sequence data in F_03 and F_04 (Figure 3-1) are used for simulating the pressure responses to pumping and recovery. For the simulation,

the fitting parameters are defined as the formation hydraulic conductivity, formation specific storage, static formation pressure, and flow dimension. The flow dimension was optimized as a result of the conceptual formation flow model that was presented in the preceding section. In addition, a well skin hydraulic conductivity and specific storage were defined as fitting parameters. The slotted (5.5-in.) casing intervals are enclosed by a gravel pack, whose radial thickness is defined as the skin thickness, within the larger diameter (12.5-in.) borehole. As discussed, these well skin parameters are given arbitrary values, are used to improve the model fit to the data, and cannot in reality be constrained. Their physical validity is questionable; however, the well construction warrants their inclusion in the simulation.

As reported, the formation thickness was defined as the composite thickness (557-ft) of both the upper and lower slotted casing intervals. Therefore, the parameter estimates, in particular the formation hydraulic conductivity, are simulated for the composite response. The partitioning of the composite estimate into the upper and lower zone components is addressed below (Section 3.1.4).

3.1.3 Parameter Estimates, Numerical Uncertainty, and Physical Uncertainty

Initial simulations of the pressure response data showed that multiple parameter estimates (solutions) were able to equivalently fit the measured data through nonlinear optimization. A 1,000-simulation perturbation analysis was performed to assess the range of parameters, both for individual parameters and between parameters, that are able to provide equivalent numerical fits. A horsetail diagram of the best numerical-fit simulated data is shown in Figure 3-3 (top); each simulated response is defined by a different set of fitting parameters. Figure 3-4 (top) shows the large range of formation K and S_s solution pairs that correspond to the simulated responses, plotted against the fit statistic sum of squared errors (SSE). It is important to note that these solutions reflect only the numerical uncertainty of the parameter solutions that is inherent to the inverse method; they do not reflect actual (physical) uncertainty because the aquifer storage parameter cannot be constrained from single-well pump-test data. A scatterplot of the same solution pairs are plotted in Figure 3-4 (bottom), as well as are the initial parameter estimates used in the perturbation analysis. The initial estimates show that a sufficiently large range of parameter-space was considered for the simulations.

Figure 3-4 shows that, from a purely numerical perspective, the solution sets are poorly constrained and that the solution "surface" does not contain an apparent global (best-fit) minimum. To constrain the uncertainty in estimated hydraulic conductivity within a physically realistic range, a realistic range of specific storage for the AA is defined. From first principles,

$$S_s = \rho g(\alpha + n\beta) \qquad (3\text{-}1)$$

Fluid density (ρ = 1,000 kg m^{-3}), gravity (g = 9.8 m s^{-2}), and fluid compressibility (β = 4.4 x 10^{-10} m s^2 kg^{-1}) are assumed constant. n is effective porosity and α is vertical matrix compressibility. α in this context represents bulk compressibility,

which considers the effects of both pore volume reduction and inter-matrix compression under hydrostatic pressure. However, under the assumption that the rock inter-matrix grains are incompressible, bulk (total) compressibility is equivalent to pore volume compressibility.

Representative specific storage values for the AA are presented in Table 3-1. Defining the K-S_s solution pairs presented in Figure 3-4 with respect to this storage range, the K solution range becomes well constrained. Figure 3-5a shows the cluster of K solutions that define the physical uncertainty for this parameter, and Figure 3-3 (bottom) show the corresponding set of simulated responses. Under the reasonable assumption that each fit is equivalent and equiprobable, the K estimates are uniformly distributed and range from 1.6×10^{-6} - 3.2×10^{-6} m s^{-1}. Figure 3-4 (bottom) shows that the K range is numerically insensitive to S_s within this range.

Table 3-1
Calculated HSU Specific Storage

Well Name	Rock Type	n_{min} (-)	n_{max} (-)	alpha$_{min}$ (m^2 N^{-1})	alpha$_{max}$ (m^2 N^{-1})	$S_{s\ min}$ (m^{-1})	$S_{s\ max}$ (m^{-1})
ER-5-4	Alluvium	0.238[a]	0.402[a]	5.2×10^{-9}[b]	1.0×10^{-8}[b]	5.0×10^{-5}	1.0×10^{-4}
ER-5-4#2	Tuff (bedded, non-welded to welded)	0.10[a]*	0.55[a]*	5.1×10^{-10}[c]	2.3×10^{-9}[c]	5.4×10^{-6}	2.5×10^{-5}

[a] Shaw (2003)
[b] Domenico and Schwartz (1990)
[c] Touloukian and Ho (1981)
* Assuming all storage from the porous matrix

The constrained response simulations, shown in Figure 3-3 (bottom), show that the optimized static formation pressure accurately reproduces the measured data.

The optimized flow dimension is about 2.04 (radial), as shown in Figure 3-5b. However, this single value is representative of the late-time, final flow geometry within the area of influence, centered at ER-5-4. That is, the flow dimension represents the largest volume of aquifer that was tested; therefore, it is representative of the flow geometry averaged over that volume. However, the flow dimension varies through response time as the formation pressure transient travels into the formation and the effective area of flow contribution increases with radial distance into the formation. Figure 3-5c shows a plot of the flow dimension through both pumping and recovery time, and in fact shows that in the earlier periods of each sequence the flow dimension is greater than 2.0. This supports the conjecture that there may be a vertical component of flow or some strong change in storage properties near the well above/below the completion zone. This result is confirmed by analysis of the ER-5-4 observation well response during the MWAT, where the data are representative of a significantly longer duration response (see Section 3.3.4).

The well skin parameter estimates are not presented. As appropriate, the data were poorly constrained and uncorrelated with the formation hydraulic property estimates, confirming their lack of physical meaning.

3.1.4 Partitioning of Formation Hydraulic Conductivity

The best-fit hydraulic conductivity solution set is representative of the composite response derived from measured flow through both slotted casing intervals. In order to reduce uncertainty within the K solutions presented, the composite response is partitioned respective to the upper and lower completion intervals. The analysis requires that both the formation head and percent of total flow contribution are known at each interval.

The upper completion head is, on average, higher than that in the lower completion. This was shown from the 3.99-ft head difference between the zones that was measured after the bridge plug installation at 2,290 ft bgs (Section 2.1.1). The gradient direction is confirmed from ambient flow logging using the DRI thermal flowmeter tool; there is natural downward flow between the completions at a depth averaged rate of 0.52 gpm.

Impeller flow logs measured during pumping conditions show that the percent contribution to well production from each completion varies with the production rate. Flow logs were measured at rates of 70, 125, and 175 gpm. In general, formation zones with higher head will contribute more flow to the well. This is unquestionably true when the transmissivity of the zones are equal. At the 70 gpm rate, the majority of inflow to the well was through the upper zone; there was on average an 8 percent inflow contribution from the lower zone. At the 125 and 175 rates, inflow from the lower zone increased to 9 and 11 percent, respectively. These data show that the interval flow rates should not be accepted completely at their measured values; the flow logging data are not strictly representative of the formation interval transmissivity. By increasing the pumping rate, the measured production from the lower interval will increase as the head gradient between the formation zone and wellbore increases. However, if well losses (turbulent and friction induced) attributed to the lower zone are greater than the entrance losses of the upper slotted completion, then the head gradient between the formation and wellbore in the lower completion will not increase with an increase in the pumping rate and the rate of inflow in the lower completion will remain biased low. As evidenced from the change in formation inflow rates with the pumping rate, such an occurrence does exist in ER-5-4. However, the magnitude of the well loss (Section 2.1.2.1), and quantitative implication for how it reduces production from the lower interval, is unknown. That is, the well loss cannot be added to the head difference between the lower and upper completion.

On the contrary, the pumping rate (175 gpm) during which interval flow rate measurements were made appears sufficiently high that the induced drawdown is significantly greater than the head difference between the formation intervals tested; this is an optimal condition for production. The maximum measured drawdown through the constant-rate test (at 160 gpm) was about 120 ft; therefore, the head difference between the upper and lower completions is about 3 percent of the induced drawdown. The small percentage implies that the transmissivity of

the lower completion is significantly less than that of the upper. Therefore, partitioning of the K-estimates into their interval components is performed by weighting the composite K data by the percent of flow, relative to the interval thicknesses, that each completion zone contributed to production (based on the logs at 175 gpm).

An exact partitioning of the composite K cannot be performed because the head gradient between the formation and the wellbore, at both completion intervals, is unknown (although the difference between the two are known). This implies that the influence of well loss on the reduction of head in the lower interval is unknown. In other words, well losses probably decrease the amount of contribution that the lower screened interval would contribute in their absence. Because the composite K-estimate is weighted in part by the production across each interval, the partitioned K for the lower interval is biased low and, accordingly, the partitioned K for the upper interval is biased high. The partitioned K-estimate for each interval is presented in Table 3-2.

Table 3-2
Hydraulic Conductivity Range: Well ER-5-4 Lower and Upper Completion Zones

	Composite K ($m\ s^{-1}$) Range		Percent Flow at 175 gpm	Percent of Total Casing Interval Thickness	Weight (-)	Weighted K ($m\ s^{-1}$) Range	
	Min	Max				Min	Max
Lower Slotted Interval	1.6×10^{-6}	3.2×10^{-6}	11	38	0.29	4.6×10^{-7}	9.3×10^{-7}
Upper Slotted Interval			89	62	1.44	2.3×10^{-6}	4.6×10^{-6}

3.2 Well ER-5-4#2 Single-Well Constant-rate Test

Well ER-5-4#2 is cased to a TD of 7,000 ft bgs. The borehole is completed with blank casing from ground surface to 6,486 ft bgs, with slotted casing from 6,486 to 6,658 ft bgs, and is open below 6,658 ft bgs to the well TD (Figure 1-6). There is an open annulus between the casing and borehole wall between 4,848 and 6,658 ft bgs. The slotted-casing interval extends across the Tcb, a hydrostratigraphic section of the LTCU. Flow and temperature logging under pumping conditions indicated that inflow to the well occurred not only from the formation exposed through the slotted casing interval, but also through the open annulus from the formation above the slotted casing (Section 2.2.2.2).

The constant-rate test was performed for eleven days between November 12, 2002 (JD 316) and November 23, 2002 (JD 186). A production rate of 170 gpm was chosen as the optimal rate for the test. Control problems with the pump resulted in varying production rates during the first two days of constant-rate production, making the early-time portion of the test difficult to interpret. The recovery of the well was monitored for nine days until December 2, 2002 (JD 336).

The following sections present the conceptualization of the model flow domain, the LTCU hydraulic property estimates derived from simulation of the measured response at ER-5-4#2, and the estimate uncertainties.

3.2.1 Formation Flow Model Conceptualization

The production rate and formation pressure response at ER-5-4#2 through development and constant-rate production are shown in Figure 3-6. The complete response record is discretized into a set of flow and pressure sequences. The well development record is included in the simulation to account for lingering pressure transients in the formation. The constant-rate test drawdown and recovery sequences are respectively identified as flow sequences F_02 and F_03 in the figure.

As performed for the analysis of the ER-5-4 single-well testing data, the response log-log diagnostic plots are used to assist in the identification of flow regimes within the wellbore and the formation. The log-log diagnostics for the buildup flow sequence F_03 are shown in Figure 3-7. Variability in the production rate during drawdown resulted in uninterpretable diagnostic plots for flow sequence F_02; these are not presented. A general assessment of the buildup plots is presented. The early-time wellbore storage period and $1^1/_2$ log cycle transition (from storage to formation response) period are identifiable. Flow contribution from the open annulus above the screened interval probably convolutes the observed response. Following this period, the derivative plot shows an upward trending feature for the duration of the sequence. In general, such a feature indicates a flow geometry that restricts the pressure response through the formation, e.g., the pinching out of a hydrostratigraphic unit (Horne, 1995). Several such scenarios could be applied to describe the observed response; there is no information to constrain the interpretation, in particular because the drawdown sequence diagnostics are uninterpretable. However, it can be said that the response is indicative of a single-porosity formation. The features indicative of a double/fractured-porosity formation are not shown, e.g., a local minima on the derivative plot that results from the shift between steady fracture and matrix dominated flow (Horne, 1995). The LTCU tested (across the 1,810-ft formation thickness) consists of partially welded tuff above 6,530 ft bgs and bedded to nonwelded tuff below. Although fracture zones have been identified in tuff units across the NTS (Shaw, 2003), the data show that a double-porosity model is inappropriate for the simulation.

3.2.2 Simulation of the Formation Response

The Cartesian flow sequence data in F_02 and F_03 (Figure 3-6) are used for simulating the pressure responses to pumping and recovery. For the simulation, the fitting parameters are defined as the formation hydraulic conductivity, formation specific storage, static formation pressure, and flow dimension. The flow dimension was optimized as a result of the nonradial, yet unknown, flow geometry, indicated by the recovery period log-log diagnostics. In addition, a well skin hydraulic conductivity and specific storage were defined as fitting parameters. The open annulus between the borehole and casing justifies their

inclusion into the model. It was anticipated that these parameters would account for a significant portion of the annulus storage that would have affected the measured early-time responses in the drawdown and buildup sequences.

The formation thickness is defined as the 1,810-ft interval below the cemented borehole and above the base of the slotted casing interval. Flow and temperature logging indicated that the large majority of production was contributed from the 4.13-in. open annulus above the slotted interval. Although it is possible that the formation thickness is less, no data are available that can be used to constrain the upper bound, located at an unknown point above the slotted casing interval. This datum presents a significant source of uncertainty.

3.2.3 Parameter Estimates, Numerical Uncertainty, and Physical Uncertainty

A 500-simulation perturbation analysis was performed in which both the drawdown (F_02) and buildup (F_03) flow sequences were simultaneously used as fits for the simulated response. A horsetail diagram of the best numerical-fit simulated data is shown in Figure 3-8 (top); each simulated response is defined by a different set of fitting parameters. The simulated responses show poor fits. Recall that the measured pressure response data were pre-processed, or corrected, for the measured components of thermal volume expansion/contraction and well loss. Both corrections were shown to significantly influence the magnitude and curvature of the drawdown and buildup responses (Section 2.2.2.1, Figure 2-10). It is conjectured that deficiencies, or incompleteness, of the corrective terms result in the poor fits. In particular, the variable production rate during drawdown resulted in complex wellbore conditions that may not have been fully accounted for in the correction. Therefore, a second perturbation analysis was completed in which only the buildup sequence (F_03) was used as the fit for the simulated response. The drawdown sequence was defined as the (corrected) measured data. An advantage of this method is that the shape of the buildup sequence is not affected by well loss. The simulated responses are shown in Figure 3-8 (bottom).

The scatterplot in Figure 3-9 (top) shows the large range of formation K and S_s solution pairs that correspond to the responses derived from simulation of the buildup sequence F_03 (Figure 3-8 (bottom)), as well as the initial parameter estimates used in the perturbation analysis. Again, these solutions reflect only the numerical uncertainty of the parameter solutions that is inherent to the inverse solution method; they do not reflect actual (physical) uncertainty because the aquifer storage parameter cannot be constrained by single-well pump-test data. The initial estimate locations show that a sufficiently large range of parameter-space was considered for the simulations. From a numerical perspective, the solutions sets are poorly constrained; a large and unrealistic range of hydraulic properties are able to provide equivalent fits to the measured data.

To constrain the hydraulic conductivity estimate, a physically realistic range of specific storage for the LTCU tested is defined. The remaining fitting parameters (static formation pressure, flow dimension, well skin hydraulic conductivity and storage) provide no insight with respect to constraining the K and S_s estimates. The static formation pressure is equivalently reproduced by all K-S_s solution pairs.

The flow dimension parameters are poorly constrained (Figure 3-9 [bottom]) and are, in any case, highly suspect due to the unknown influence of the annular contribution on the flow geometry. The skin parameters, as theoretically appropriate, are poorly constrained and display no correlation with the formation parameters. Therefore, a physically realistic range of the S_s, relative to the LTCU tested, is defined to constrain the K solutions shown in Figure 3-9 (top). The assumptions for this calculation were presented in Section 3.1.3. The range is presented in Table 3-1.

The range of K solutions, constrained by the physically realistic range of the local LTCU specific storage, is 2.2×10^{-7} to 1.7×10^{-6} m s^{-1}. This is a relatively large spread, just under one order of magnitude in width. There is no apparent quantitative means by which to rank, or assign relative goodness of fit values, to the corresponding simulated response data shown in Figure 3-8 (bottom). Therefore, each fit is assumed to be equivalent and equiprobable; the K solutions are presented as a uniform distribution.

3.3 Well Cluster RNM-2s Multiple-Well Constant-rate Test

To briefly review the MWAT activities, RNM-2s was pumped for 75 days (JD 116 through 191) and monitored for recovery to JD 253. A clear response to constant-rate production was observed in the pumping well, RNM-2s, and three observation wells, RNM-2, RNM-1, and the ER-5-4 upper completion zone. These data were presented in Section 2.3.3.1 to Section 2.3.3.4, respectively. All well completion intervals are located in the AA. Across the well cluster, the AA is characterized as a 3,676-ft section of poorly consolidated sand, silt, and minor gravel. From depth-to-water measurements made under static conditions, the alluvium is saturated below about 722 ft bgs (Table 2-7); therefore, the saturated thickness is about 2,954 ft. With the exception of the ER-5-4 upper completion zone, the pumping- and observation-well completion intervals are located at or near to the water table. The unconfined system requires that the water table response is included in the conceptual and theoretical model of formation flow during the MWAT.

Section 3.3.1 describes the unconfined flow model applied in the analysis. Section 3.3.2 through Section 3.3.4 presents the conceptual flow model and geometry that are interpreted from each observation well response. The response measured at RNM-2s is not applied in the estimation of formation hydraulic properties, but is used only to assist in the interpretation of the observation well responses measured. Recall from Section 2.3.3.1 that unquantifiable well losses, that are presumed to comprise a significant component of the well pressure response at RNM-2s, make these data uncertain and unsuitable for interpretation. Section 3.3.2 through Section 3.3.4 also includes the analysis methods and formation hydraulic property estimates, presented individually for each well. A summary and comparison of results is presented in Section 4.2.

3.3.1 Unconfined Flow Model

The well-test analysis code nSIGHTS is used for the interpretation and analysis of the well responses measured during the RNM-2s MWAT. A version of the code capable of simulating unconfined aquifer conditions, relative to that which was presented in Section 3.0, is applied. Modifications to the code and verification information are presented below; otherwise, the theoretical description of the code presented in Section 3.0 is the same.

The modified version assumes a two-dimensional, liquid, non-leaky, single porosity system. A gridded two-dimensional (an)isotropic domain is defined radially in the horizontal and layered, or slabbed, in the vertical. The (vertical) formation thickness, and therefore discretization, is permitted to vary through time with the water table elevation. Hydraulic properties are assumed homogenous with depth, but may vary with radial distance into the formation if specified by the user. The upper layer boundary condition is defined as the water table. A flow dimension of 2.0 (radial) is assumed. Although other flow dimensions are possible, they would be theoretically suspect; it is difficult to distinguish between a change in flow geometry versus a water table response, i.e., delayed gravity drainage and specific yield.

Both fully penetrating and partially penetrating wells are implemented for the unconfined solution in nSIGHTS. If partially penetrating, a completion zone interval may be defined at the production well. The interval thickness varies if it intersects the water table. Observation well responses are defined differently. The response is incorporated relative to the depth below the water table (or above the bottom of the formation) at which the response was measured (e.g., the location of a pressure transducer); therefore, neither a well penetration depth nor completion zone interval is required for an observation well.

The unconfined implementation was verified by comparing nSIGHTS results to those produced by the analytic code WTAQ (Barlow and Moench, 1999). A number of different configurations were analyzed:

1. Full penetration well, no wellbore storage
2. Full penetration well, wellbore storage
3. Water-table partial penetration with wellbore storage
4. Saturated partial penetration with wellbore storage
5. Saturated partial penetration with wellbore storage, anisotropy and skin

Agreement between numerical and analytical solutions was good in all cases. A graphical comparison of the verification simulations with the analytical solutions is documented in SNJV Central Files (LVCF058653).

3.3.2 Interpretation and Analysis of the RNM-1 Response

The RNM-1 wellhead is located 707 ft north of the RNM-2s production well. The well was drilled at an average angle of 21° from the vertical into the CAMBRIC test cavity. The RNM-1 completion interval, between 857.96 to 884.10 ft bgs, is about 100 ft above the cavity. The extent to which the nuclear test affected the area of the formation hydraulically stressed at the RNM-1 completion is uncertain. The steady, equilibrium water level measured in RNM-1 is approximately 8.5 ft below that measured in other wells across the RNM-2s cluster. One interpretation of the discrepancy between water levels is that a low permeability skin surrounds the cavity that is slowing the local water-level recovery to the regional static condition. In this case, the recovery must be sufficiently gradual that the RNM-1 water level appears static over short time periods (on the order of months). The existence of such a skin within 100 feet of the cavity is highly plausible. However, as reported in Section 2.3.2, the water-level differential may also reflect uncertainty in the true RNM-1 completion interval depth resulting from the lack of a borehole deviation survey. A borehole deviation of less than 2° between the actual and measured value would account for the 8.5 ft water-level difference to within one-hundredth of a foot of the SWL measured at RNM-2. The latter interpretation of the discrepancy between the local water levels is more plausible when the RNM-1 well response to MWAT production is considered.

The log-log diagnostic plots, shown in Figure 3-10, provide insight into the plausible flow geometry that exists between RNM-2s and RNM-1. The diagnostic responses appear stable for both the drawdown (top) and recovery (bottom) sequences, indicating that possible flow boundaries within the radius of influence (of the well test) do not interfere with the response measured during the buildup sequence. Both the pressure and the derivative plot, for both sequences, have an approximate $^1/_4$-slope. In addition, the pressure change and derivative are separated approximately by a factor of four through the earlier periods of the response. Together, these features are indicative of a measured response through a finite conductivity vertical fracture (FCVF) (Horne, 1995). Similar diagnostic responses (i.e., long-time linear responses in which there is little difference between drawdown and buildup) have been observed in flow to a well through a sand channel (Horne, 1995). Similarly, the strip (linear composite) model has been suggested by Liu and Butler (1990) in which a linear strip of high transmissivity in an otherwise homogenous and unconfined aquifer controls flow to/from a well. Their diagnostic plots (for a drawdown sequence) are remarkably similar to those observed for the RNM-1 response. They noted that a Neuman delayed gravity response model has difficulty modeling such a response because flow is governed by a linear (channel) system in combination with a delayed gravity drainage system.

The complete RNM-1 response to the MWAT production and recovery is simulated using nSIGHTS. The fitting parameters defined are the formation horizontal hydraulic conductivity, the vertical hydraulic conductivity, specific storage, and specific yield. The inclusion of anisotropy in the model is justified given the hydrogeologic conceptualization of preferentially layered alluvium deposits. As discussed in detail, the formation thickness is defined as the saturated 2,954-ft section of the AA. However, consideration of the partially penetrating

RNM-2s completion zone (Section 2.3.3) permits flow to/from the well through only a portion of this thickness. The vertical extent of the zone of influence is dependent on the estimated aquifer hydraulic properties; therefore, the problem becomes circular and definition of the actual formation thickness tested is somewhat arbitrary. This matter is discussed in greater detail in the analysis of the RNM-2 observation response (Section 3.3.3). The discussion is not completed in this section because the influence of the CAMBRIC cavity on the vertical component of flow through the AA is highly uncertain.

It was reported in Section 2.3.3.1 that there is some ambiguity as to the definition of the RNM-2s completion interval. The well casing is perforated between 1,038 and 1,119 ft bgs; however, a gravel pack surrounds the perforation from 690 ft bgs, above the water table to 1,120 ft bgs. Initial simulations showed that either assumption produced equivalent results (not only for the RNM-1 data, but for the RNM-2 and ER-5-4 upper completion data as well). The aquifer is both sufficiently thick and permeable that the impact of the exact definition of the RNM-2s completion interval is negligible. For this and all other analyses, the perforated-casing interval is defined as the penetration (pumping) interval.

The best-fit simulated response is shown in Figure 3-11. As reported, optimization of the simulated response was too computationally intensive (using the two-dimensional model) to perform a perturbation analysis in a realistic time period. In lieu, several optimizations were performed using markedly different sets of initial parameter estimates. In all cases, the fit converged to approximately the same set of solutions; it is presumed that the solution set presented corresponds to the fit-statistic global minimum for the realistic range of parameter space that was tested. The best-fit solution set is: $K_h = 3.2 \times 10^{-5}$ m s^{-1}, $K_v = 1.0 \times 10^{-5}$, $S_y = 0.287$, $S_s = 7.9 \times 10^{-4}$ m^{-1}.

Although K_h is relatively high compared to previous estimates of the FF hydraulic conductivity (see Section 4.2), the flow regime between RNM-2s and RNM-1 may be anomalous because of the proximity of the RNM-1 completion zone to the CAMBRIC cavity. However, the measured well response at RNM-1 indicates that the CAMBRIC cavity did not significantly influence groundwater flow between RNM-1 and RNM-2s. Recall that the diagnostic plots (Figure 3-10) for both the drawdown and recovery sequence were nearly identical. Had the cavity influenced the response, presumably early in the 75-day test, it would be expected that some lingering boundary effect would be observed in the buildup diagnostics. Further, the RNM-1 well response is similar to the RNM-2 well response; the RNM-2 completion zone was not impacted by the CAMBRIC test (see next Section 3.3.3).

A definite conclusion concerning the representativeness of the local RNM-1 hydraulic property estimates to the AA is not determined. The uncertainty is qualitative in nature given that the impact of the nuclear test on the formation interval tested (i.e., the actual flow geometry) is unknown.

3.3.3 Interpretation and Analysis of the RNM-2 Response

The RNM-2 wellhead is located 314 ft northeast of RNM-2s. The observation well casing is perforated from 720 to 820 ft bgs and intersects the water table (Table 2-7). The measured well response at RNM-2 (Figure 2-16) is similar to that measured at RNM-1 (Figure 2-17). This would qualitatively imply that the CAMBRIC test cavity beneath the RNM-1 completion zone did not significantly influence the well response measured at RNM-1, although this contradicts the speculation of a low permeability cavity skin that is evidenced by the low RNM-1 water level. This apparent contradiction was reported above and is discussed further at a later point in the text. The RNM-2 response log-log diagnostics shown in Figure 3-12, for both the drawdown (top) and recovery (bottom) sequences, have similar long-time linear features to those observed in the RNM-1 data. A $^1/_2$-slope to $^1/_4$-slope transition is observed for both the pressure change and derivative profiles, in both sequences. $^1/_2$-slopes are characteristically representative of infinite conductivity vertical fractures (ICVF) (Horne, 1995). ICVF responses also result in a factor-of-two offset between the early time pressure change and derivative, which the RNM-2 response shows through some periods. Further, the $^1/_2$- to $^1/_4$-slope is a distinct indicator of a linear strip feature(s) with transmissivity much larger than that of the surrounding composite matrix (Butler and Liu, 1991). The strip model corresponds well with the conceptual model of preferentially layered alluvial deposits in the horizontal plane.

The RNM-2 response is simulated using nSIGHTS. The fitting parameters defined are the formation horizontal hydraulic conductivity, the vertical hydraulic conductivity, specific storage, and specific yield. Again, the inclusion of anisotropy in the model is justified given the flow domain conceptualization of a preferentially layered alluvium. The formation thickness is defined as the saturated 2,954-ft section of the AA.

The best-fit simulated response is shown in Figure 3-13 (top). Although a perturbation analysis was not performed for reasons discussed earlier, several sections of parameter space were defined as the initial parameter estimate sets. In all cases, the response fit converged to approximately the same set of solutions. The best-fit solution set is: $K_h = 3.6 \times 10^{-5}$ m s^{-1}, $K_v = 8.5 \times 10^{-7}$, $S_y = 0.031$, $S_s = 5.7 \times 10^{-6}$ m^{-1}.

Observation of the simulated radial and vertical head distribution across the formation domain shows that the interval tested is significantly less than the total thickness of the AA. The two-dimensional head distribution corresponding to the time of maximum drawdown in RNM-2 is shown in Figure 3-13 (bottom). In general, the head varies less than one-foot through the lower 1,400-ft interval of the AA. Definition of the actual formation thickness tested is arbitrary and must be based on a user defined criterion that specifies a critical head value below which the difference from static is negligibly small. However, under the assumption that hydraulic conductivity is an intrinsic property of the AA tested, it is only important to show that the formation thickness tested is not significantly influenced by the lower (no flow) boundary condition, which it is not in actuality.

This type of boundary condition is not a physically realistic model; the AA is underlain by the Timber Mountain Formation, a volcanic aquifer. However, nSIGHTS does not permit another type of boundary to be specified.

3.3.4 Interpretation and Analysis of the ER-5-4 Upper Completion Zone Response

The ER-5-4 upper completion zone is located 1,191.58 ft northeast of RNM-2s. In map view, RNM-2s, RNM-2, and ER-5-4 fall approximately along a straight line (Figure 1-5). The observation well casing is perforated from 1,770 to 2,113 ft bgs, about 1,000 feet below the water table. Therefore, the vertical displacement is on the order of the horizontal displacement between the production and observation wells, and the interpretation and analysis of the observation well data must consider anisotropy. In addition, it is not clear whether the observation well response behaves as a confined or unconfined response given the depth of the completion. The negligibly small specific yield estimate derived in the analysis (see below) suggests a confined response. The following discussion addresses this issue.

The ER-5-4 response log-log diagnostic plots are shown in Figure 3-14, for both the drawdown (top) and buildup (bottom) sequences. In light of the RNM-1 and RNM-2 response interpretation, and also the large vertical distance below RNM-2s, several flow geometries can be conceptualized that would result in the observed response. The exact interpretation is uncertain. However, it is certain that the flow geometry of the pressure response, as it propagates through the formation, varies over the first 10 to 20 days. Through this earlier period of the test, the derivative plots trend downward (especially evident in the buildup sequence) and indicate that the formation pressure response dissipates at a faster rate than it would under Theis-like conditions. For example, a constant pressure boundary would effectively dissipate the response at the boundary location, decreasing the amount of drawdown in the formation, and therefore result in a downward trending pressure derivative. Conceptually, linearized flow through preferential flow features would also provide such a response. Although a delayed gravity drainage response characteristic of unconfined aquifers is not observed in the diagnostics, linearized flow may mask this feature. This interpretation is consistent with those of the RNM-1 and RNM-2 responses. Regardless, after the period (10 to 20 days) of flow geometry change, the pressure response through the formation appears to approach an approximate radial condition.

To account for the proximity of the RNM-2s pumping well to the water table and the vertical displacement between the pumping and observation wells, the ER-5-4 response is simulated using the unconfined version of nSIGHTS. The fitting parameters defined are the formation horizontal hydraulic conductivity, the vertical hydraulic conductivity, specific storage, and specific yield. The formation thickness is defined as the saturated 2,954-ft section of the AA.

The best-fit simulated response is shown in Figure 3-15. Again, a perturbation analysis was not performed for reasons discussed earlier, although several sections of parameter space were defined as the initial parameter estimate sets. The response fit converged to approximately the same set of solutions in all of the cases. It was anticipated that the large vertical distance between RNM-2s and

ER-5-4 would result in a large uncertainty range, or large (negative) correlative structure, between K_h and K_v. The best-fit solution set is: $K_h = 7.2 \times 10^{-6}$ m s^{-1}, $K_v = 2.0 \times 10^{-8}$, $S_y = 0.002$, $S_s = 1.4 \times 10^{-7}$ m^{-1}. A discussion of these parameters in relation to others derived for the FF AA is presented in Section 4.2.1.

Before concluding this section, the choice to individually analyze the MWAT observation well responses at RNM-2 and ER-5-4 is discussed. That both wells are located in line with RNM-2s would suggest that the observation well data could be simultaneously simulated in nSIGHTS. However, the data show that the flow geometries at each well were different, which would make simultaneous fitting problematic. Insufficient data was available to specify within the numerical model how the geometry varied with spatial scale. Inclusion of such descriptive parameters (e.g., a spatial model of flow geometry with radial distance into the formation from RNM-2s) would have introduced unbounded uncertainty into the hydraulic property estimates. Therefore, the observation well responses were analyzed independently so that the data interpretation and analysis for each observation well response would both honor the measured data and permit a better constrained solution. This approach, as opposed to the simultaneous fitting of well responses when multiple-well hydraulic testing data are available, is preferred when apparent heterogeneity in the flow system cannot be captured by a simple hydrogeologic (conceptual and numerical) model (Herweijer, 1997). The assumed approach is particularly appropriate because the hydraulic properties derived will be used for contaminant transport prediction, where insight is required as to the geometry of flowpaths and the variability of hydraulic conductivity.

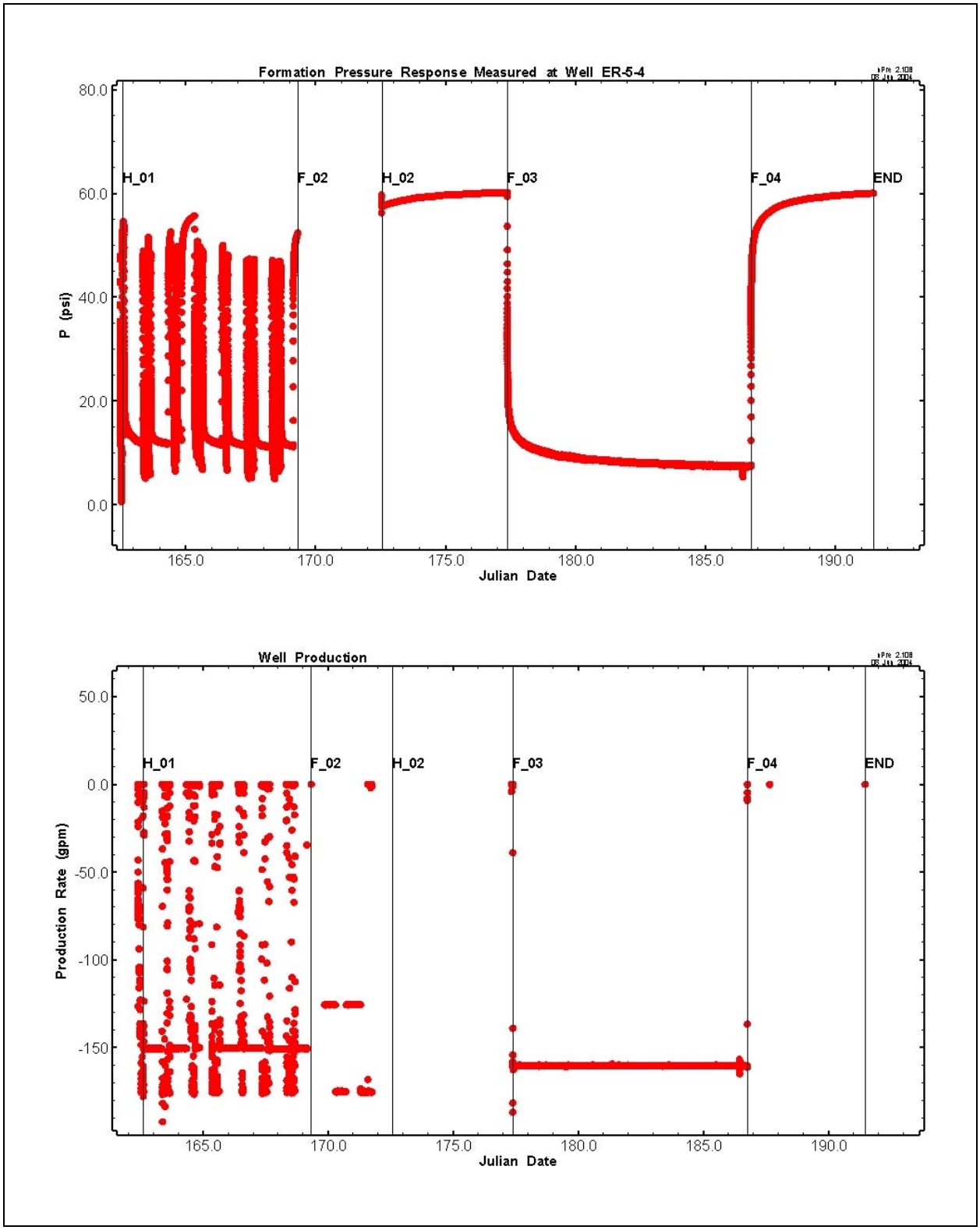

Figure 3-1
ER-5-4 Single-Well Test: Pressure History and Flow Sequences (top) Based on Variation of the Well Production Rate (bottom)

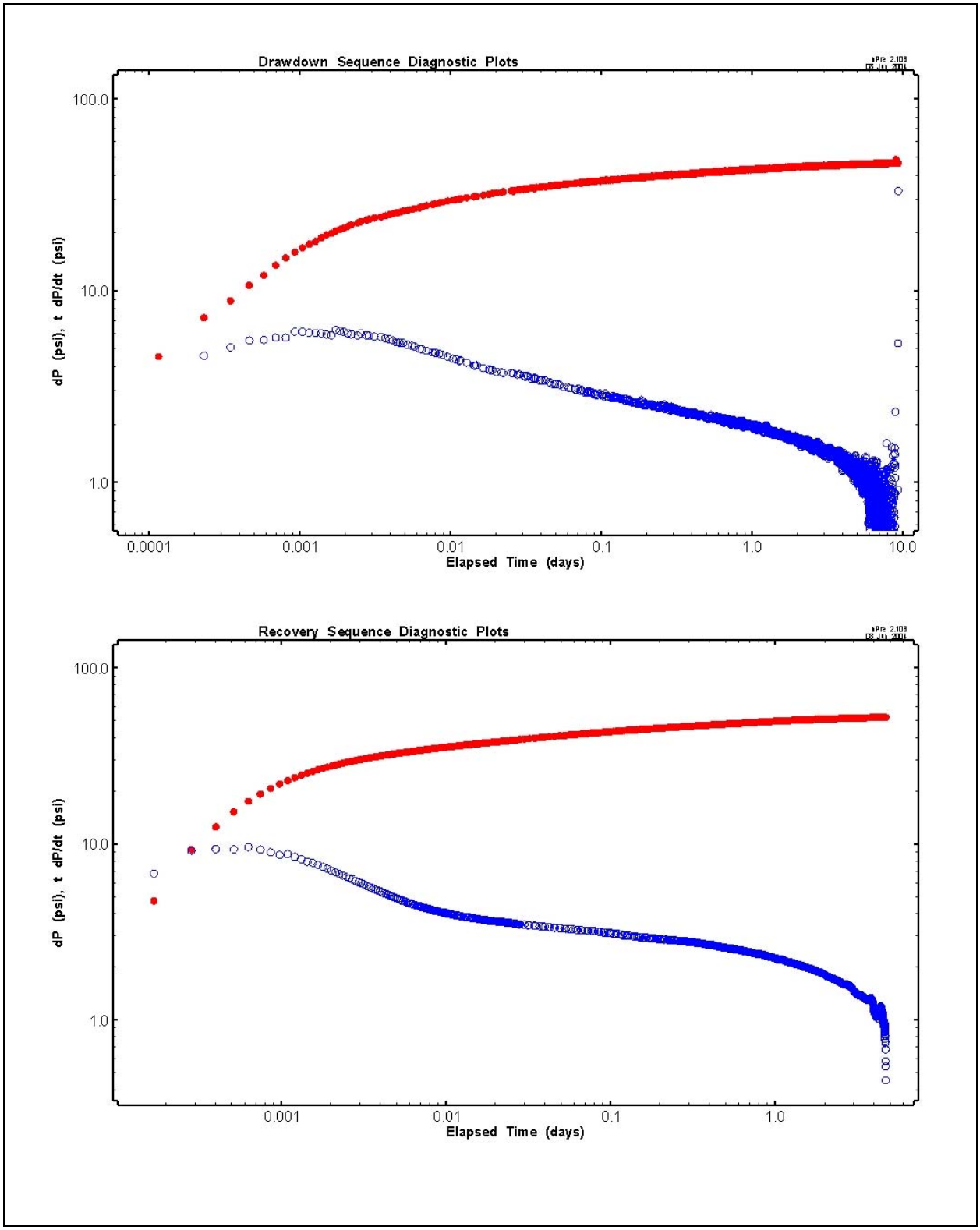

Figure 3-2
ER-5-4 Single-Well Test: Drawdown (a) and Recovery (b) Sequence Log-Log Diagnostic Plots

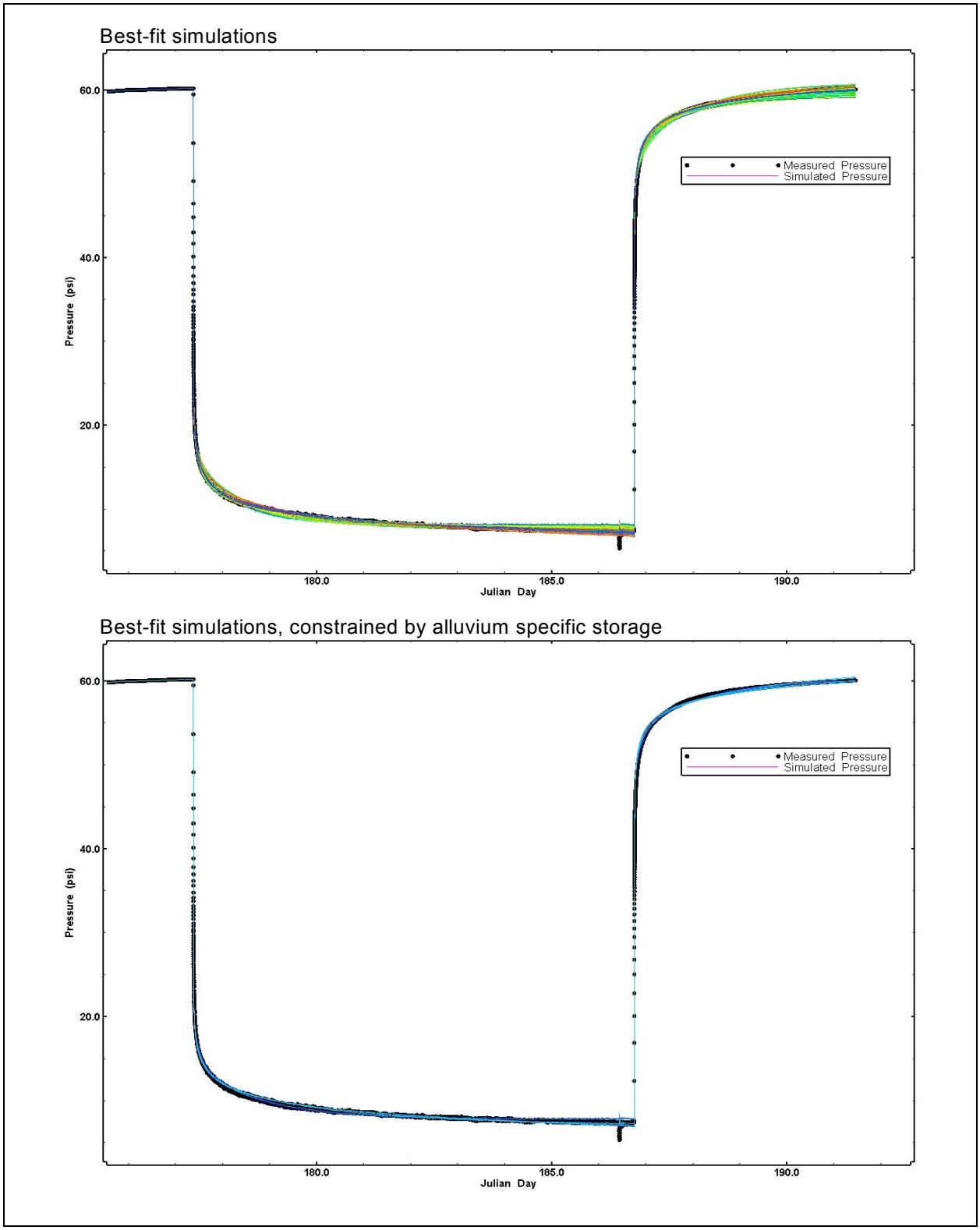

Figure 3-3
ER-5-4 Single-Well Test Perturbation Analysis: All Best-fit Well Response Simulations (top) and Best-fit Simulations Constrained by AA S_s (bottom)

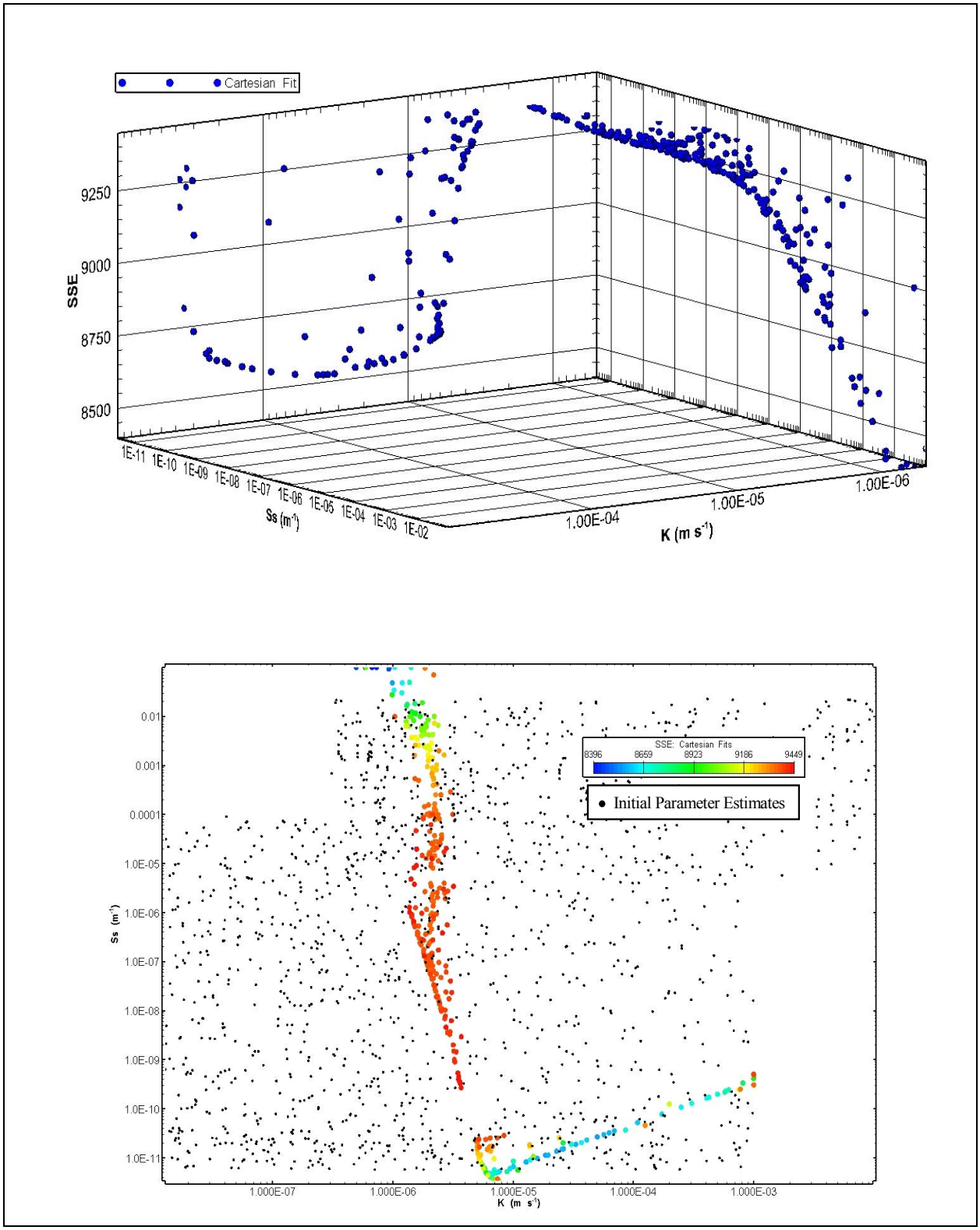

Figure 3-4
ER-5-4 Single-Well Test: Scatterplot of K and S_S Solution Pairs Plotted Against the Fit SSE (top) and Projected onto Parameter Space (bottom)

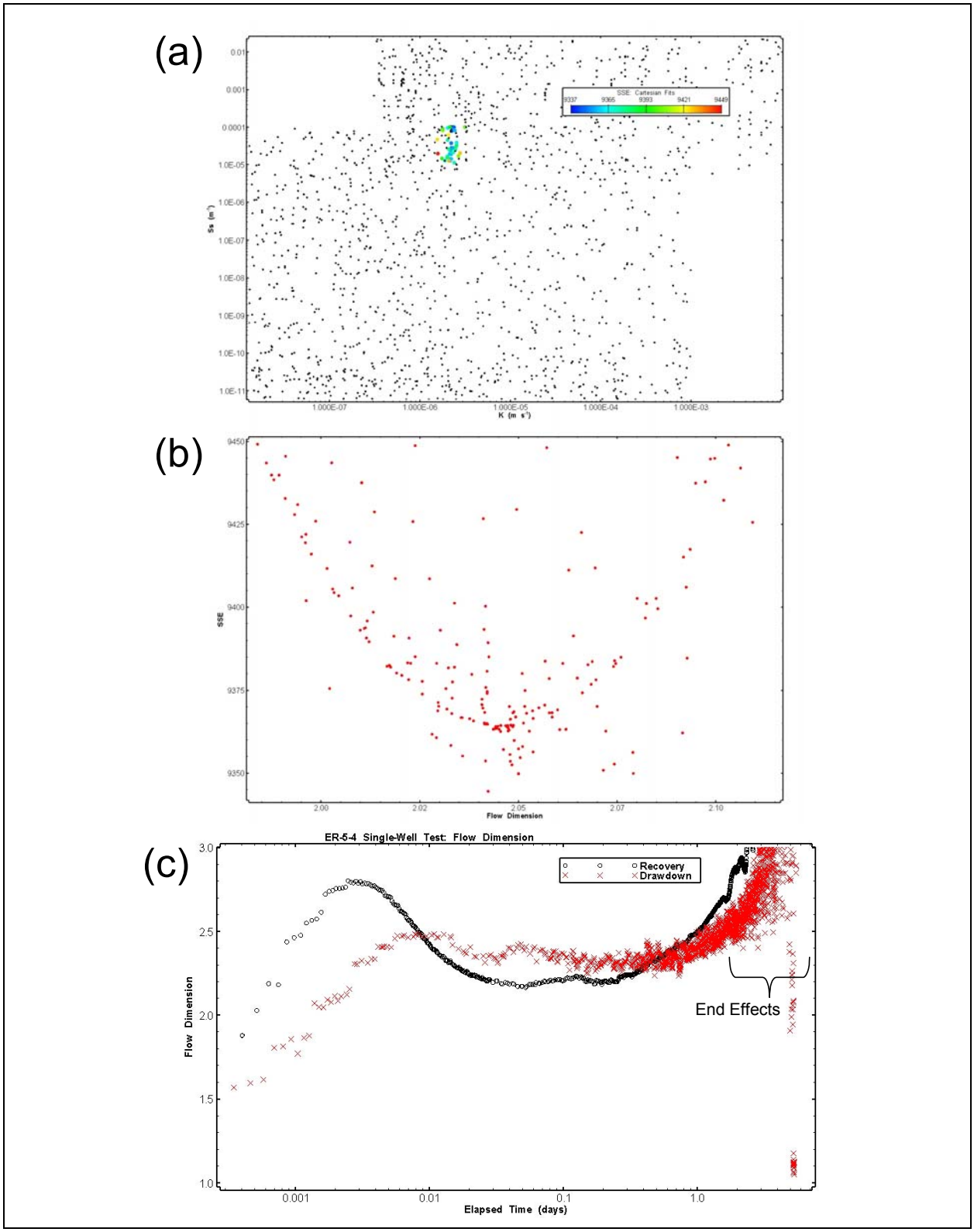

Figure 3-5
ER-5-4 Single-Well Test: Best-fit and Constrained K Solution Set (a) and Flow Dimension (b), and Measured Flow Dimension through Constant-rate Pumping and Recovery Sequences (c)

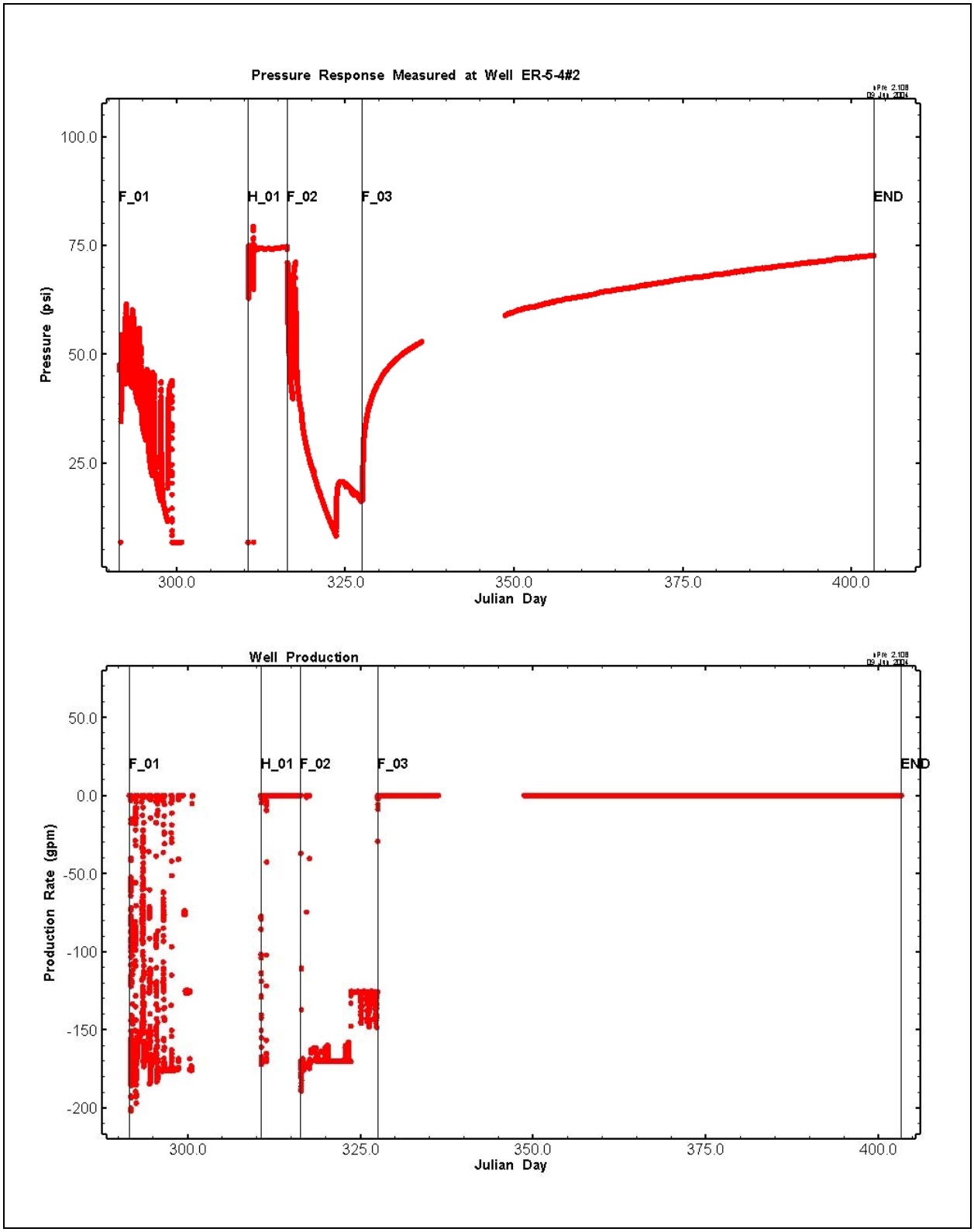

Figure 3-6
ER-5-4#2 Single-Well Test: Pressure History and Flow Sequences (top) Based on Variation of the Well Production Rate (bottom)

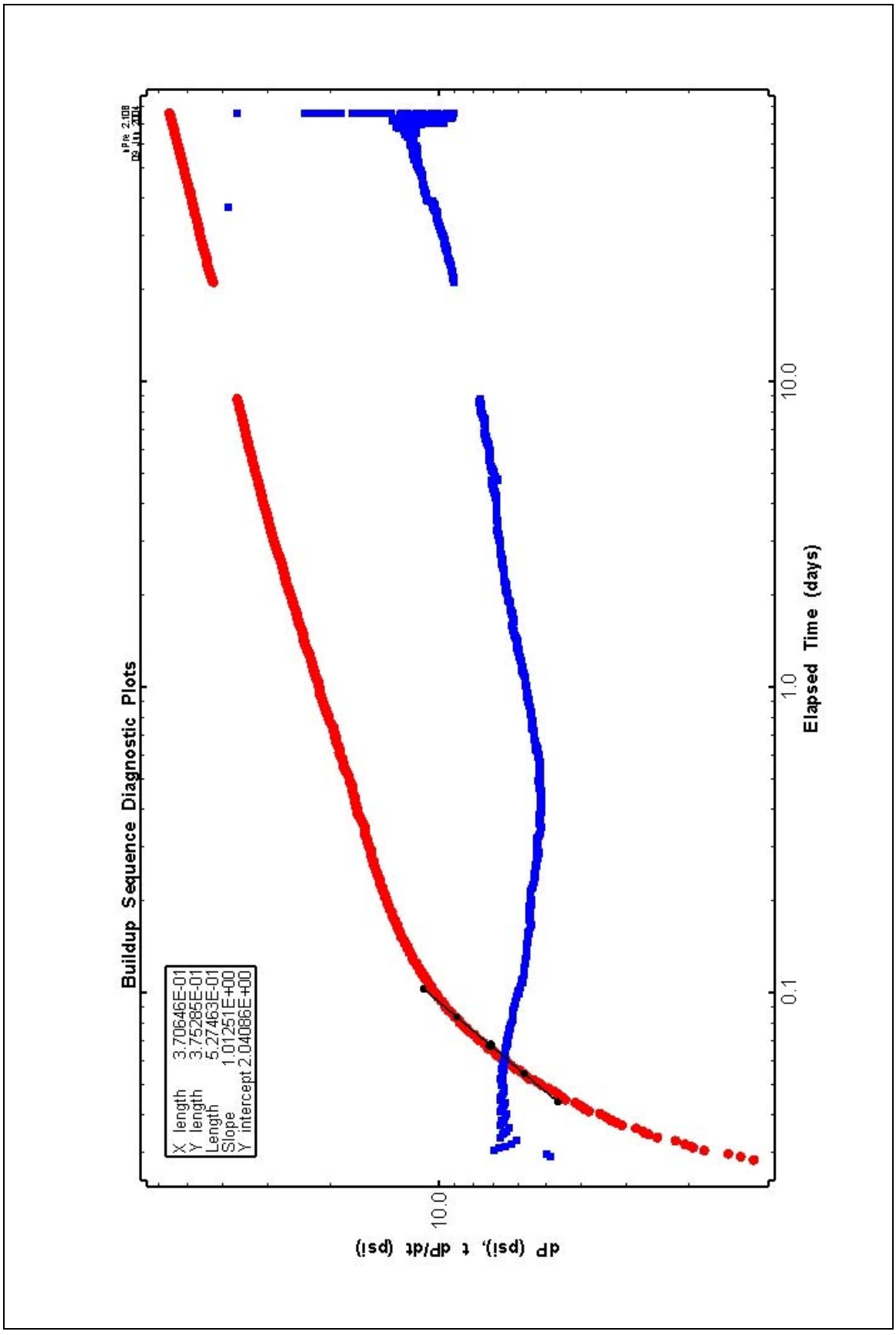

Figure 3-7
ER-5-4#2 Single-Well Test: Recovery Sequence Log-Log Diagnostic Plots

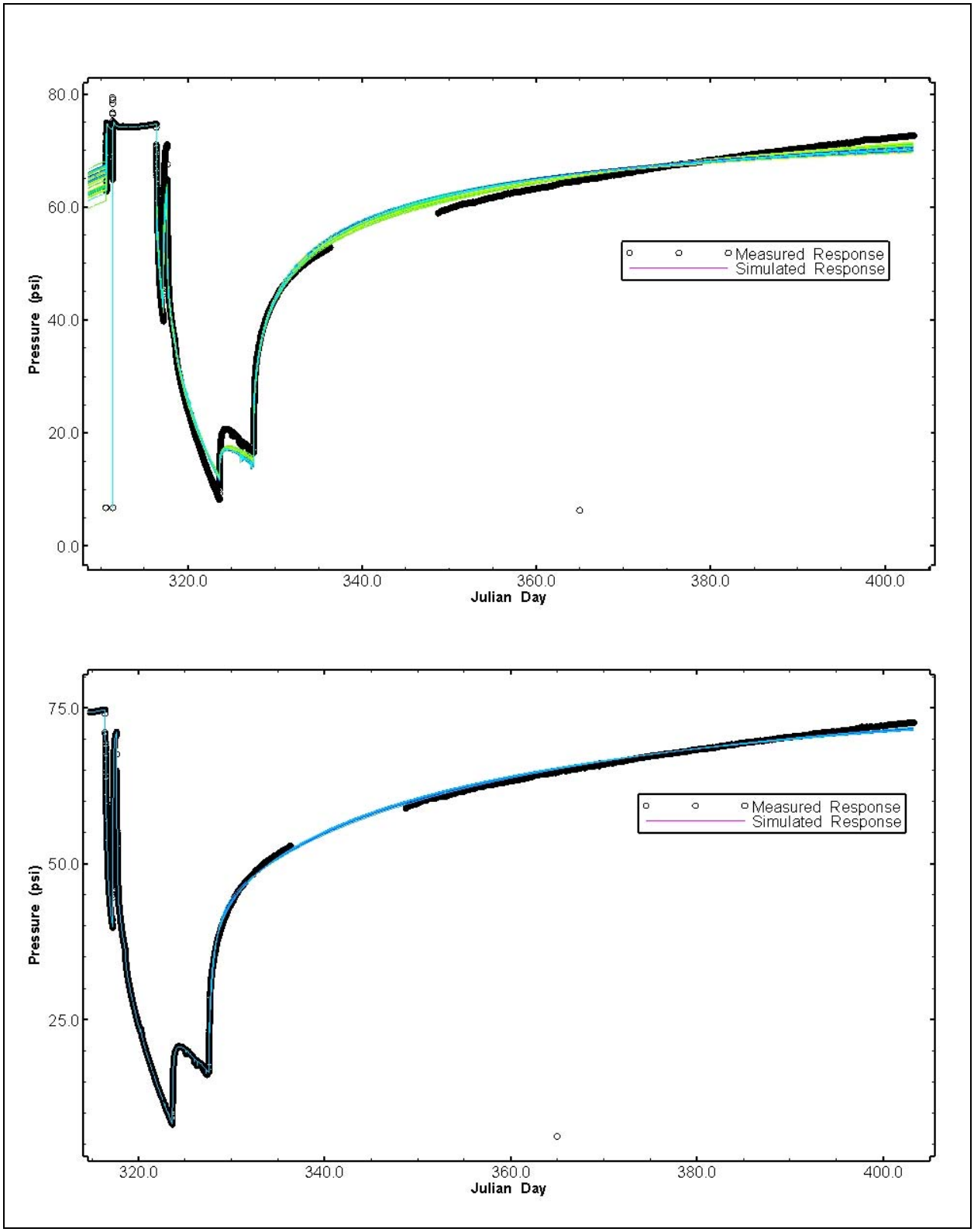

Figure 3-8
ER-5-4#2 Single-Well Test Perturbation Analysis: The Best-fit (Drawdown and Recovery) Well Response Simulations (top) and the Best-fit (Recovery) Response Simulations (bottom)

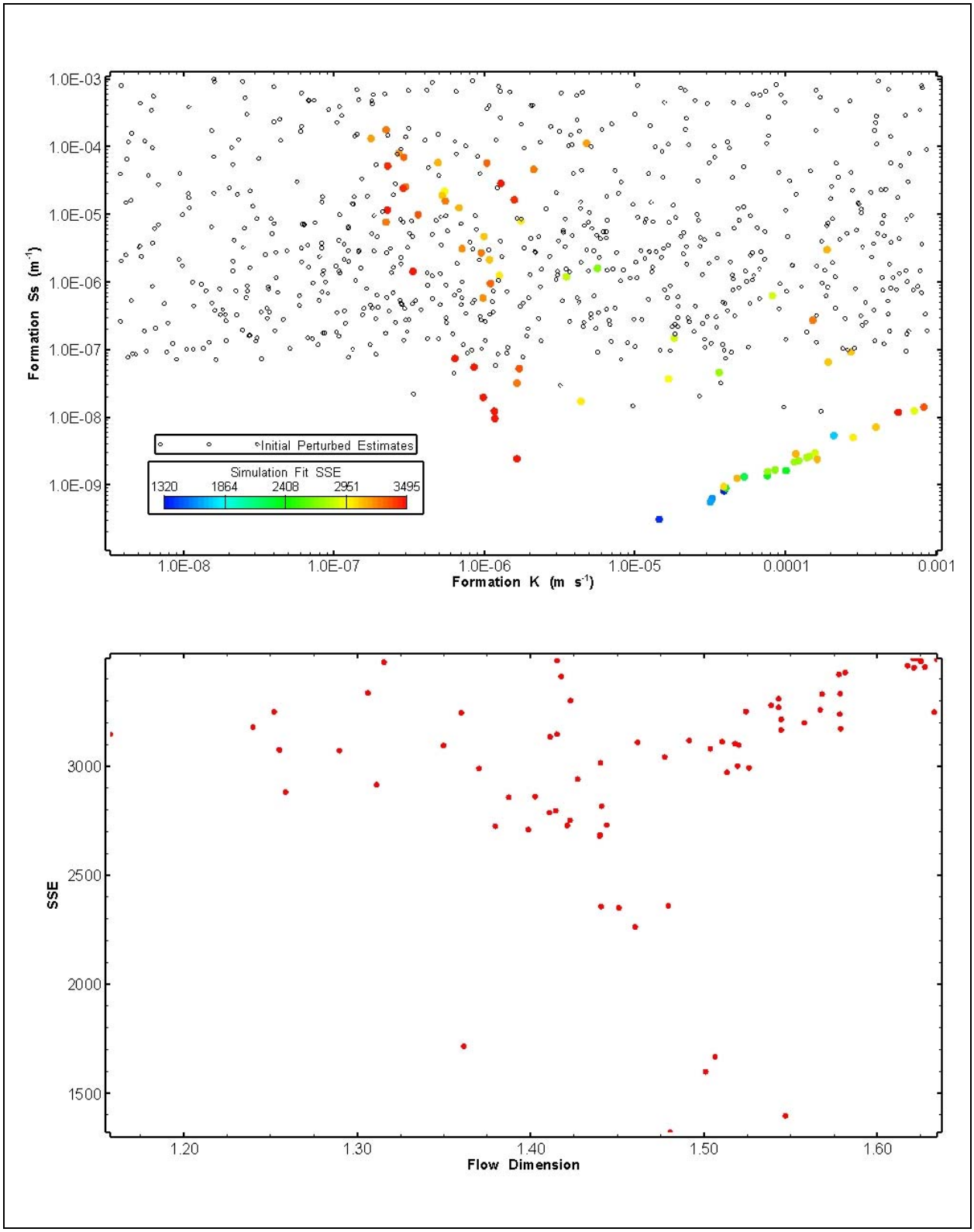

Figure 3-9
ER-5-4#2 Single-Well Test: Scatterplot of K and S_s Solution Pairs (top) and Flow Dimension (Bottom). All Solution Sets are Poorly Constrained.

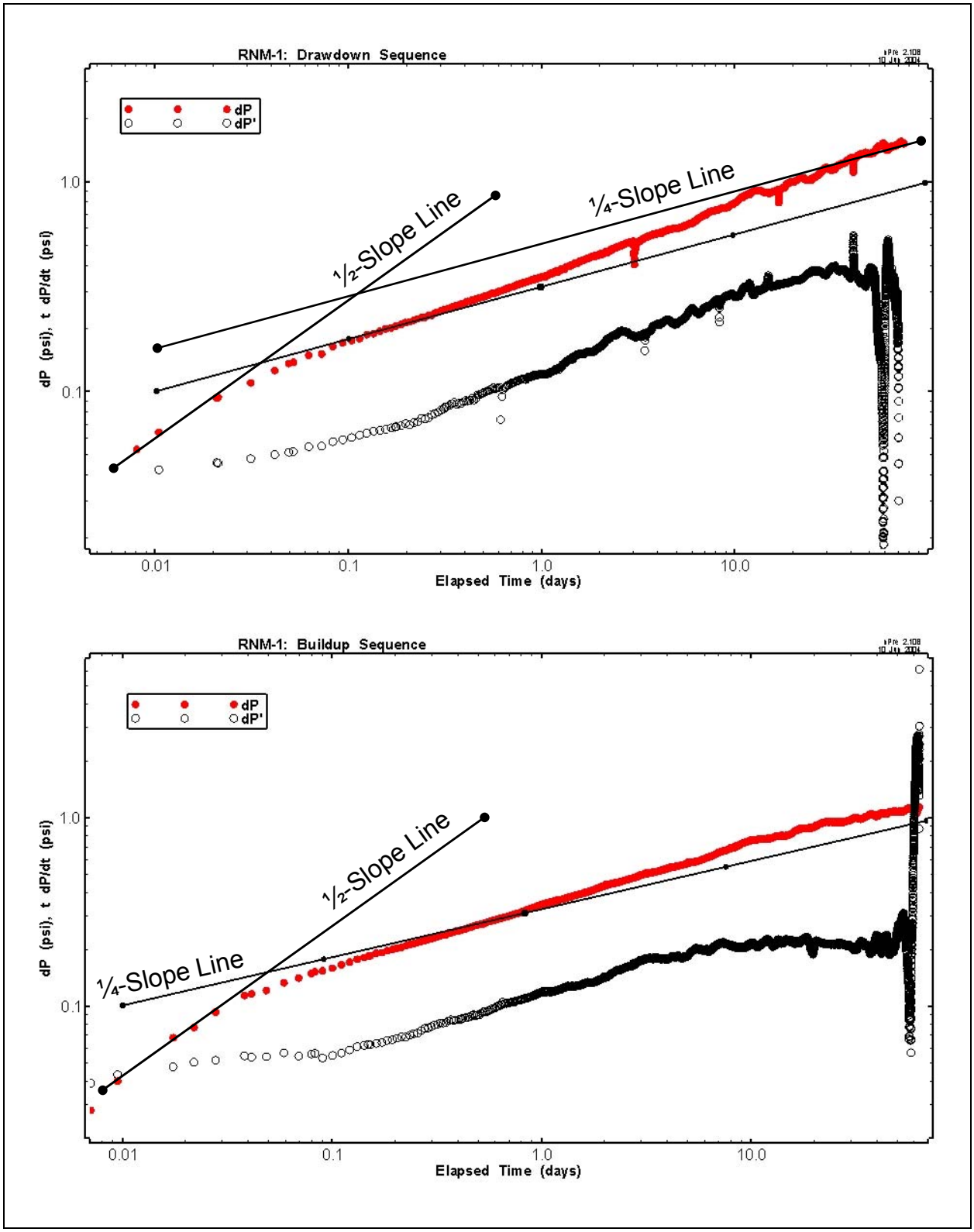

Figure 3-10
RNM-1 MWAT Measured Response: Drawdown (a) and Recovery (b) Sequence Log-Log Diagnostic Plots

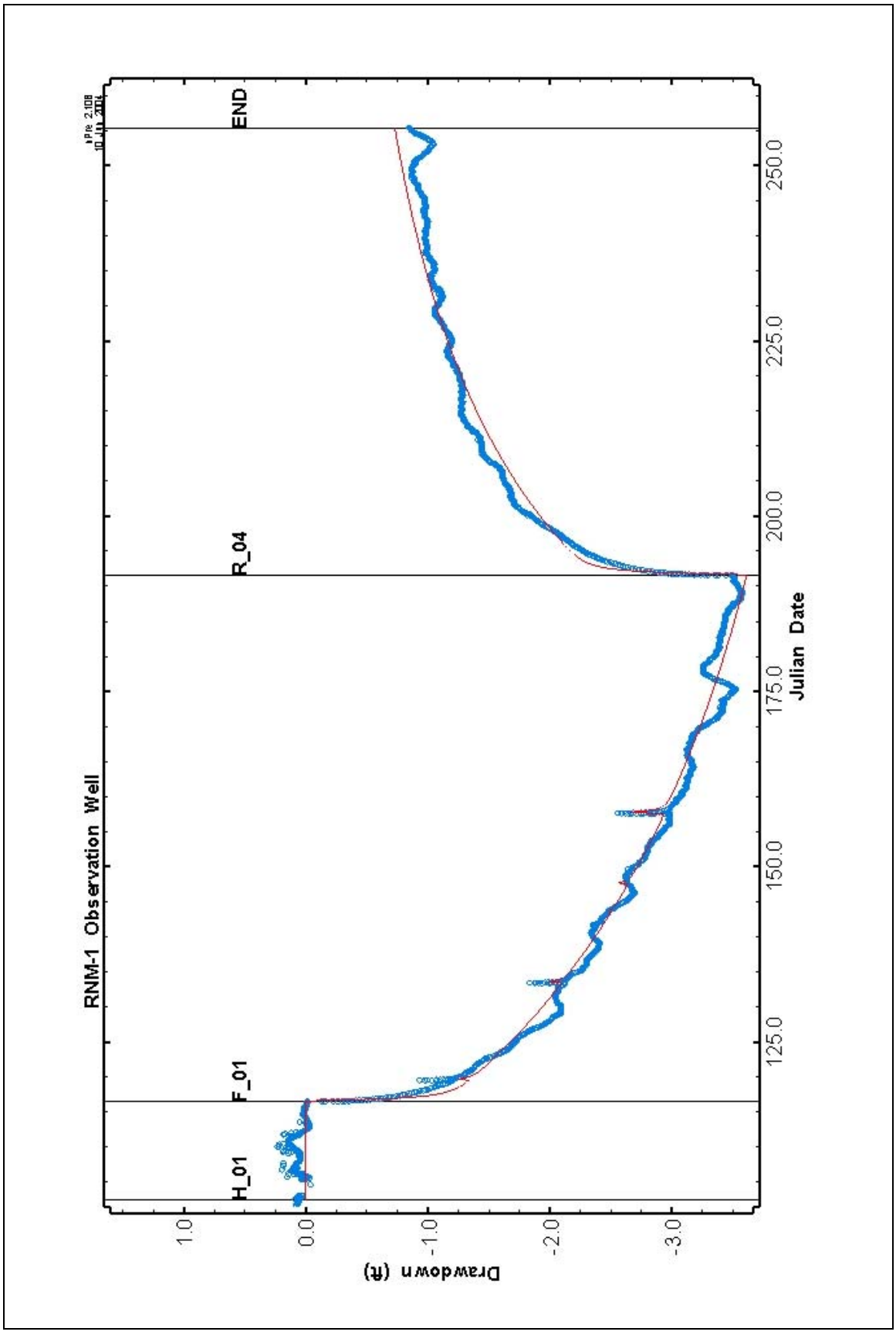

Figure 3-11
RNM-1 MWAT Measured and Simulated Drawdown

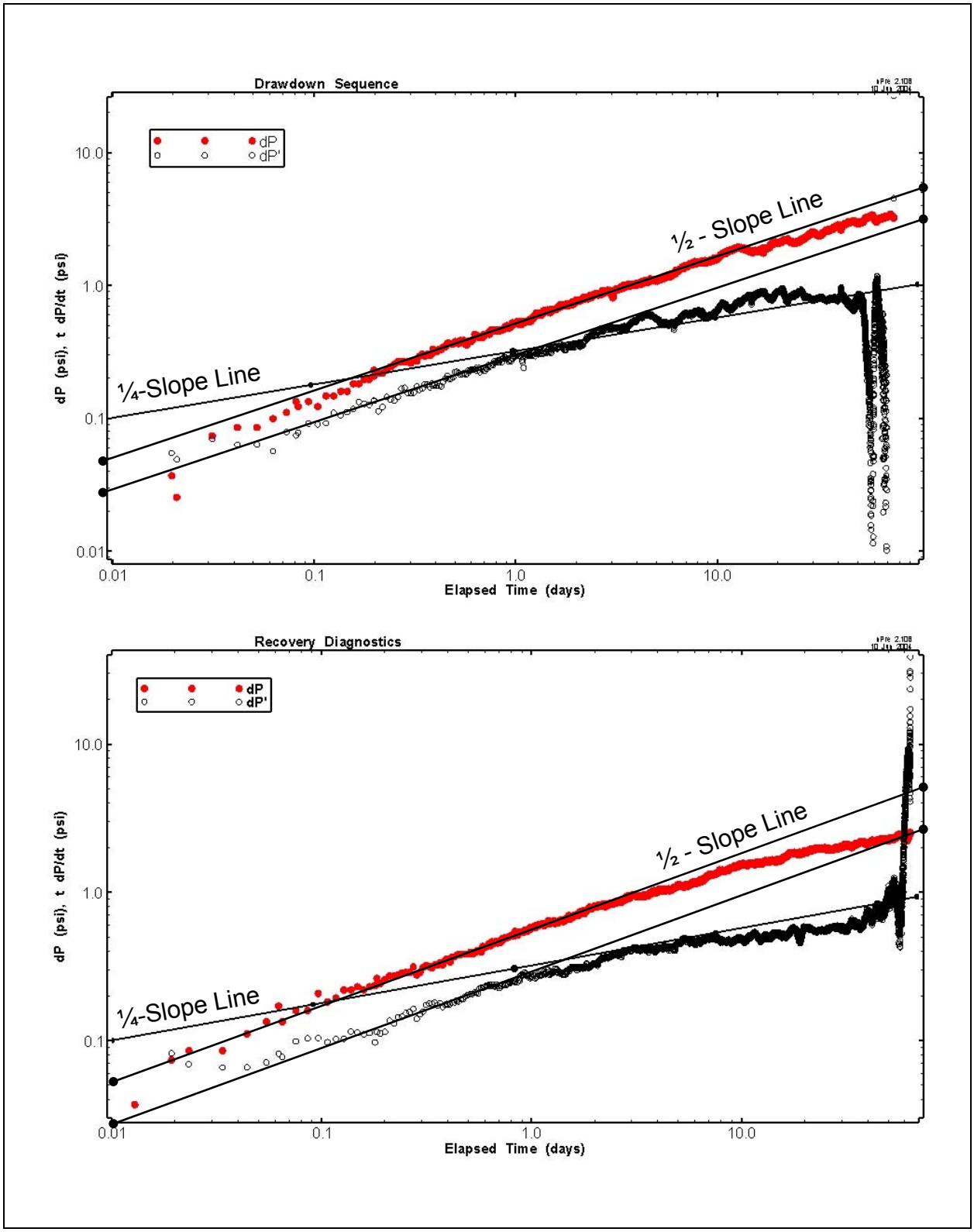

Figure 3-12
RNM-2 MWAT Measured Response: Drawdown (a) and Recovery (b) Sequence Log-Log Diagnostic Plots

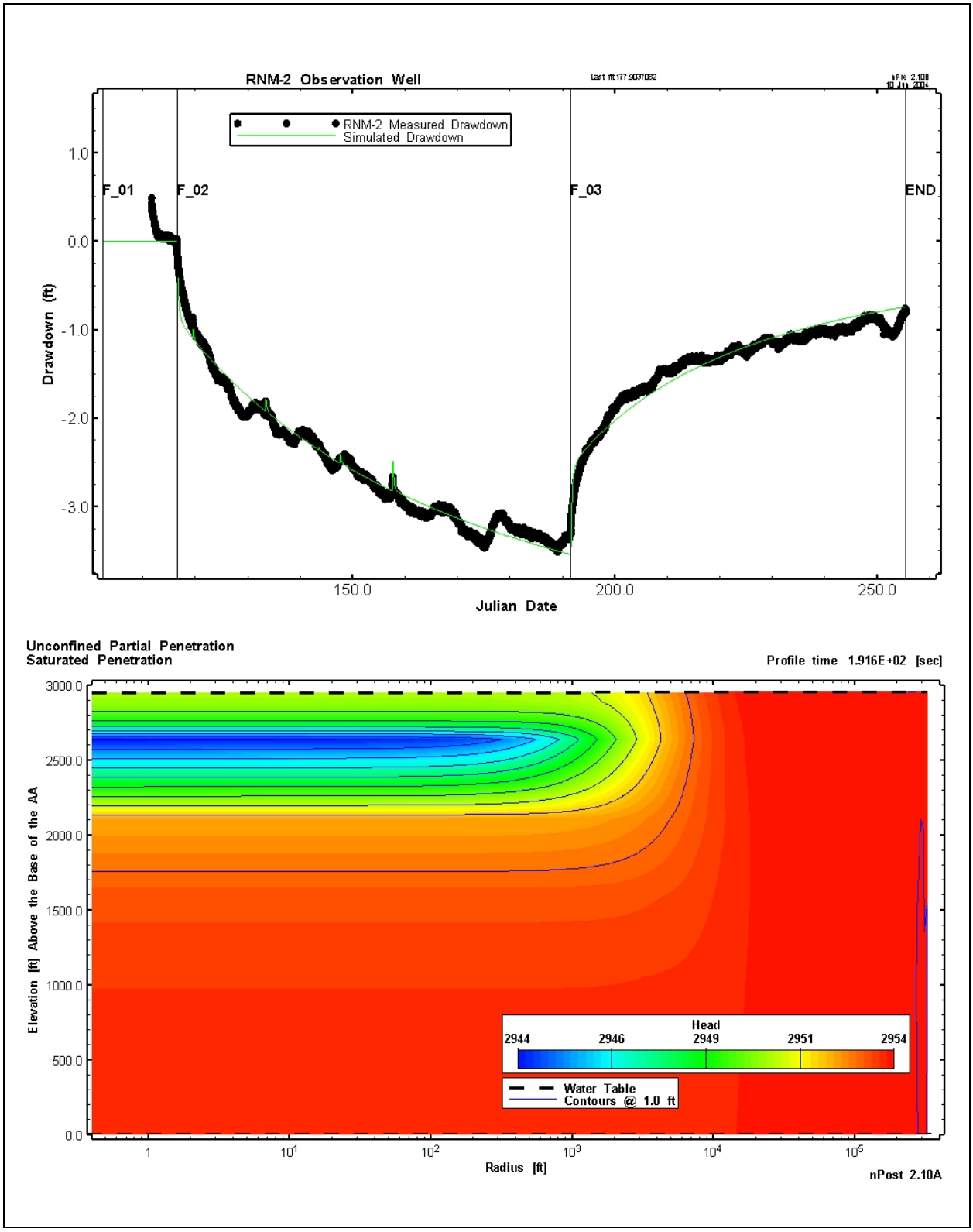

Figure 3-13
Top: RNM-2 MWAT Measured and Simulated Drawdown (top). Bottom: Simulation of the 2-D Head Distribution Through the AA Using Best-fit Hydraulic Properties (Corresponding to the Top Plot)

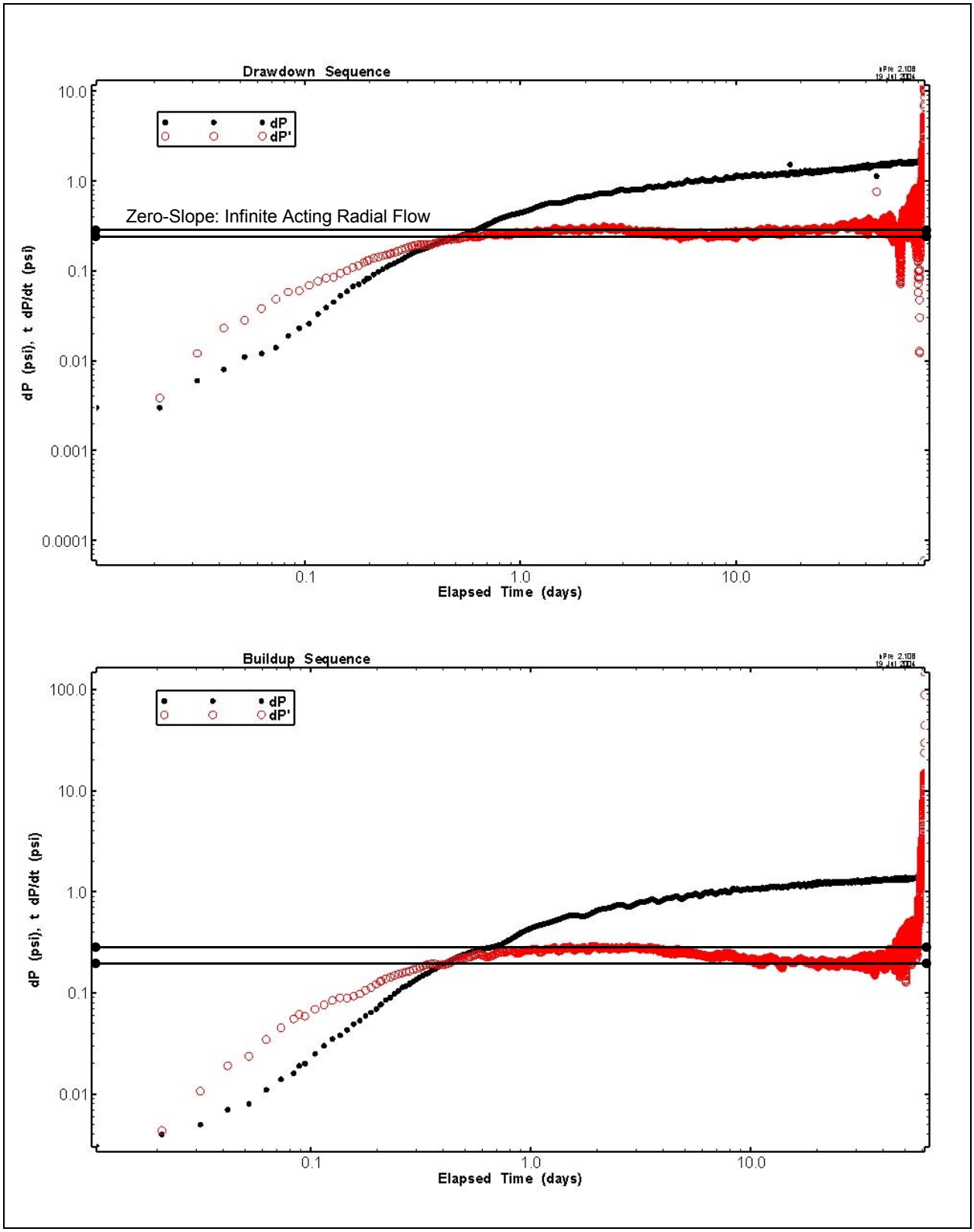

Figure 3-14
ER-5-4 Upper CZ MWAT Measured Response: Drawdown (a) and Recovery (b) Sequence Log-Log Diagnostic Plots

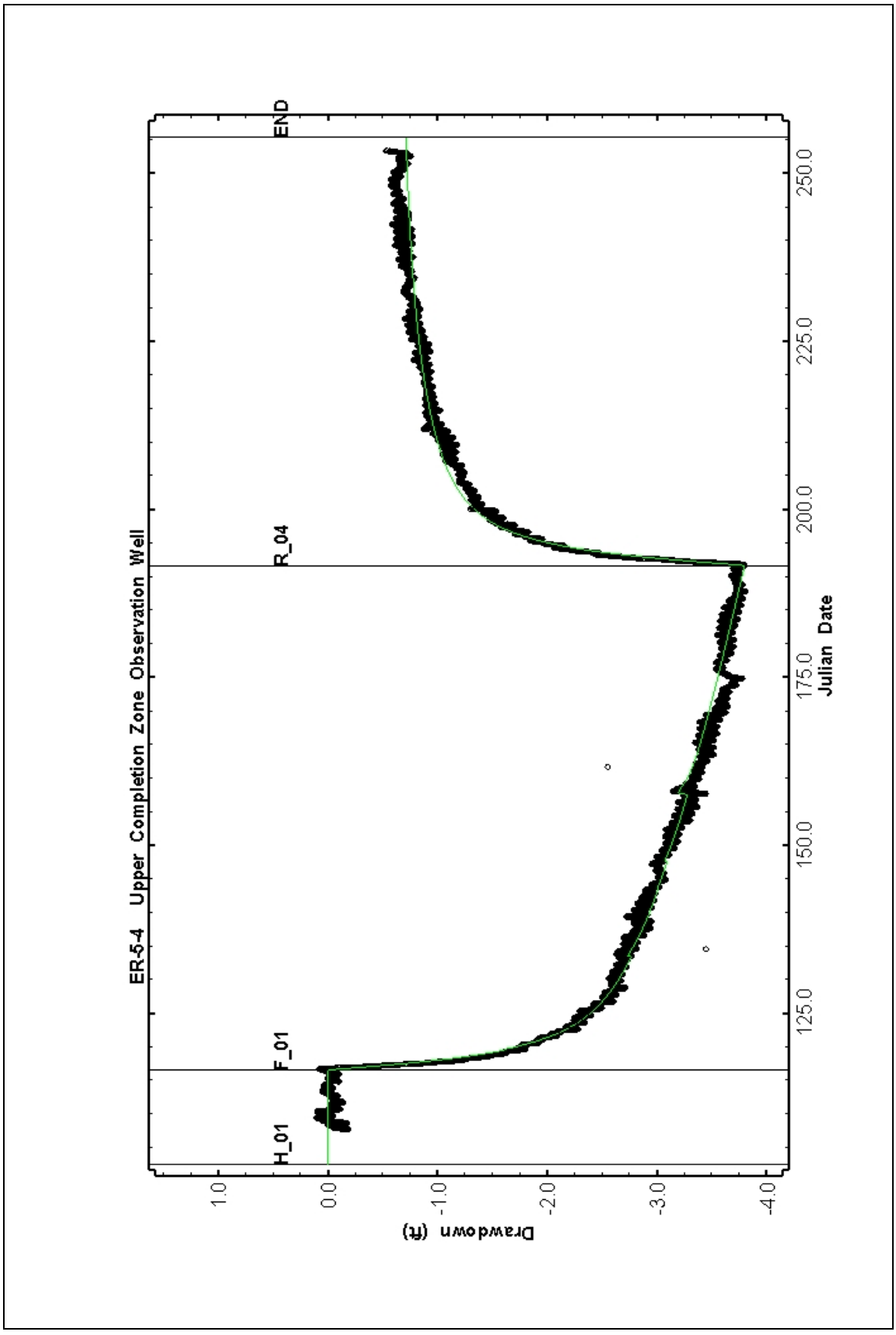

Figure 3-15
ER-5-4 Upper CZ MWAT Measured and Simulated Drawdown

4.0 Summary of Hydraulic Test Interpretation Results

This section summarizes the HSU hydraulic properties derived from the analyses of well-testing data collected across the RNM-2s well cluster. A review of hydraulic gradients across the cluster is presented in Section 4.1. Section 4.2 presents the HSU hydraulic properties representative of the well cluster and compares these data with spatially averaged properties across FF. Section 4.3 presents the comparative study of the RNM-2s MWAT performed by the USGS. The USGS MWAT data interpretation, methods of analysis, and HSU hydraulic property estimates are both summarized and compared with those derived by SNJV in this report.

4.1 Hydraulic Gradients

Horizontal hydraulic gradients across the well cluster were presented in Section 2.3.2. Of the 11 wells in the cluster at which water levels were measured, 9 are completed in the AA. ER-5-4#2 is completed in the LTCU, and TW-3 is completed in the LCA. Therefore, horizontal gradients cannot be determined in HSUs other than the AA. Figure 2-14 presented a table and schematic of the magnitude and direction of gradients in the AA between individual wells from depth-to-water measurements taken immediately prior to the RNM-2s MWAT. In general, flow in the AA across the well cluster is directed east; the exact direction is uncertain. The gradient magnitudes varied from 0.0003 (within measurement uncertainty) to 0.0013.

One vertical gradient was measured in the AA. Prior to the RNM-2s MWAT, a bridge plug was installed in ER-5-4 separating the upper and lower completion zones. The gradient measured across the zones, between 1,942 and 3,234 ft bgs (the completion zone midpoint depths bgs) is 0.0031. That the vertical gradient is a factor of three greater than the maximum horizontal gradient, over an equivalent distance, suggests anisotropy of the hydraulic conductivity ($K_h/K_v > 1$). Static conditions were at no time observed in water-level measurements at ER-5-4#2, and water-level measurements were not collected at TW-3. Therefore, the gradients across the AA into the deeper HSUs were not determined.

4.2 Formation Hydraulic Properties

Single-well testing was performed at Well ER-5-4 and Well ER-5-4#2 to estimate hydraulic properties of the local AA and LTCU, respectively. The 75-day RNM-2s MWAT tested a larger-scale area of the AA through the well cluster. Responses to MWAT production at RNM-2s were observed at wells RNM-1, RNM-2, and the

ER-5-4 upper completion interval, all completed within the AA. The interpretation, analysis, and results derived from each of the these tests were presented in detail in Section 3.0. This section summarizes these results. Table 4-1 presents a composite list of the hydraulic properties interpreted, and Table 4-2 presents FF HSU hydraulic property data for comparison.

4.2.1 Alluvial Aquifer (AA)

Four observation well responses were individually interpreted and analyzed to estimate hydraulic properties of the AA. The MWAT responses were analyzed individually because evidence of a scale-dependent flow geometry was interpreted. The interpretation of the log-log diagnostics for each of the tests imply that the AA hydraulic properties are laterally heterogeneous. It was suggested that the heterogeneity corresponds to the strip model in which groundwater flow is through high transmissivity channelized features in the formation. Although the exact form of such strips are unknown, the model is conceptually permissible given that alluvium deposits likely contain remnant flow features from the time of deposition. Further, the diagnostic plots suggest that the heterogeneity, whatever its actual form may be, is scale dependent. Interpretation of the RNM-1 and RNM-2 responses to MWAT pumping indicate a linear response to pumping at the hundreds-of-feet scale. Interpretation of the ER-5-4 response to MWAT pumping showed that the strip model geometry may have been detected in the early (first 10 to 20 days) period of pumping, but gradually changed to an approximate radial flow response during the later periods. Conceptually, this is reasonable given that in late (constant-rate) pumping time a large volume of the aquifer is tested and lateral heterogeneity at smaller spatial scales would be averaged-out, resulting in an effective radial-flow response.

Horizontal hydraulic conductivity estimates from the four tests (Table 4-1) fall well within the range defined from previous hydraulic testing of the AA across the NTS at the pump-test scale (Table 4-2). The ER-5-4 single-well test estimate was derived using a confined, one-dimensional radial flow model assuming isotropic properties. Due to the inherent numerical uncertainty in the hydraulic conductivity solution set, the conductivity was constrained by a physically realistic range of alluvium specific storage. The MWAT estimates were derived using an unconfined, two-dimensional, anisotropic model. The conductivity estimates range from 7.2×10^{-6} to 3.6×10^{-5} m s^{-1}, just over one order of magnitude. The RNM-1 and RNM-2 MWAT response analyses produced similar high-valued hydraulic conductivities. These data support the strip model conceptualization of the flow domain. However, the RNM-1 response is somewhat suspect because the completion is directly above the CAMBRIC test cavity. If the cavity is hydraulically connected to the RNM-1 completion zone, this may explain the relatively high specific storage and specific yield produced from the analysis. However, a large amount of uncertainty surrounds the nature of the hydraulic connection to the RNM-1 completion zone. The ER-5-4 MWAT response analysis produced hydraulic conductivity estimates that are representative of the AA at the thousands-of-feet scale. It is again noted that the specific yield estimate derived from the ER-5-4 response analysis is negligibly small and suggests a confined formation response. This results from the depth of the ER-5-4

Table 4-1
Single- and Multiple-Well Test Analysis Results

Production Well	Observation Well	Distance Between Wells (ft)	Interval Tested		HSU	K_h (m s^{-1})		K_V (m s^{-1})	S_S (m^{-1})		S_y (-)	Comment(s)
			Top (ft bgs)	Bottom (ft bgs)		Minimum	Maximum		Minimum	Maximum		
ER-5-4	ER-5-4 (upper completion zone)	N/A	1,770	2,113	AA	2.3×10^{-6}*+	4.6×10^{-6}*+	N/A	5.0×10^{-5}	1.0×10^{-4}	N/A	S_S is derived from rock physical properties because the data were poorly constrained in the well-test analysis (Section 3.1.3); K solutions are assumed uniformly distributed
	ER-5-4 (lower completion zone)		3,136	3,350		4.6×10^{-7}*+	9.3×10^{-7}*+					
ER-5-4#2	ER-5-4#2	N/A	4,848	6,658	LTCU	2.2×10^{-7}*	1.7×10^{-6}*	N/A	5.4×10^{-6}	2.5×10^{-5}	N/A	
RNM-2s	RNM-1	706.58	722	3,676	AA	3.2×10^{-5}		1.0×10^{-5}	7.9×10^{-4}		0.287	Properties may not be representative of the local AA because of the test-area proximity to the CAMBRIC nuclear test cavity
	RNM-2	314.05	722	3,676	AA	3.6×10^{-5}		8.5×10^{-7}	5.7×10^{-6}		0.031	The formation interval tested (transmissive interval) is defined as the total AA thickness. Simulation of the 2-D AA head distribution through time shows that the head does not appreciably change in the lower 1,400-ft section of the aquifer
	ER-5-4 (upper completion zone)	1191.58	722	3,676	AA	7.2×10^{-6}		2.0×10^{-8}	1.4×10^{-7}		0.002	

*The well-test analysis assumed isotropic formation hydraulic properties
+Estimates are biased high (upper completion zone) and low (lower completion zone); insufficient information is available to quantify both the bias and uncertainty bounds (see Section 3.1.4)

Table 4-2
Regional and NTS AA Hydraulic Properties
(Page 1 of 4)

Observation Well	Transmissive Thickness (m)	Lithologic Description	Analysis Method	Hydraulic Conductivity (m s^{-1})	Specific Storage (m^{-1})
18S/51-07db2	73.80	Clay, marl, and limestone	Boulton (1963)	1.9E-04	4.1E-04
18S/51-07db2	73.80	Clay, marl, and limestone	Boulton (1963)	3.9E-04	8.1E-06
Airport Well	118.90	Cobble-boulder gravel, gravelly sand, fine sand, and sandy to gravelly clay	Bourdet (1985)	2.6E-05	
CL-VF-O-1	94.50	Sand, gravel, and boulders with minor intermixed/interbedded silt and clay	Neuman (1975)	4.2E-05	
CL-VF-T-1A	62.20	Sand, gravel, and boulders with minor intermixed/interbedded silt and clay	Neuman (1975)	5.6E-05	
Doing well	38.10	Sandy gravel, cobble-boulder gravel, and gravelly, sandy clay with cobbles	Hantush and Jacob (1955)	6.1E-05	7.9E-06
ER-5-3#3	102.50		Neuman unconfined, delayed gravity drainage	3.9E-07	5.5E-06
Franklin Lake #14	16.30	Clay, silt, sand. and gravel	Theis (1935)	3.1E-05	
Furnace Creek test well	45.70	Coarse sand, sandy to clayey gravel, conglomerate, gravelly mudstone and ss	Cooper and Jacob (1946)*	1.5E-03	
GN-IO-2	58.30	Sand, gravel, and boulders with minor intermixed/interbedded silt and clay	Neuman (1975)	2.2E-04	1.0E-05
GN-IT-2	112.80	Sand, gravel, and boulders with minor intermixed/interbedded silt and clay	Cooper and Jacob (1946)	3.1E-05	
GS-4	0.00	Alluvium		1.6E-05	
HC-SO-1	71.30	Sand, gravel, and boulders with some intermixed/interbedded silt and clay	Neuman (1975)	2.9E-04	1.4E-05
HC-S-O-2	39.50	Sand, gravel, and boulders with some intermixed/interbedded silt and clay	Neuman (1975)	4.4E-05	2.5E-06
HC-ST-1	67.90	Sand, gravel, and boulders with some intermixed/interbedded silt and clay	Theis (1935)	1.3E-04	
HC-S-T-2	58.80	Sand, gravel, and boulders with some intermixed/interbedded silt and clay	Theis (1935)	4.5E-05	

Table 4-2
Regional and NTS AA Hydraulic Properties
(Page 2 of 4)

Observation Well	Transmissive Thickness (m)	Lithologic Description	Analysis Method	Hydraulic Conductivity (m s^{-1})	Specific Storage (m^{-1})
Klondike #1	46.30	Gravelly sandstone with interbedded claystone	Cooper and Jacob (1946)	7.2E-05	
Klondike #1	46.30	Gravelly sandstone with interbedded claystone	Cooper and Jacob (1946)	7.2E-05	
Klondike #1	45.70	Gravelly sandstone with interbedded claystone	Cooper and Jacob (1946)	7.0E-05	
Klondike #2	46.30	Gravelly sandstone with interbedded claystone	Cooper and Jacob (1946)	2.7E-05	
NC-EWDP-9SX	15.70	Tuffaceous, silty, sandy gravel and gravelly, silty sand	Cooper and Jacob (1946)*	5.0E-04	
Nye County Land Co	115.80	Limestone, marl, clay, sand, and variably cemented gravel	Boulton (1963)	5.7E-06	
Point of Rocks North Well	110.00	Clay, marl, limestone, and variably cemented gravel	Boulton (1963)	5.9E-05	
RE-VF-O1	25.50	Sand, gravel, and boulders with minor intermixed/interbedded silt and clay	Neuman (1975)	2.1E-04	3.9E-06
RE-VF-O1	12.80	Sand, gravel, and boulders with minor intermixed/interbedded silt and clay	Neuman (1975)	8.4E-04	1.6E-05
RE-VF-T1	104.10	Sand, gravel, and boulders with minor intermixed/interbedded silt and clay	Theis (1935)	1.1E-04	
Richard Washburn	74.00	Sandy gravel, cobble-boulder gravel, and gravelly clay with cobbles	Theis (1935)	4.7E-05	
RNM-1	21.20	Fine to coarse-grained sand and gravelly sand with thin silty clay intervals	Neuman (1975)*	5.3E-04	2.4E-04
RNM-2s	120.70	Silt/clay sand/gravel volcanics and/or carbonate rocks	Moench 1984; Leaky Case 1, 1985	1.7E-06	1.7E-05
RNM-2s	36.00	Fine to coarse-grained sand and gravelly sand with thin silty clay intervals	Theis (1935) recovery*	1.9E-04	
Spring Meadows #1	73.20	Clay, marl, and limestone with variably cemented gravel	Boulton (1963)	6.6E-05	4.1E-05

Table 4-2
Regional and NTS AA Hydraulic Properties
(Page 3 of 4)

Observation Well	Transmissive Thickness (m)	Lithologic Description	Analysis Method	Hydraulic Conductivity (m s^{-1})	Specific Storage (m^{-1})
Spring Meadows #1	73.20	Clay, marl, and limestone with variably cemented gravel	Boulton (1963)	2.1E-04	
Spring Meadows #2	73.10	Clay, marl, and limestone with variably cemented gravel	Boulton (1963)	2.1E-04	5.5E-04
Spring Meadows #4	121.90	Clay, marl, and limestone with variably cemented gravel	Boulton (1963)	1.7E-04	2.5E-04
UE-5n	120.70	Silt/clay sand/gravel volcanics and/or carbonate rocks	Moench 1985; Leaky Case 1, 1985	3.8E-06	2.5E-04
W-14	0.00	Alluvium		3.1E-05	
W-5	0.00	Alluvium		6.3E-06	
WW-3	69.50	Sandstone, conglomerate, and tuff	Theis (1935)	2.0E-06	
WW-3	69.50	Sandstone, conglomerate, and tuff	Theis (1935)	1.5E-06	
WW-3	69.50	Sandstone, conglomerate, and tuff	Theis (1935)	2.7E-06	
WW-5b	64.90	Variably indurated silty sand, fine- to coarse-grained sand, and gravelly sand	Theis (1935)	1.6E-05	
WW-5c	92.00	Variably indurated sand, gravel, cobbles, and boulders with thin silt layers	Theis (1935)	3.9E-06	
WW-5c	92.00	Variably indurated sand, gravel, cobbles, and boulders with thin silt layers	Cooper and Jacob (1946)	3.8E-06	
WW-5c	92.00	Variably indurated sand, gravel, cobbles, and boulders with thin silt layers	Theis (1935) recovery	4.0E-06	
Spring Meadows #13	102.40	Limestone, marl, clay, gypsum, sand, and variably cemented gravel	Boulton (1963)	1.9E-04	2.0E-05
Watertown 3 WW	79.00	Fine to coarse-grained sand, gravel and clay	Theis (1935) recovery	5.0E-05	
NC-EWDP-19D	78.80	Gravelly sand and sandy gravel with silty intervals	Hantush (1961)*	3.1E-06	
WW-A (527.3 m)	80.80	Calcite-cemented, poorly sorted, silty sand and gravel with interbedded clay	Cooper and Jacob (1946)	2.2E-05	
WW-A (527.3 m)	80.80	Calcite-cemented, poorly sorted, silty sand and gravel with interbedded clay	Cooper and Jacob (1946)	2.3E-05	

Table 4-2
Regional and NTS AA Hydraulic Properties
(Page 4 of 4)

Observation Well	Transmissive Thickness (m)	Lithologic Description	Analysis Method	Hydraulic Conductivity (m s^{-1})	Specific Storage (m^{-1})
UE-5c WW	137.90	Fine to coarse-grained sand and gravelly sand with thin silty clay intervals	Neuman (1975)*	1.2E-06	
Data Ranges			**Minimum**	**3.9E-07**	**2.5E-06**
			Maximum	**1.5E-03**	**5.5E-04**

Source: UGTA Groundwater Database

completion zone and is, therefore, not representative of shallower sections of the AA. The specific yield estimate derived from the RNM-2 response analysis is representative of the shallow alluvium (with respect to the strip model).

4.2.2 Lower Tuff Confining Unit

Hydraulic properties of the LTCU were derived from the ER-5-4#2 single-well test analysis. The test data collected were difficult to interpret because the large majority of groundwater inflow to the well was from the open annulus (between the blank well casing and borehole wall) above the slotted casing interval. Therefore, the contributing interval was uncertain. Also, temperature effects and well losses comprised a significant component of the measured drawdown response to pumping that required correction. Uncertainty in the data and conceptualization of the flow domain near and in the well translated into uncertainty into the hydraulic property estimates. The hydraulic conductivity estimates are not well constrained and range just under one order of magnitude (Table 4-1). As performed in the ER-5-4 single-well test analysis, the numerically derived hydraulic conductivity estimates were constrained by a physically realistic range of tuff-specific storage. The LTCU has not been previously tested at FF; therefore, these data stand alone. From testing over the entire NTS area, the LTCU (horizontal) hydraulic conductivity is shown to range between about 10^{-8} and 10^{-4} m s^{-1}. Although the range derived in this analysis is wide (2.2 x 10^{-7} to 1.7 x 10^{-6}), it falls well within that defined for other tuff confining units at the NTS.

4.3 USGS RNM-2s MWAT Analysis

The USGS performed an independent analysis of hydraulic data collected during the RNM-2s MWAT. Their interpretation, analysis methods, and results are summarized in Section 4.3.1. A comparison of the interpretive methods and results between the SNJV and USGS analyses is presented in Section 4.3.2. Appendix A contains a copy of the USGS RNM-2s MWAT analysis report.

4.3.1 USGS Method of Analysis

Observation well responses at RNM-1, RNM-2, the ER-5-4 upper completion zone, and the ER-5-4 piezometer were analyzed to estimate hydraulic properties of the northern FF AA HSU. The base of the AA was defined at 2,300 ft bgs, although it was acknowledged that the base could be as deep as 3,700 ft bgs. Lithologic descriptions of the local AA indicate that below the 2,300 to 2,800 ft bgs interval, the alluvium is less permeable than that above to the ground surface.

The observation well responses, measured in the field as the pressure of the wellbore water column, were converted to head for the analyses. Barometric and earth-tide effects were removed from the pressure record before conversion to head. The response analyses were completed for the drawdown sequence of the MWAT; recovery data were not analyzed.

Both analytical and numerical models were applied to estimate hydraulic properties of the AA. Specifically, the properties estimated were transmissivity,

specific yield, specific storage, and vertical anisotropy. Both the analytical and numerical methods employed simultaneous simulation of the four observation well responses. The analytical method applied was the Moench solution for unconfined aquifers. The model assumes that hydraulic conductivity of the alluvium is homogenous and vertically anisotropic. Model uncertainty was incorporated through variation of the (production and observation) well penetration thicknesses and consideration of wellbore storage. The numerical model applied was MODFLOW, and was used to incorporate the effect of the CAMBRIC test cavity on the simulated observation well responses. The hydraulic conductivity of the alluvium was assumed homogenous (with the exception of the vicinity near CAMBRIC) and vertically anisotropic, as in the analytical model. Changes in the saturated thickness of the alluvium were not simulated because of the small (measured) water-level variation relative to the total thickness of the AA.

The alluvium hydraulic property estimates derived from the analytical and numerical models were similar. Results are presented in Table 4-3 for the two assumptions of varying alluvium thickness.

Table 4-3[1]
Hydraulic Property Estimates from Analytical and Numerical Multiple-Well Simultaneous Solutions

METHOD	Transmissivity ($m^2 s^{-1}$)	Hydraulic Conductivity ($m s^{-1}$)[3]	Vertical-to-Horizontal Anisotropy	Specific Yield	Specific Storage (m^{-1})
Analytical Multiple Well 1600[2]	1.9×10^{-3}	3.9×10^{-6}	0.5	0.19	7×10^{-6}
Analytical Multiple Well 3000[2]	2.7×10^{-3}	2.8×10^{-6}	0.4	0.19	3×10^{-6}
Numerical Multiple Well 1600[2]	2.0×10^{-3}	4.2×10^{-6}	0.9	0.22	1×10^{-5}
Numerical Multiple Well 3000[2]	2.8×10^{-3}	3.2×10^{-6}	0.7	0.21	7×10^{-6}

1 Reproduced from Appendix A. Some units were converted from British to International System to correspond with those presented in the main body of this document.

2 Value is the assigned thickness of the alluvial aquifer in feet.

3 Hydraulic conductivity is the transmissivity divided by the saturated thickness of the aquifer.

4.3.2 Comparison of SNJV and USGS Analyses

The spatial array of the pumping and observation wells for the RNM-2s MWAT permit the analysis of the hydraulic testing data using two different approaches. One entails the simultaneous analysis of drawdown/recovery at all observation wells, and the other approach (the more classic) analyzes each observation well response individually. Further subdivisions in the approach are possible; for instance the nSIGHTS tool used by the SNJV is a 1- or 2-dimensional axisymmetric radial numerical model, while the USGS used a fully 3-dimensional flow model. Both are numerical models. The USGS also used an analytic, basically 1-dimensional radial solution, to fit all observation wells simultaneously (other packages have this option as well). nSIGHTS can be used to fit responses individually, or multiple responses simultaneously, and the same is true of MODFLOW. The SNJV approach was to fit each response individually, and the USGS chose to fit them all simultaneously.

The USGS estimates for horizontal hydraulic conductivity, accounting for uncertainty in the alluvium thickness, range from 2.8 x 10^{-6} to 4.2 x 10^{-6} m s^{-1}. The estimates derived by SNJV range from 7.2 x 10^{-6} to 3.2 x 10^{-5}. Although the ranges to do not overlap, in total they span just over one order of magnitude. The USGS estimates are less variable (factor of 1.5) than those of the SNJV (factor of 4.5). Given the different methods of analysis the results are in reasonable agreement. Specific storage estimates are also similar, although those from the USGS vary less (within one order of magnitude). The SNJV specific storage estimate derived from the RNM-1 response is high and reflects the uncertainty associated with the hydraulic connection between the observation well and the CAMBRIC cavity.

Both specific yield and vertical hydraulic conductivity estimates differed significantly between the SNJV and USGS analyses. The differences are probably a result of the dissimilar conceptual models and approaches to the flow regime diagnosis applied to the alluvium flow system in the two analyses. Observation of both the drawdown and recovery response log-log diagnostic plots showed distinct heterogeneity in the alluvium flow geometry at multiple spatial scales, and did not show a convincing delayed yield effect. The SNJV did not constrain the specific yield values during fitting because the evidence for such an effect was ambiguous. This also permitted the specific yield estimate to indicate how well the data supported the conceptual model. For example, the SNJV specific yield estimate derived from the ER-5-4 response was negligibly small, indicating that the response may act like a confined system, which corresponds well with the proposed conceptual model (see Section 3.3.4)

In general, the difference between the SNJV and USGS hydraulic property estimates stems from how heterogeneity within the alluvium was conceptually and numerically approached. Distinct linear flow features were observed on the log-log diagnostics at at least two observation wells. The flow regime observed at Wells RNM-1 and RNM-2 were identified as preferential flow strips with conductivity higher than that of the composite alluvium matrix. In the 3-dimensional model the aquifer was assumed to be homogenous and vertically anisotropic with the exception of the volume near CAMBRIC; no other heterogeneity was accounted for. The proximity of these wells to the pumping well indicates that their responses are representative of a relatively small aquifer volume. A similar subradial (linear) flow feature was identified at ER-5-4, 1,192 ft from RNM-2s, in early time of the MWAT. The apparent heterogeneity warranted the individual analysis of the observation well responses to pumping at RNM-2s, rather than forcing the same model of heterogeneity on all responses. Clearly the well-by-well approach may not provide an integrated view of the heterogeneity that an appropriately parameterized 3-dimensional model might. Lavenue and deMarsily (2001) show just this benefit from using a numerical model to interpret a MWAT in conjunction with more conventional well-by-well analysis.

The incorporation of alluvium heterogeneity is particularly important in this case because the parameters will be used for contaminant transport prediction (likely at not much greater scale than the observation wells in the test) which requires that preferential flow features and their hydraulic properties are identified. Therefore, the individual-response analysis approach assumed by SNJV was consistent with

the overall goal of the task. To have idealized the alluvium flow regime would have resulted in parameter estimates that neither honored the heterogeneity observed from the measured data nor provided data unique to the alluvium of northern FF.

5.0 References

ASME, see American Society of Mechanical Engineers.

American Society of Mechanical Engineers. 1990. "Quality Assurance Requirements of Computer Software for Nuclear Facility Applications," ASME NQA-2a-1990 addenda, Part 2.7. New York, NY.

Barlow, P.M., and A.F. Moench. 1999. *WTAQ--A Computer Program for Calculating Drawdowns and Estimating Hydraulic Properties for Confined and Water-Table Aquifers*, USGS-WRIR-99-4225, 74 p. Denver, CO: U.S. Geological Survey.

Boulton, N.S. 1963. "Analysis of Data from Nonequilibrium Pumping Tests Allowing for Delayed Yield from Storage." In Proc. Inst. Civil Engrs., 26, pp. 469-482.

Bourdet, D., 1985, Pressure behavior of layered reservoirs with crossflow, *in* Proceedings, Society of Petroleum Engineers California regional meeting, Bakersfield, California, March 27-29, 1985: Dallas, Texas.

Bouwer, H. and R.C. Rice. 1976. "A Slug Test Method for Determining Hydraulic Conductivity of Unconfined Aquifers with Completely or Partially Penetrating Wells." In *Water Resources Research*, Vol. 12, No. 3, p. 423 - 428.

Bouwer, H. 1989. "The Bouwer and Rice Slug Test--an Update." In *Groundwate*r, Vol. 27, No. 3, p. 304 - 309.

Bredehoeft, J.D. and S.S. Papadopulos. 1980. "A Method for Determining the Hydraulic Properties of Tight Formations." *In Water Resources Research*, 16(1), 233-238.

Bryant, E.A. 1992. *The Cambric Migration Experiment: A Summary Report*, LA-12335-MS. Los Alamos, NM: Los Alamos National Laboratory.

Butler, J.J., and W.Z. Liu. 1991. "Pumping tests in non-uniform aquifers - the linear strip case." In *Journal of Hydrology*, Vol. 128, p. 69 - 99.

Cooper, H.H., J.D. Bredehoeft, and S.S. Papadopulos. 1967. "Response of a Finite-Diameter Well to an Instantaneous Charge of Water." In *Water Resources Research*, Vol. 3, No. 1, p. 263 - 269.

Cooper, H.H., Jr. and C.E. Jacob. 1946. "A Generalized Graphical Method for Evaluating Formation Constants and Summarizing Well-Field History." In Transaction American Geophysical Union, Vol. 27:526-534. Washington, DC.

DOE/NV, see U.S. Department of Energy.

Domenico, P.A., and F.W. Schwartz. 1990. *Physical and Chemical Hydrogeology.* New York, NY: John Wiley & Sons, Inc.

Hantush, M.S. and C.E. Jacob. 1955. Non-steady radial flow in an infinite leaky aquifer. Trans. Amer. Geophys. Union, Vol. 36, pp. 95-100

Herweijer, J.C. 1997. "Sedimentary Heterogeneity and Flow Towards a Well." Vrije University, Ph.D. dissertation, p. 103.

Horne, R.N. 1995. *Modern Well Test Analysis*. Palo Alto, CA: Petroway, Inc.

Hvorslev, M.J. 1951. *Time Lag and Soil Permeability in Ground Water Observations, Bull No. 36, Waterways Experiment Station*, p. 1 - 50. Vicksburg, MS: U.S. Army Corps of Engineers.

Kruseman, G.P., and N.A. de Ridder. 1990. "International Institute for Land Reclamation and Improvement." *In Analysis and Evaluation of Pumping Test Data*, Publication No. 47. The Netherlands: Wageningen.

Liu, W., and J.J. Butler, Jr. 1990. Software for the evaluation of analytical and semi-analytical solutions for pumping induced drawdown in complex geologic settings. Kansas Geological Survey Computer Program Series 90-4, p. 52.

Lavenue, M., and G. deMarsily. 2001. "Three-dimensional interference test interpretation in a fractured aquifer using the pilot point inverse method." In *Water Resources Research*, Vol. 37, No. 11, p. 2659-2675.

Lohman, S.W. 1972. *Ground-Water Hydraulics*, Professional Paper 708. Denver, CO: U.S. Geological Survey

Moench, A.F. 1984. "Double-porosity models for a fissured groundwater reservoir with fracture skin." In *Water Resources Research*, Vol. 20, No. 7, p. 831 - 846.

Moody, L.F. 1944. "Friction factors for pipe flow." Trans. ASME, 66:671-678.

Neuman, S.P. 1974. "Effect of Partial Penetration on Flow in Unconfined Aquifers Considering Delayed Gravity Response." In *Water Resources Research*, Vol. 10, No. 2, p. 303 - 312.

Neuman, S.P. 1975. "Analysis of pumping test data from anisotropic unconfined aquifers considering delayed gravity response." In *Water Resources Research*, Vol. 11, p. 329 - 342.

Novakowski, K.S. 1990. "Analysis of Aquifer Tests Conducted in Fractured Rock: A Review of the Physical Background and the Design of a Computer Program for Generating Type Curves." In *Groundwater*, Vol. 28(1): 99-108. Dublin, OH: National Water Well Association

Oberlander, P.L., and C. Russell. 2003. *Final Report: Depth-Specific Hydraulic Testing of Yucca Flat Environmental Restoration Wells FY 2003*. Las Vegas, NV: Desert Research Institute, Division of Hydrologic Sciences.

Pickens, J.F., G.E. Grisak, J.D. Avis, D.W. Belanger, and M. Thury. 1987. "Analysis and Interpretation of Borehole Hydraulic Tests in Deep Boreholes: Principles, Model Development, and Applications." In *Water Resource Research*, Vol. 23(7), 1341-1375. Washington, DC: American Geophysical Union.

Roscoe Moss Company. 1990. *Handbook of Ground Water Development*. New York, NY: Wiley & Sons.

Shaw Environmental, Inc. 2003. *Contaminant Transport Parameters for the Groundwater Flow and Transport Model of Corrective Action Units 101 and 102: Central and Western Pahute Mesa, Nye County, Nevada*, Shaw/13052--201-CD Rev. 0, August 2003. Las Vegas, NV.

Theis, C.V. 1935. "The Relation Between the Lowering of the Piezometric Surface and the Rate and Duration of Discharge of a Well Using Groundwater Storage." In Trans Amer. Geophys. Union, 2, pp. 519-524.

Touloukian, Y.S., and C.Y. Ho. 1981. "McGraw Hill/Cindas Data Series on Material Properties." In *Physical Properties of Rocks and Minerals*. Volume II-2. New York, NY: McGraw Hill Book Company.

U.S. Department of Energy, Nevada Operations Office. 2000. *Addendum to the Corrective Action Investigation Plan for Corrective Action Unit 98: Frenchman Flat, Nevada Test Site, Nevada*, DOE/NV--478-REV.1-ADD. Las Vegas, NV.

U.S. Geological Survey. 2004. Nevada District web site. As accessed at http://nevada.usgs.gov/doe/nv/sitepage_temp.cfm?site_id=364927115574801.

Walker D.D., and R.M. Roberts. 2003. "Flow Dimension Corresponding to Hydrogeologic Conditions." In Water Resources Res., 39(12), pp. 1349-1356.

Weisbach, J. 1845. "Lehrbuch der Ingenieur-und Maschinen-Mechanik," Vol. 1. In *Theoretische Mechanik*, Vieweg and Sohn, Braunschweig, 535 pages (in German).

Zlotnik, V. 1994. "Interpretation of Slug and Packer Tests in Anisotropic Aquifers." In *Ground Water*, Vol. 32, No. 5, p. 761 - 766.

APPENDIX A

Analysis of RNM-2s MWAT Data

(Provided by USGS)

United States Department of the Interior

U. S. GEOLOGICAL SURVEY

160 N. Stephanie Road
Henderson, Nevada 89074
Phone: (702) 564-4604

June 6, 2004

MEMORANDUM

To: Devin Galloway, Ground-Water Specialist, Western Region, WRD

From: Michael T. Pavelko, Hydrologist and Keith J. Halford, Ground-Water Specialist, Nevada District, WRD

Subject: AQUIFER TEST—Analysis of multiple-well aquifer test RNM-2s, Frenchman Flat, Nevada

A multiple-well aquifer test was conducted in Frenchman Flat, Nevada, to estimate the hydraulic properties of the alluvial aquifer in the vicinity of well RNM-2s (Figure 1). RNM-2s was pumped for 75 days at 600 gpm between April 26, 2003 and July 10, 2003. The test was funded by the U.S. Department of Energy, National Nuclear Security Administration Nevada Site Office. Shaw Environmental, Inc. was the lead contractor responsible for providing site supervision and testing services. Stoller-Navarro Joint Venture was responsible for the primary analysis of the aquifer-test data. The U.S. Geological Survey provided quality assurance by also analyzing aquifer-test results from pumping RNM-2s. Hydraulic property estimates from the RNM-2s aquifer test will constrain calibration of local contaminant transport models (DOE/NV, 1999 and DOE/NV, 2000).

Site and Geology

The aquifer test occurred in Area 5 of the Nevada Test Site, northwest of Frenchman Lake (Figure 1). The alluvial aquifer is comprised of largely undifferentiated intervals of silt, sand, and gravel from 0 to 3,700 ft below land surface (IT Corporation, 2003).

The hydraulic base of the alluvial aquifer ranges was assumed to be 2,300 ft below land surface, but could be as deep as 3,700 ft below land surface. An interval between 2,300 and 2,800 ft below land surface has been differentiated in wells ER-5-4 and ER-5-4#2 (IT Corporation, 2001; IT Corporation, 2003). The differentiated interval

was described as silty to sandy clay in well ER-5-4 and as sand and silt deposits in well ER-5-4#2. Both lithologic descriptions suggest the differentiated interval is less permeable than the interbedded very fine to coarse sand from 760 to 2,300 ft below land surface (IT Corporation, 2001).

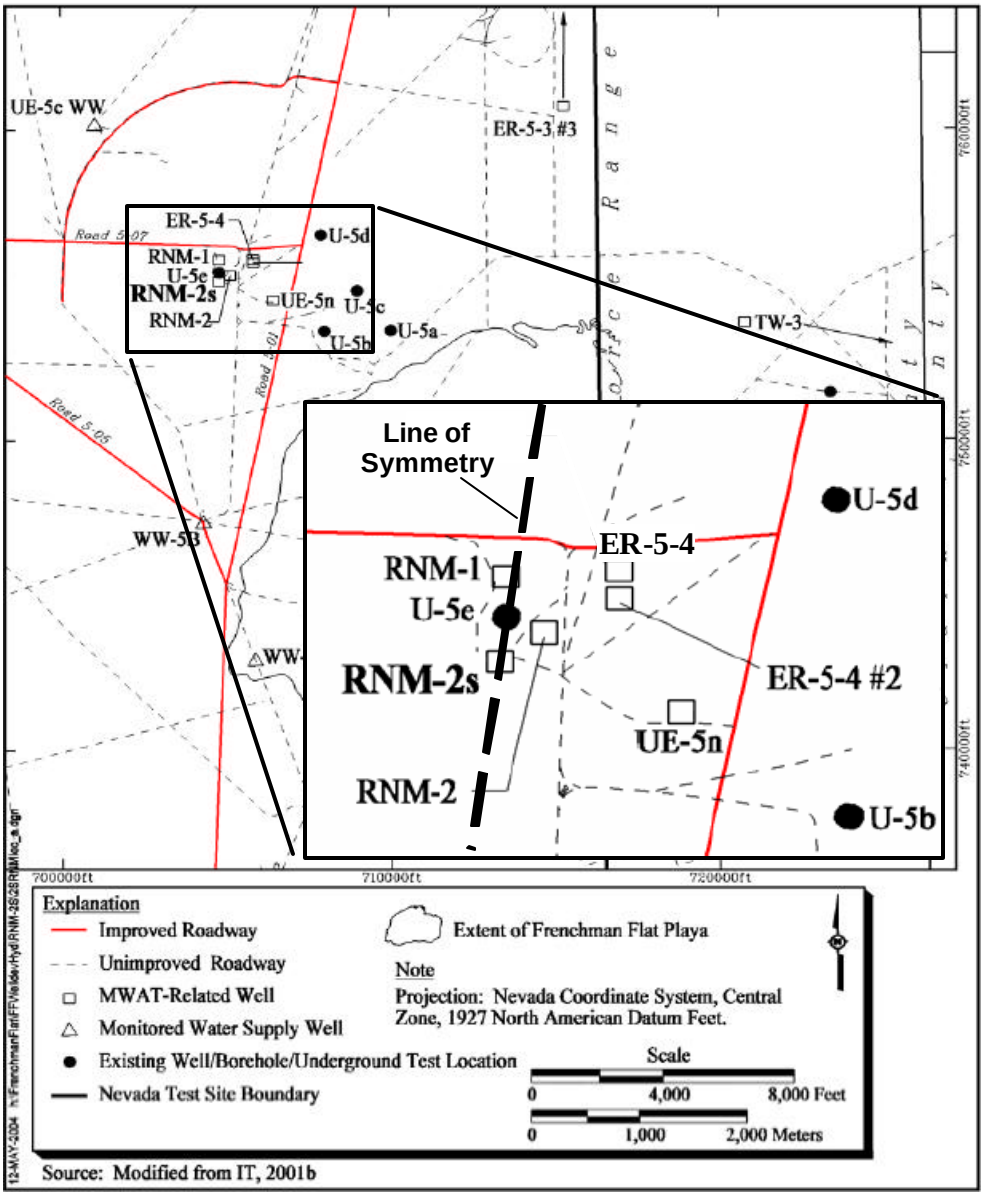

Figure 1.—Location of RNM-2s aquifer test, Frenchman Flat, Nevada.

The alluvial aquifer in the immediate vicinity of pumping well RNM-2s was altered by the Cambric Event, an underground nuclear experiment (Bryant, 1992). A 50 to 75 ft diameter cavity and chimney were created by the 0.75-Kt event. The cavity and

chimney extend above the water table, 710 ft below land surface, and below the working point, 970 ft below land surface. Hydraulic conductivity likely is increased in the rubble-filled cavity and chimney (Tompson and others, 1999). A zone of compressed rock and melt glass exists around the cavity which likely decreases hydraulic conductivity. Hydraulic conductivity around the chimney also could be affected by the Cambric event, but the effect is unknown.

Many observation wells were not designed for aquifer testing which affected drawdowns. Well RNM-1 was completed with perforated casing, instead of screen, in the Cambric cavity. RNM-2 also was completed with perforated casing, has filled with formation material, and has an obstruction at 770 ft below land surface (Stoller-Navarro, 2004). RNM-2s (Outer West Piezometer) was completed as an open tube with no screen. ER-5-4 (shallow) was not developed and communicates poorly with the aquifer because of entrained drilling fluid (Stoller-Navarro, 2004).

Table 1.—Well location and construction data for RNM-2s multiple-well aquifer test.

[Latitude and longitude are in degrees, minutes, and seconds and referenced to North American Datum of 1927; ft amsl, feet above sea level; ft bgs, feet below ground surface; wells without a bottom perforation are open-tube piezometers without screens and open at the top of perforations depth.]

Well name	Latitude	Longitude	Ground surface elevation (ft amsl)	Hole depth (ft bgs)	Perforations	
					Top (ft bgs)	Bottom (ft bgs)
RNM-2s	36°49'22"	115°58'01"	3130.22	1156	1038	1119
RNM-2s (Outer West Piezometer)	36°49'22"	115°58'01"	3130.22	1156	1038	open tube
RNM-2	36°49'23"	115°57'57"	3128.80	935	720	820
RNM-1[1]	36°49'28"	115°58'01"	3135.17	936	858	929
ER-5-4#2	36°49'27"	115°57'48"	3127.00	7000	6486	6658
ER-5-4 (deep)	36°49'27"	115°57'48"	3127.00	3732	1769	2113
ER-5-4 (shallow)	36°49'27"	115°57'48"	3127.00	3732	723	813
UE-5n	36°49'15"	115°57'41"	3113.04	1687	720	730
ER-5-3#3	36°52'23"	115°56'17"	3337.40	1800	1492	1744
TW-3	36°48'30"	115°51'26"	3484.12	1860	1356	open tube

[1] RNM-1 was drilled 21° from the vertical towards the U-5e emplacement hole.

Measurements

One production well and nine observation wells were used for the aquifer test (Table 1, Figure 1). Each well was instrumented with a pressure transducer and water-levels were measured at least once an hour. Water levels were measured between April 11, 2003 and September 12, 2003 which was two weeks before the test to two months after the test.

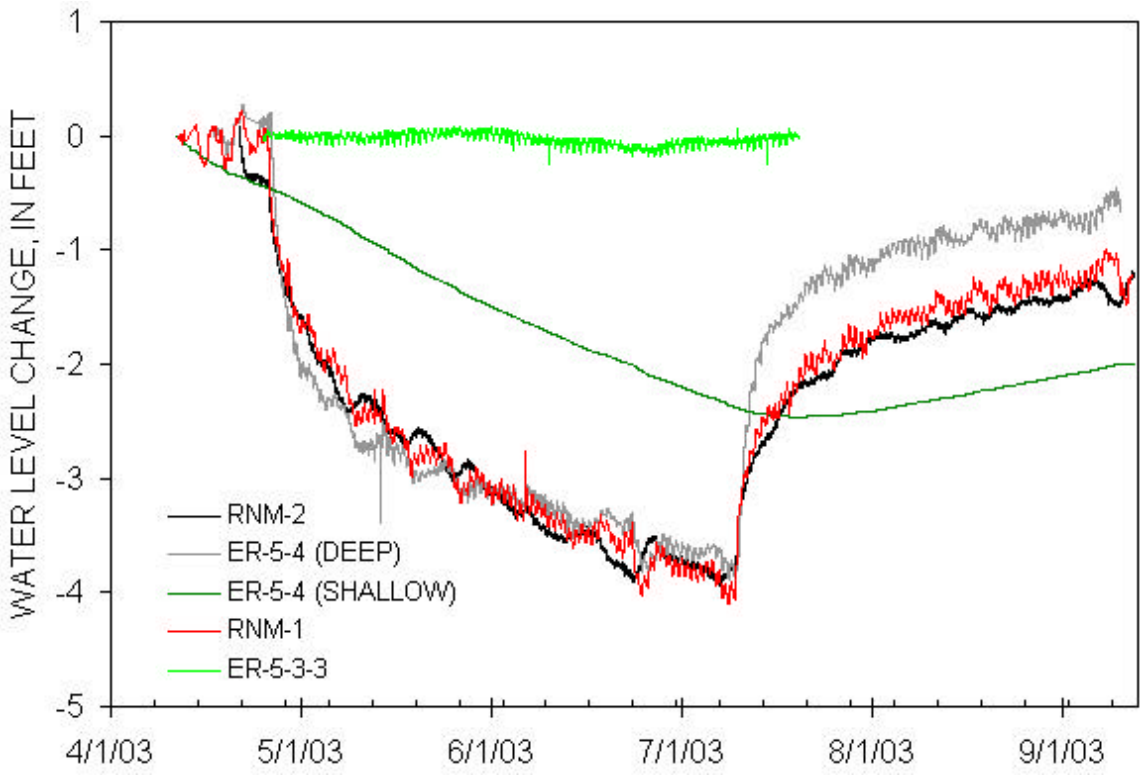

Figure 2.—Water level changes in selected observation wells.

Well RNM-2s began pumping April 26, 2003 and discharged about 600 gpm for 75 days. Production rates were measured with a 4.0-inch magnetic flowmeter system (Stoller-Navarro, 2004). Production ceased three times for periods of 3 hours or less during the 75-d test. Drawdowns were affected negligibly by these brief pauses in pumping.

Results were not affected by pumping from water supply wells near the RNM-2s aquifer test. Well WW-5B was the closest water supply well and was located 1.5 miles

south of RNM-2s (Figure 1). Monthly pumping rates averaged 50 gpm during 2003. Well WW-5C was 2.5 miles from RNM-2s and pumped less than 40 gpm during 2003.

Drawdowns were estimated by subtracting the water level prior to pumping from subsequent water levels. Barometric and earth-tide effects were removed from measured water levels before drawdowns were estimated. Drawdowns were estimated only for the pumping phase of the test. Recovery data were not analyzed because uncertainty of drawdown estimates increases while drawdowns decrease during recovery.

Drawdowns were not estimated from water levels in wells RNM-2s (Outer West Piezometer), ER-5-4#2, UE-5n, ER-5-3#3, and TW-3. Water-levels in wells ER-5-4#2 and TW-3, completed low-permeability, air-fall tuff below the alluvial aquifer, did not respond to pumping. Well ER-5-3#3 was 4 miles from RNM-2s and did not respond to pumping. Well RNM-2s (Outer West Piezometer) communicated very poorly with the aquifer so meaningful drawdowns could not be estimated (Stoller-Navarro, 2004).

Analysis

Hydraulic properties of the alluvial aquifer were estimated with analytical and numerical models. Transmissivity, specific yield, specific storage, and vertical anisotropy were estimated with all models. The analytical model was the Moench solution for unconfined aquifers (Barlow and Moench, 1999). Hydraulic properties associated with the Cambric cavity were estimated with a numerical model which was solved with MODFLOW (Harbaugh and McDonald, 1996).

All hydraulic properties were estimated by minimizing weighted sum-of-squares differences between simulated and measured drawdowns. The analytical model was calibrated with the Solver in Excel. The numerical model was calibrated with MODOPTIM (Halford, 1992). Observations from well ER-5-4(DEEP) were weighted most because the completion was good and the surrounding aquifer was unaffected by the Cambric event. Simulated and measured drawdowns from 1 day after pumping began were compared in well RNM-2s. This was done so that hydraulic properties of the aquifer affected calibration results more than the construction of the pumping well.

Analytical model: Unconfined Moench Solution

The analytical model that best approximated the alluvial aquifer was the unconfined Moench solution (Barlow and Moench, 1999). This analytical model assumes that hydraulic conductivity is homogeneous and vertically anisotropic. Effects of a partially penetrating production well and observation wells with finite screens and wellbore storage also are simulated.

Simulated drawdowns were fitted to measured drawdowns in wells ER-5-4(DEEP), ER-5-4(SHALLOW), and RNM-2s. Drawdowns in these wells were not affected by the Cambric event. Well RNM-1 penetrated the Cambric cavity. Measured drawdowns were about an order of magnitude less than any homogeneous model could explain so drawdowns in well RNM-1 were not compared. Drawdowns in well RNM-2 parallel drawdowns in well RNM-1 and likewise could not be explained. Simulated drawdowns matched measured drawdowns with a root-mean-square (RMS) error of 0.12 ft (Figure 3). The RMS error was less than 2 percent of the 7-ft range in drawdowns that were analyzed.

Hydraulic property estimates were reasonable for an alluvial aquifer (Table 2). Hydraulic conductivity is 1.1 ft/d if a 1,800-ft^2/d transmissivity is divided by a 1,600-ft aquifer thickness. Specific-storage of 2×10^{-6} ft^{-1} and specific yield of 0.19 agree with other estimates for alluvial material. A vertical-to-lateral anisotropy of 0.5 is more than expected but still plausible.

Transmissivity increased 40 percent to 2,500 ft^2/d if the alluvial aquifer was assumed to be 3,000 ft thick instead of 1,600 ft thick. Simulated drawdowns from the 1,600-ft thick and 3,000-ft thick models were very similar. Vertical-to-lateral anisotropy decreased slightly to 0.4 (Table 2). Estimates of specific-storage and specific yield were unchanged.

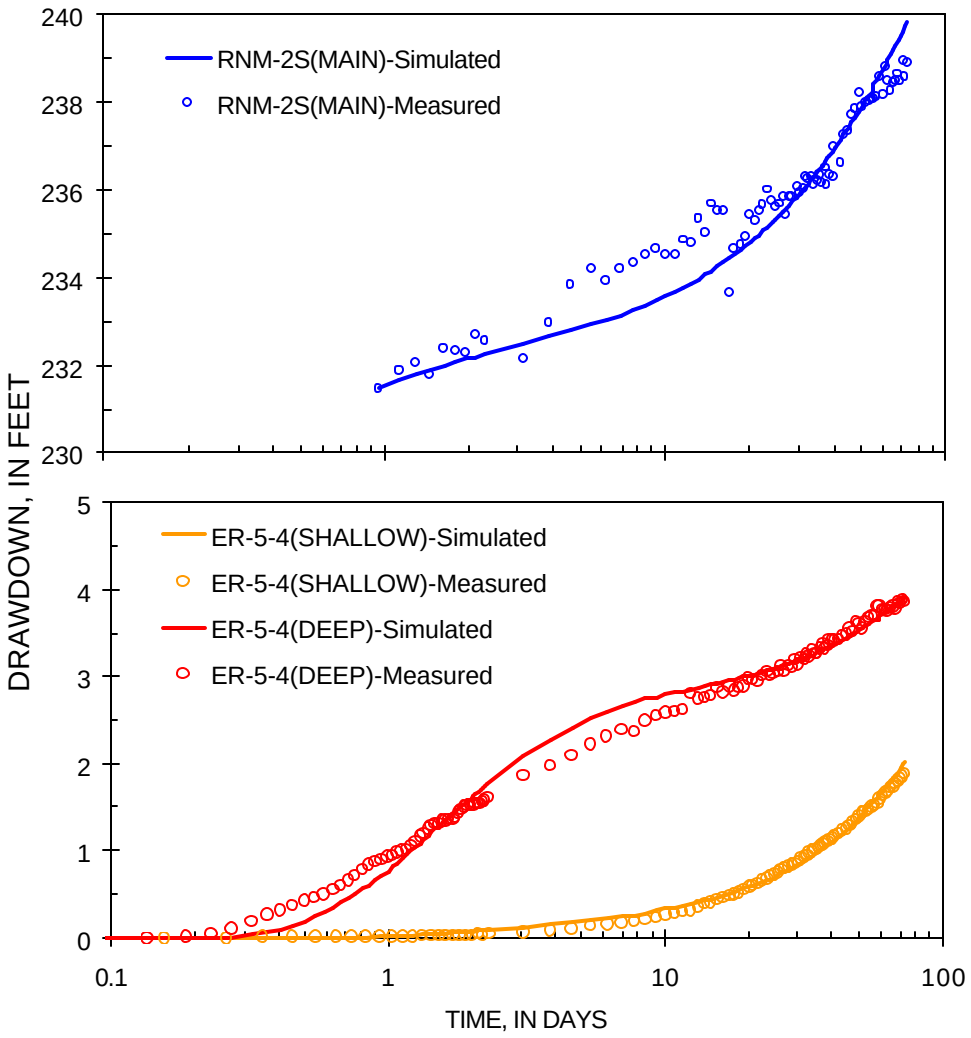

Figure 3.—Simulated drawdowns from unconfined Moench solution and measured drawdowns in wells RNM-2s, ER 5-4(Shallow), and ER 5-4(DEEP).

Table 2.—Hydraulic property estimates from analytical multiple-well, numerical multiple-well, and geometric mean of single-well solutions.

METHOD	Transmissivity, ft²/d	Hydraulic Conductivity, ft/d [a]	Vertical-to-Horizontal Anisotropy	Specific Yield	Specific Storage, ft^{-1}
Analytical Multiple Well 1600 [1]	1,800	1.1	0.5	0.19	2.E-06
Analytical Multiple Well 3000 [1]	2,500	0.8	0.4	0.19	1.E-06
Numerical Multiple Well 1600 [1]	1,900	1.2	0.9	0.22	3.E-06
Numerical Multiple Well 3000 [1]	2,600	0.9	0.7	0.21	2.E-06
Simple Geometric Mean	8,000	5.0	0.4	0.15	1.E-05

[1] Value is the assigned thickness of the alluvial aquifer in feet.

[a] Hydraulic conductivity is the transmissivity divided by the saturated thickness of the aquifer.

Numerical model: MODFLOW

Results from the RNM-2s aquifer test also were analyzed with a numerical model to test the effect of the Cambric cavity on drawdowns in well RNM-1. A line of symmetry was assumed to bisect well RNM-2s and the cavity so only half of the area of interest was simulated (Figure 4). Heterogeneities approximated the cavity-chimney interior, cavity skin, chimney skin, and developed zone around the pumping well (Figure 5). Hydraulic conductivity was assumed to be homogeneous and vertically anisotropic in the undisturbed aquifer as in the analytical model.

The model domain was discretized into 21 layers of 80 rows and 35 columns (Figures 4 and 5). The numerical model extended laterally 100,000 ft away from well RNM-2s. The vertical extent was from 710 to 2,300 ft below land surface. Rows and columns were assigned widths of 15 ft near well RNM-2s and the cavity (Figure 4). Row and column widths were multiplied by 1.3 from near well RNM-2s to the edges of the model. Layer thicknesses ranged from 1 ft at the water table to 100 ft at the base of the aquifer (Figure 5). All external boundaries were no-flow. Changes in the wetted thickness of the aquifer were not simulated because the maximum drawdown near the water table was small relative to the total thickness. The RNM-2s aquifer test was simulated with a 99-d stress period.

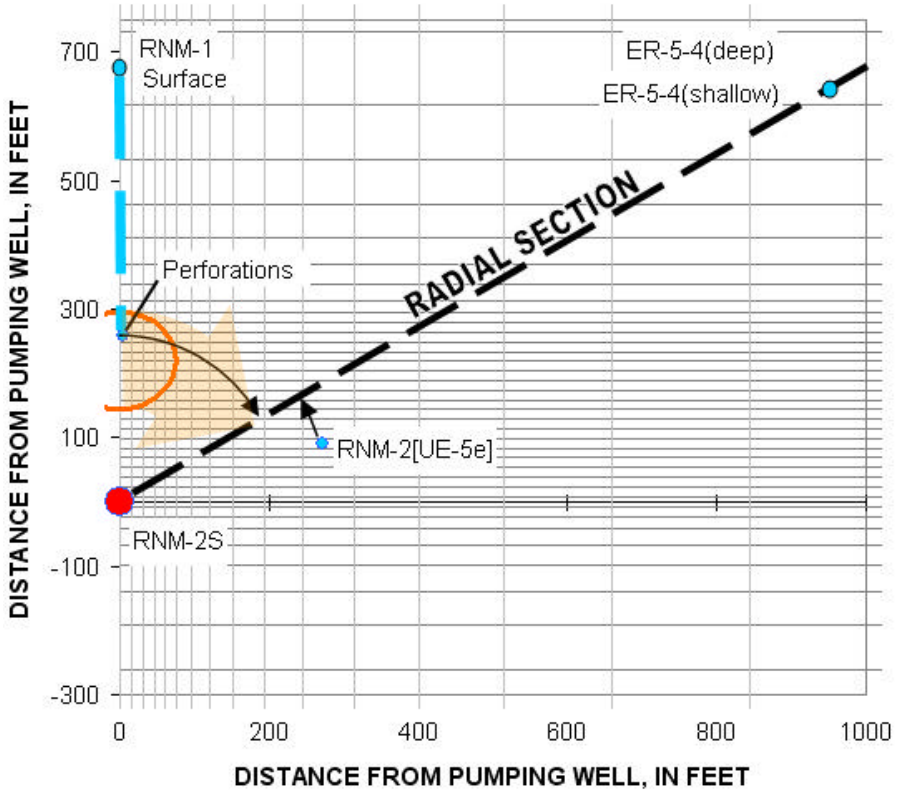

Figure 4.-- Numerical model grid and observation wells near RNM-2s oriented about the line of symmetry through well RNM-2s and the cavity.

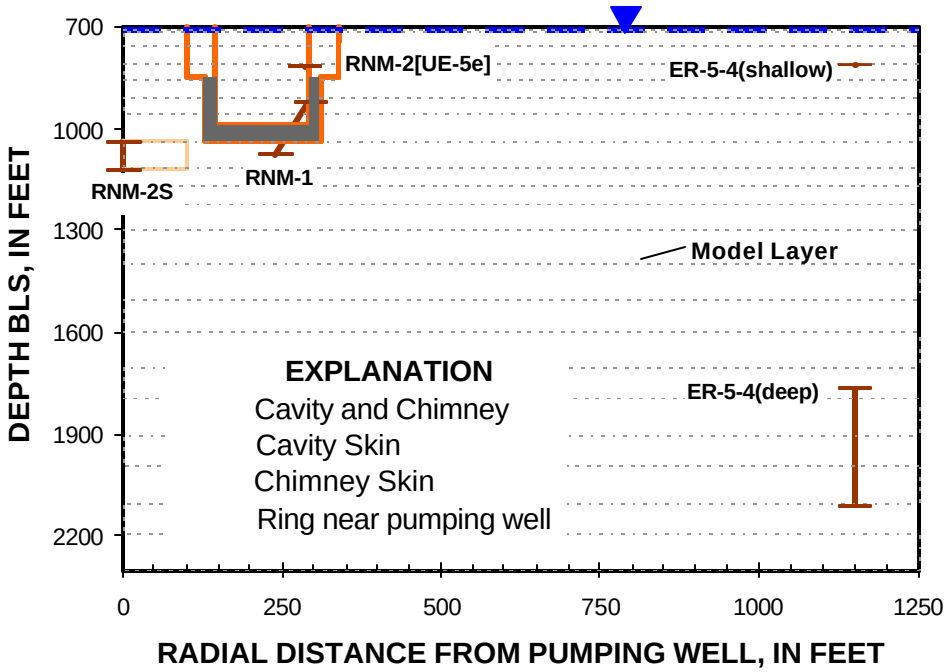

Figure 5.-- Radial cross section with hydrologic features and observation wells.

Measured drawdowns in well RNM-1 were compared with simulated drawdowns from the numerical model. Hydraulic conductivity estimates for the cavity-chimney, cavity skin, and chimney skin were constrained by observations from well RNM-1. Simulated drawdowns also were fitted to measured drawdowns in wells ER-5-4(DEEP), ER-5-4(SHALLOW), and RNM-2s as was done with the analytical models. Simulated drawdowns matched measured drawdowns with a root-mean-square (RMS) error of 0.08 ft (Figure 6). The RMS error was about 1 percent of the 7-ft range in drawdowns that were analyzed.

Measured drawdowns in well RNM-2 could not be explained with any reasonable model (Figure 7). Measured drawdowns in wells RNM-1 and RNM-2 paralleled one another which suggested that both wells were completed in the cavity. The reported position of the RNM-2 completion is more than 200 ft from the likely edge of the Cambric cavity. Simulated drawdowns were more than 3 times greater than measured drawdowns in well RNM-2 after 50 d of pumping (Figure 7).

Hydraulic property estimates for the alluvial aquifer from the analytical and numerical models differed little (Table 2). Hydraulic conductivity is 1.2 ft/d if a 1,900-ft^2/d transmissivity is divided by a 1,600-ft aquifer thickness. The vertical-to-lateral anisotropy of 0.9 was double the estimate from the analytical model. This was the only hydraulic property estimate for the alluvial aquifer that differed significantly between analytical and numerical models. Specific-storage of 3×10^{-6} ft^{-1} and specific yield of 0.22 agree with estimates from the analytical model.

The Cambric cavity is connected poorly to the surrounding alluvial aquifer. Hydraulic conductivity estimates of the cavity and chimney skins were 0.001 and 0.003 ft/d, respectively (Table 3). Conductance estimates of the cavity and chimney skins were equal because the thicknesses of the cavity and chimney skins were 15 and 45 ft, respectively. Hydraulic conductivity of the cavity-chimney fill is 2 ft/d which is similar to the hydraulic conductivity of the undisturbed aquifer.

Drawdown surfaces were predominantly spherical shells between the pumping well and the most distant observation well ER-5-4(DEEP) (Figure 8). Spherical

drawdown resulted from an 80-ft pumping interval which was 5 percent of the aquifer thickness. The Cambric cavity affected drawdown locally. Water flowed around the Cambric cavity which was hydraulically similar to an impermeable cylinder (Wheatcraft and Winterberg, 1985).

Transmissivity increased 40 percent to 2,600 ft^2/d if a 3,000-ft thickness was simulated instead of a 1,600-ft thickness. Simulated drawdowns from the 1,600-ft thick and 3,000-ft thick numerical models differed little. Vertical-to-lateral anisotropy decreased slightly to 0.7 (Table 3). Estimates of specific-storage and specific yield were unchanged. Hydraulic conductivity estimates for the cavity-chimney, cavity skin, and chimney skin were not affected by simulating a 3,000-ft thick aquifer.

Table 3.—Hydraulic properties estimated with the numerical model.

Hydraulic Property	Numerical 1600 [1]	Numerical 3000 [1]	Units
Transmissivity	1,900.	2,600.	ft^2/d
Vertical-to-Horizontal Anisotropy	0.9	0.7	d'less
Specific Yield	0.22	0.20	d'less
Specific Storage	0.000003	0.000002	ft^{-1}
Hydraulic Conductivity of Cavity-Chimney	1.9	2.0	ft/d
Hydraulic Conductivity of Cavity Skin	0.0014	0.0011	ft/d
Hydraulic Conductivity of Chimney Skin	0.003	0.003	ft/d
Specific Yield of Chimney [2]	0.50	0.50	d'less
Hydraulic Conductivity of developed zone around pumping well [2]	15.	15.	ft/d

[1] Value is the assigned thickness of the alluvial aquifer in feet.

[2] Value was assigned and was not estimated.

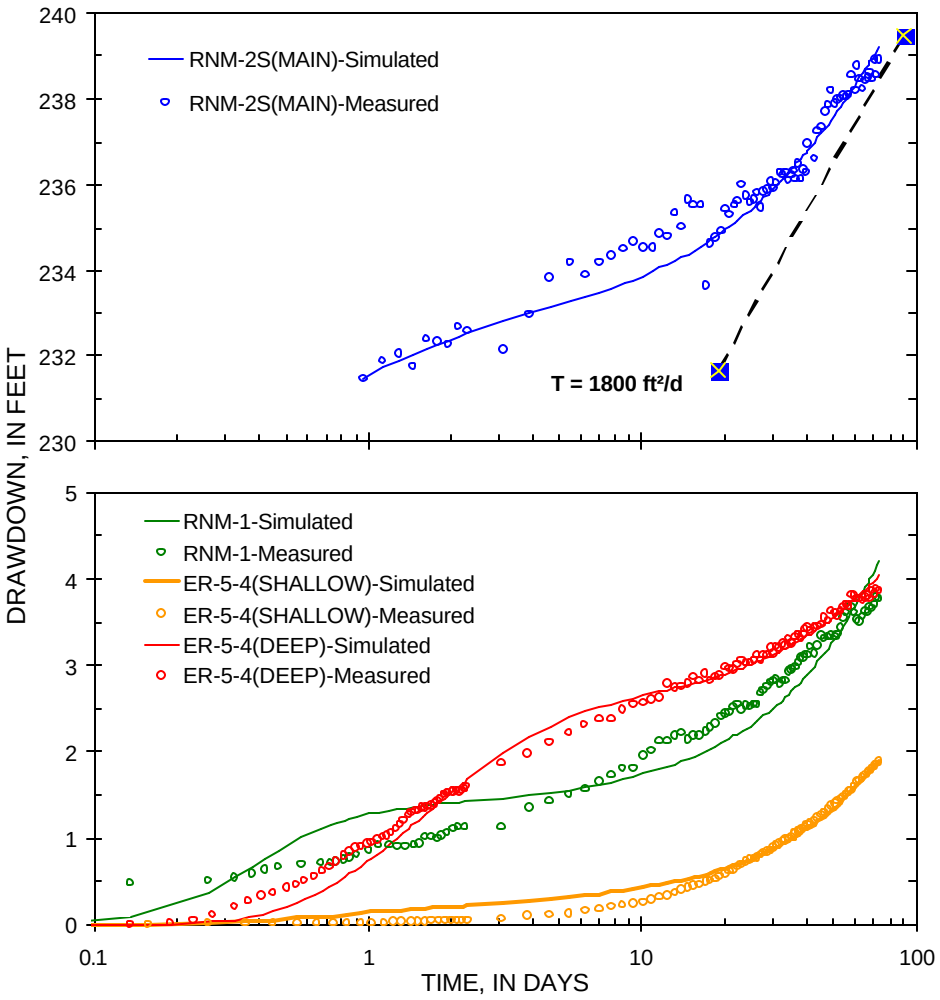

Figure 6.-- Simulated drawdowns from numerical model and measured drawdowns in wells RNM-2s, RNM-1, ER 5-4(Shallow), and ER 5-4(DEEP).

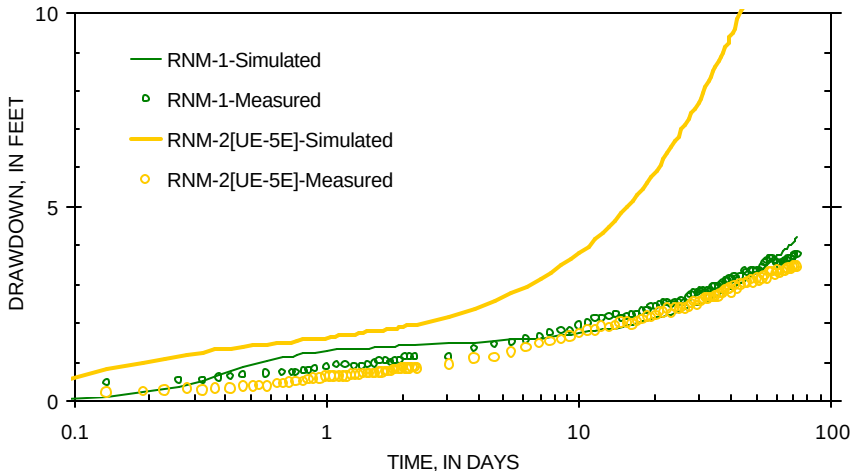

Figure 7.-- Simulated drawdowns from numerical model and measured drawdowns in wells RNM-1 and RNM-2[UE-5E].

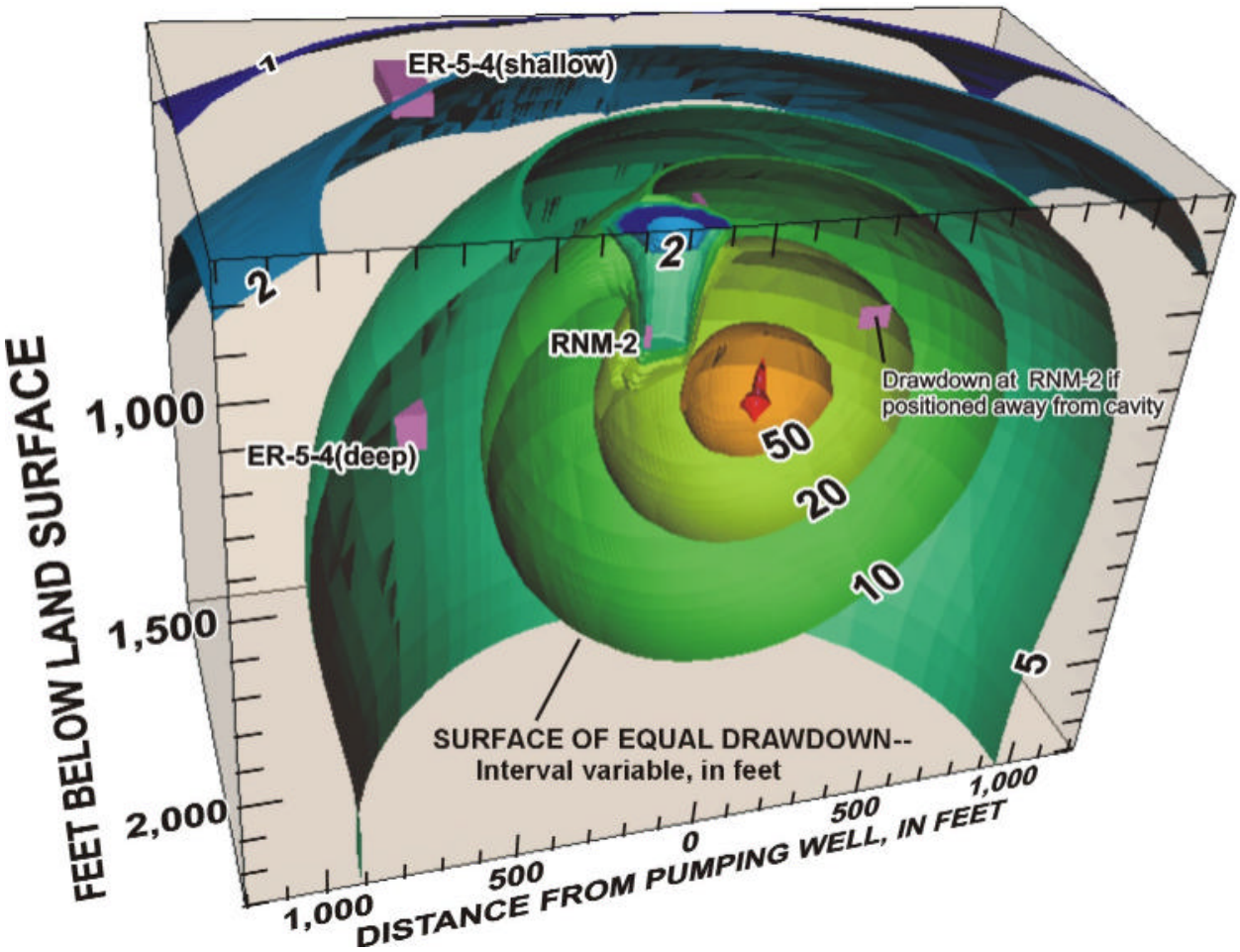

Figure 8.-- Simulated drawdown surfaces from numerical model after 50 d of pumpage at 600 gpm.

Simple Approach

Multiple-well aquifer tests have been interpreted by independently analyzing drawdowns in each well. Drawdowns that resulted from a single pumping event are interpreted and multiple transmissivity estimates are reported (Goode and Senior, 1998). Best estimates of transmissivity and other hydraulic properties are averages of individual estimates (Geldon and others, 2002). This method will be referred to as the "Simple Approach" in this memo.

Hydraulic property estimates from the RNM-2s aquifer test are non-unique if interpreted with the Simple Approach. For example, transmissivity could be estimated to be 3,000 or 14,000 ft^2/d by fitting an unconfined Moench solution to drawdowns in well ER-5-4(DEEP) (Figure 9). Fit between simulated and measured drawdowns is the

same for both models, but the aquifer system is interpreted quite differently. The aquifer with a transmissivity of 14,000 ft²/d would be interpreted incorrectly as confined because the response is Theis like and a specific yield of 0.0001 is too small for unconfined aquifers. The aquifer with a transmissivity of 3,000 ft²/d would be interpreted correctly as unconfined.

The RNM-2s aquifer test should not be interpreted with the Simple Approach despite good fits between simulated and measured drawdowns (CompareALL+IndependentTests_RNM-2s.xls). Transmissivities estimated from the RNM-2s test with the Simple Approach range from 1.5 to 10 times the multiple-well estimate of 2,000 ft²/d (Table 4). The geometric mean of Simple-Approach estimates is 8,000 ft²/d (Table 2). Transmissivity estimates departed most from the multiple-well estimate where the analyzed well had a poor completion or was in the cavity. Estimates of specific-storage, specific yield, and vertical-to-lateral anisotropy each range over an order of magnitude. Treating the five sets of parameter estimates from the Simple Approach as equivalent, independent results suggests a greater uncertainty than exists.

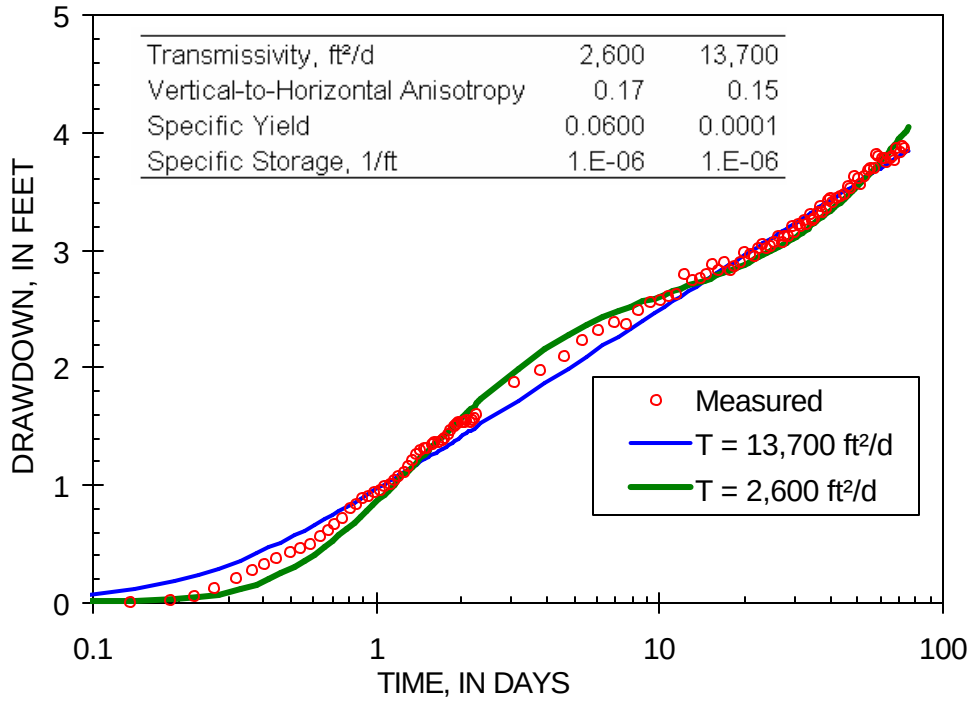

Figure 9.—Simulated drawdowns from alternative, unconfined Moench solutions and measured drawdowns in well ER 5-4(DEEP).

Table 4.—Hydraulic property estimates from five alternative Moench models that were matched to wells individually.

Observation Well	Transmissivity, ft²/d	Hydraulic Conductivity, ft/d	Vertical-to-Horizontal Anisotropy	Specific Yield	Specific Storage, ft^{-1}
ER-5-4(shallow)	9,000	5.7	0.59	0.18	8.E-06
ER-5-4(deep)	2,600	1.6	0.17	0.06	1.E-06
RNM-1	13,000	8.2	2.43	0.51	3.E-05
RNM-2[UE-5e]	22,000	14.0	0.07	0.09	4.E-05
RNM-2S	5,000	3.2	0.65	0.17	8.E-06

References

Barlow, P.M. and Moench, A.F., 1999, WTAQ—A Computer Program for Calculating Drawdowns and Estimating Hydraulic Properties for Confined and Water-Table Aquifers, U.S. Geological Survey Water-Resources Investigation Report 99-4225

Bryant, E.A. 1992. The Cambric Migration Experiment: A Summary Report, LA-12335-MS. Los Alamos, NM: Los Alamos National Laboratory.

Geldon, A.L., Umari, A.M.A., M. F. Fahy, J. D. Earle, J. M. Gemmell and Jon Darnell, 2002, Results of hydraulic tests in Miocene tuffaceous rocks at the C-hole complex, 1995 to 1997, Yucca Mountain, Nye County, Nevada: U.S. Geological Survey Water-Resources Investigations Report 02-4141, 58 p.

Goode, D.J. and L. A. Senior, 1998, Review of Aquifer Test Results for the Lansdale Area, Montgomery County, Pennsylvania, USGS Open-File Report 98-294, 70 p.

Halford, K.J., 1992, Incorporating Reservoir Characteristics for Automatic History Matching: Baton Rouge, La., Louisiana State University, Ph.D. dissertation, 150 p.

Harbaugh, A.W., and McDonald, M.G., 1996, Programmer's documentation for MODFLOW-96, an update to the U.S. Geological Survey modular finite difference ground-water flow model: U.S. Geological Survey Open-File Report 96-486, 220 p.

IT Corporation. 2001. Frenchman Flat Well ER-5-4 Data Report for Development and Hydraulic Testing. Preliminary. September 2001. Las Vegas, NV.

IT Corporation. 2003. Frenchman Flat ER-5-4 #2 Well Data Report. Preliminary. March 2003. Las Vegas, NV.

McDonald, M.G., and Harbaugh, A.W., 1988, A modular three-dimensional finite-difference ground-water flow model: U.S. Geological Survey Techniques of Water-Resources Investigations, book 6, chapter A1, 576 p.

Stoller-Navarro. 2004. Integrated Data Report for the RNM-2s Multi-Well Aquifer Test at Frenchman Flat, Nevada Test Site, Nevada. Preliminary, May, 2004. Las Vegas, NV.

Tompson, A.F.B., C.J. Bruton, Pawloski, G.A., 1999, Evaluation of the Hydrologic Source Term from Underground Nuclear Tests in Frenchman Flat at the Nevada Test Site: The Cambric Test, Lawrence Livermore National Laboratory, UCRL-ID-132300

U.S. Department of Energy, Nevada Operations Office. 1999. Corrective Action Investigation Plan for Corrective Action Unit 98: Frenchman Flat, Nevada Test Site, Nevada, DOE/NV--478-REV.1. Las Vegas, NV

U.S. Department of Energy, Nevada Operations Office. 2000. Addendum to the Corrective Action Investigation Plan for Corrective Action Unit 98: Frenchman Flat, Nevada Test Site, Nevada, DOE/NV--478-REV.1-ADD. Las Vegas, NV.

Wheatcraft, S.W. and F. Winterberg, 1985, Steady-state flow passing through a cylinder of permeability different from the surrounding medium, *Water Resources Research*, 21(12):1923-1929.

Distribution

	Copies
Robert M. Bangerter, Jr. U.S. Department of Energy National Nuclear Security Administration Nevada Site Office Environmental Restoration Division P.O. Box 98518, M/S 505 Las Vegas, NV 89193-8518	2 HC/1 CD
Bill Wilborn U.S. Department of Energy National Nuclear Security Administration Nevada Site Office Environmental Restoration Division P.O. Box 98518, M/S 505 Las Vegas, NV 89193-8518	1 HD/1 CD
Charles Russell The Desert Research Institute 755 E. Flamingo Road Las Vegas, NV 89119	1 CD
Bonnie Thompson U.S. Geological Survey 160 N. Stephanie Street Henderson, NV 89074	1 CD
Public Reading Facility Coordinator Stoller-Navarro Joint Venture 7710 W. Cheyenne, Bldg. 3 Las Vegas, NV 89129	1 HC
U.S Department of Energy National Nuclear Security Administration Nevada Site Office Technical Library P.O. Box 98518, M/S 505 Las Vegas, NV 89193-8518	1 HC/1 CD
U.S Department of Energy Office of Scientific and Technical Information P.O. Box 62 Oak Ridge, TN 37831-0062	1 (Electronic Copy)

John McCord — 1 HC/1 CD
Stoller-Navarro Joint Venture
7710 W. Cheyenne, Bldg. 3
Las Vegas, NV 89129

Greg Ruskauff — 1 HC/1 CD
Stoller-Navarro Joint Venture
7710 W. Cheyenne, Bldg. 3
Las Vegas, NV 89129

Jeffrey Wurtz — 1 HC/1 CD
Stoller-Navarro Joint Venture
7710 W. Cheyenne, Bldg. 3
Las Vegas, NV 89129

John Pickens — 1 HC/1 CD
Stoller-Navarro Joint Venture
7710 W. Cheyenne, Bldg. 3
Las Vegas, NV 89129

Bill Fryer — 1 HC/1 CD
Stoller-Navarro Joint Venture
7710 W. Cheyenne, Bldg. 3
Las Vegas, NV 89129